FOUNDED 1925
INCORPORATED BY
ROYAL CHARTER 1961

"To promote the advancement of radio, electronics and kindred subjects by the exchange of information in these branches of engineering."

THE RADIO AND ELECTRONIC ENGINEER

The Journal of the Institution of Electronic and Radio Engineers

VOLUME 38 No. 2 AUGUST 1969

Ultrasonics in Industry

WITH a few notable exceptions, advances in the science and techniques of ultrasound in the last half century have been disappointingly slow. The basic principles of using acoustic waves for echo ranging go back at least to the early part of the century, and as long ago as 1930 Sokolov in Russia and Mülhauser in Germany outlined methods by which ultrasound could be used to replace or supplement X-ray examination in the non-destructive testing of metals.

Sonar, that is the application of ultrasound in the detection of objects under water, also seems to have suffered from this malaise although, perhaps due to the rapid development of its electromagnetic counterpart, radar, it has made rapid strides since the last world war. It is possible that part of the explanation for the slow development of ultrasonics is the indifference of most educational establishments to this subject—very little attention is given in undergraduate courses to the generation, propagation and reception of elastic waves in solids, liquids and gases. Engineering departments regard the subject as being in the province of the physicists and most physicists scorn this branch of 'classical physics'.

However, the situation does seem to be improving and much more work is now being carried out in this field, as is indicated by the interest shown and the range of papers offered for the Conference on 'Industrial Ultrasonics' which is to be held at Loughborough University in September this year. The Institution of Electronic and Radio Engineers has been involved in the organization of two major Conferences in the last few years on sonar activities but this is the first Conference they have sponsored on the application of ultrasonics in industry.

Loughborough is a new and expanding University of Technology, situated on a large and pleasant campus close to the centre of England and is easily accessible by road and rail. The Conference will last for three days and there will be sessions on High-power Ultrasonics, Transducers, Non-destructive Testing Techniques, Analysis of Properties of Materials, Imaging and Instruments. High-power ultrasonics is now used widely throughout industry for such applications as cleaning and welding and a survey paper on this subject will be given at the Conference. Other papers will describe new applications such as the welding of threads in the textile industry. Numerous applications on non-destructive testing will be discussed ranging from the testing of marine boilers to rocket motors. Much more detail is now being extracted from the ultrasonic signals either by the use of scanning and appropriate displays or by the statistical study of the variation of the signal.

A field which is rapidly developing is acoustic holography. The absence of a counterpart in acoustics to the photographic plate has meant that acoustic holography has made much slower progress than has optical holography but some ingenious approaches have now brought limited but encouraging success. Although perhaps there is some way to go before we are able to 'see' three-dimensionally in opaque solids, at least the prospect is promising. The two-dimension visualization of sound in transparent solids and liquids is now established and a paper will be presented on the latest developments in this subject. A number of ultrasonic instruments will be described ranging from position-sensing devices to those making use of ultrasonics in electrical fault detection.

The provisional list of papers is printed on pages 80 and 81 of this issue. It will be seen that several of the 20 papers are being presented by authors from overseas and it is hoped that the Conference will have a strong international flavour.

J. W. R. GRIFFITHS

INSTITUTION NOTICES

Quebec Section

At the Annual General Meeting of the Quebec Section of the Institution held in Montreal in April last the following Committee was elected for the forthcoming year 1969–70:

Chairman:	R. C. Chaston (Associate)
Vice-Chairman:	R. H. Bayliss (Member)
Immediate past Chairman:	W. Willetts (Fellow)
Hon. Secretary:	P. A. Robertson (Member)
Hon. Treasurer:	B. Deadman (Member)
Programme Secretary:	L. Seymour (Member)
	C. Gyles (Graduate)
Meetings Secretary:	K. Hancock (Associate)
Membership Secretary:	R. Pemberton (Graduate)
Symposium Chairman:	M. Wearing (Student)
Other Members:	J. Watts (Member)
	E. F. Wale (Fellow)
	B. Summers (Graduate)
	A. J. Bunner (Member)

Enquiries regarding the Section's proposed activities and other local matters should be sent to the Hon. Secretary, Mr. P. A. Robertson, C.Eng., M.I.E.R.E., Plant Department, c/o C.B.C. Engineering Headquarters, 7925 Cote St. Luce Road, Montreal 29.

Television Measuring Techniques

A conference on 'Television Measuring Techniques' is being organized by the I.E.R.E. with the association of the Institution of Electrical Engineers, the Institute of Electrical and Electronics Engineers (U.K. and Eire Section), and the Royal Television Society. It will be held at the Middlesex Hospital Medical School, London, from 11th to 13th May, 1970.

Papers will cover the following broad areas: Studio Origination; Networks; Transmitters and Aerials; Receivers.

Synopses of proposed contributions should be sent as soon as possible to: The Secretary, Organizing Committee for the Conference on 'Television Measuring Techniques', The Institution of Electronic and Radio Engineers, 9 Bedford Square, London, W.C.1.

Steam Plant Availability

Resulting from the work of the Availability Definitions Panel of the Steam Plant Group of the Institution of Mechanical Engineers, a paper on 'Availability of Power Stations and their Equipment' has been published. This paper is open for written discussion and in view of its importance the I.Mech.E. invite contributions from engineers in this country and in all parts of the world. Members of the Institution of Electronic and Radio Engineers wishing to obtain a copy of the paper should write to the Secretary, Technical Committee, The Institution of Electronic and Radio Engineers, 8–9 Bedford Square, London, W.C.1.

Electronic Engineering in Ocean Technology

In September 1966 the first Conference to be held in Europe on 'Electronic Engineering in Oceanography' was organized by the I.E.R.E. at Southampton University. The past two years have seen considerable extension of the techniques then described and it is therefore appropriate to hold a second conference in which the title indicates the rather broader coverage of 'Electronic Engineering in Ocean Technology'. The Conference will be held at the University College of Swansea from 21st to 26th September, 1970. Further details of the development of the theme of 'The Gathering, Transmission, Processing and Display of Information from the Sea' will be published in the next issue of the *Journal*, together with the 'call for papers'.

An Undersea Voyage of Research

The announcement of next year's I.E.R.E. Conference on 'Electronic Engineering in Ocean Technology' is given added point by the present activities of a Member of the Institution, Mr. Kenneth R. Haigh. Just before the start of the recent *Apollo 11* flight from Cape Kennedy, Mr. Haigh set out from nearby Palm Beach, Florida, as the British crew member of the 6-man United States research submersible *Ben Franklin*. The submersible will drift along the Gulf Stream for more than a month, finally emerging east of Cape Cod, a journey of about 1500 miles. The *Ben Franklin* will make numerous oceanographic observations of underwater sound propagation, ocean currents and marine life.

Mr. Haigh is a member of the Admiralty Underwater Weapons Establishment at Portland, and is on a two-year exchange posting with the U.S. Navy. In the 1966 I.E.R.E. Conference on Oceanography he presented a paper on techniques for measuring acoustic reflectivity of the sea bed and of ocean scattering layers, and measurements of this type are being made during the cruise of the *Ben Franklin*.

Correction

The following corrections should be made to the paper 'An Introduction to Threshold Logic', which was published in the June issue of *The Radio and Electronic Engineer:*

Page 346, paragraph 3, the equations should read:

and $$t_1 = \tfrac{1}{2}(\alpha - w_0 + 1)$$

where $$t_2 = \tfrac{1}{2}(\alpha - w_0 - 1),$$

$$\alpha = \sum_{a}^{n} (\text{weights})$$

and

w_0 = 'weight' w read off against b_0, with appropriate sign of b_0.

U.D.C. 621.311.410:621.396:621.398

The Control System of the National Grid and its Communication Links

By

P. F. GUNNING, C.G.I.A.†

Reprinted from the Proceedings of the Institution's Convention on 'Electronics in the 1970s' held in Cambridge on 2nd–5th July 1968.

Summary: The C.E.G.B. generates power to meet the instantaneous demands of the eleven Electricity Boards in England and Wales (maximum 35 800 MW in January 1968). With 230 generating stations and grid transmission at 400, 275 and 132 kV and with 700 grid switching and/or high voltage transforming stations, the C.E.G.B.'s integrated power system is the largest in the world under unified control.

To control and protect this countrywide power system, the C.E.G.B. requires a correspondingly large network of more than 2000 communication links. The paper briefly describes the C.E.G.B.'s three-tier control system which operates at district, area and national levels, and was arrived at over 30 years of control of the British 'Grid'. Some of the philosophy which has gone into the planning of the networks and into the design of the associated speech, remote control, general indication, telemetering and high-speed protection installations is explained.

1. Introduction

The British National Grid is the largest power system in the world under unified control. It is controlled and protected by a correspondingly large network of more than 2000 communication links.

This paper briefly describes the C.E.G.B.'s 3-tier control system and explains some of the philosophy which has gone into the planning of the networks and into the design of the associated telemetering and high-speed protection signalling equipment.

2. The Power System

The C.E.G.B.'s power system (Fig. 1) has some 1000, 4000 and 11 000 circuit miles of transmission lines at 400 kV, 275 kV and 132 kV respectively, interconnecting 775 grid stations and 226 power stations (total generating capacity 38 468 MW s.o.), and some 1600 miles of power cable network. Hydro-electric generation represents less than 1% of the total; and, of the 153 000 million kWh generated in 1966–7 by thermal plant, 77·4%, 12·9% and 9·4% was generated by coal, oil and uranium, respectively.

Reconstruction of the Grid system for 400 kV transmission will be completed in 1972, when the power system will be fully interconnected for bulk power transmission and the total generating capacity will be approaching an output of 55 000 MW; stations of 2000 MW standard capacity with four 500 MW units each are now coming into service.

3. The Control System

The National Grid has been operated by 2-tier control for more than 30 years with grid control centres in the provinces and home counties and a

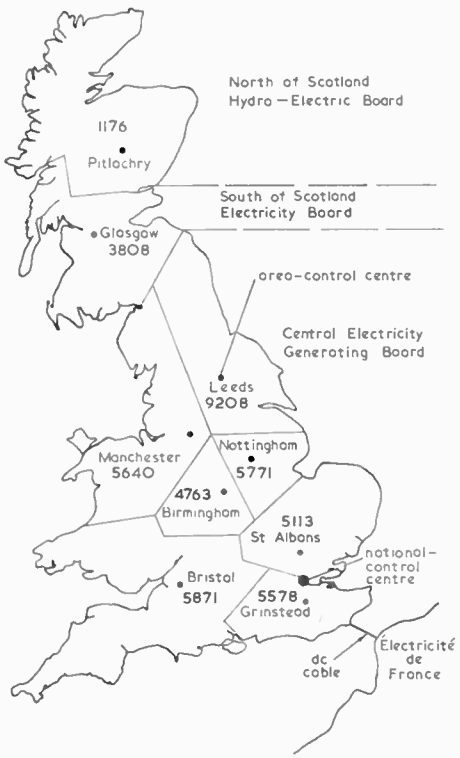

Fig. 1. Power generation in Britain. (47 528 MW output, April 1968).

† Central Electricity Generating Board, Courtenay House, London, E.C.4.

national control centre in London.[1-3] Because of congestion in the control centres, the Board is providing new control rooms for 3-tier—district, area and national—control by 1968/69.[4]

The construction of the 400 kV supergrid will be completed in the early 1970s, by which time the 275 kV and 132 kV networks (Fig. 2) will have become sub-systems interconnected by the 400 kV network. Except for their reliance on infeed from the supergrid, these sub-systems will be independent and can be separately controlled. This sub-division of the system forms the basis of 3-tier control operation (Fig. 3) and allows the formation of district controls.

District controls will deal with the switching and safety precautions of the sub-systems and supervise the power flows within the networks, and also load the associated generating plant in accordance with area economics.

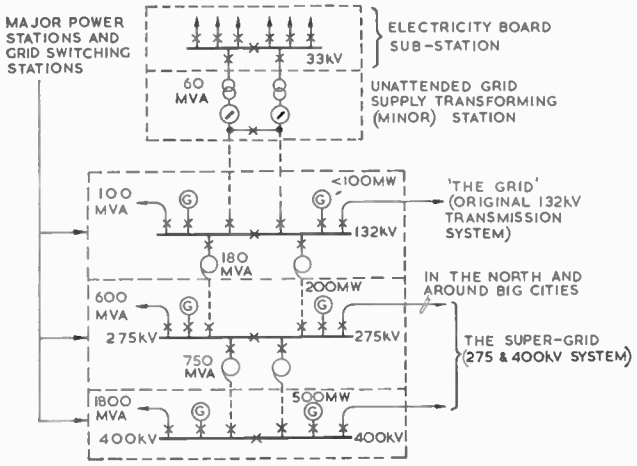

Fig. 2. The 132 kV grid and 275/400 kV super-grid systems.

Area controls will continue to be responsible for the switching and safety precautions of the supergrid and for the loading of supergrid-switched generating plant in their area. They will also continue to be responsible for operating to the inter-area power transfers set by national control for their area as a whole, and for checking the security of any interconnection between districts against probable faults or power line outage on the supergrid system.

National control will continue to co-ordinate area generation by directing economic power transfers between areas within limits which ensure the correct operation of the system.

In the control system, there are major stations and minor stations (Fig. 2). A major station is usually a large generating station or a large attended grid station. A minor station is usually a small generating station or unattended grid station, such as a bulk supply point to an Electricity Board. A minor station can only send signals to and receive signals from a major station. Major stations send signals to and receive signals from grid control centres.

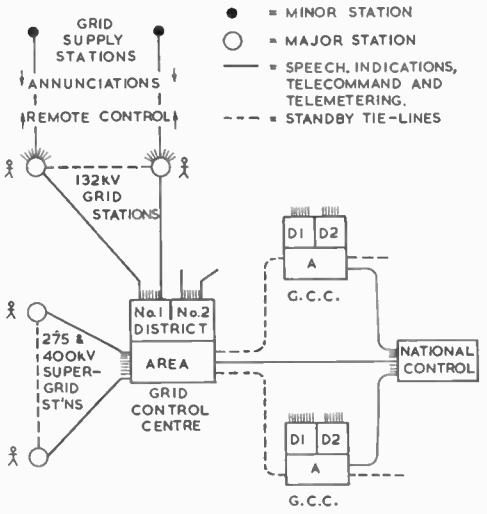

Fig. 3. 3-tier control system.

3.1. *General Facilities*

(1) Supervisory control from major stations of grid switchgear at dependent minor stations and alarm indications from minor stations at major stations.

(2) Automatic indication of switchgear condition—open or closed:

(a) from minor stations to major stations for supervisory control and thence to district control rooms;

(b) from major stations to district control rooms and, if supergrid indications, to area control rooms and thence to the national control centre.

(3) Visual instruction telegraphs:

(a) from district control rooms to district major stations;

(b) from area control rooms to area major stations and to local district control rooms;

(c) from national control centre to area control rooms.

(4) Total generation digital instruction:

(a) from district control rooms to district generating stations;

(b) from area control rooms to area generating stations.

(5) Telemetering:

(a) from minor stations to major stations to record half-hour bulk supply readings;

(b) from major stations to grid control centres for continuous indication in the appropriate control room(s) of active power (MW), reactive volt-amperes (MVAr) and direction of power flow in all supergrid power lines and transformers and in the more important grid lines; also of system volts and system frequency from selected stations, and of the total generated output (active and reactive) from each generating station;

(c) from grid control centres to national control centre of area generation, area transfer and all supergrid readings telemetered from major stations;

(d) between area control rooms to restore missing inter-area telemeter readings by telemeter patching.

(6) Automatic indication in district and/or area control rooms of current overloads at major stations and retransmission to national control centre of supergrid current overloads.

(7) Both-way priority telephone calling between each control room and its stations, between control rooms at the same centre, between area control rooms and between the national control centre and the area control rooms, Glasgow (S.S.E.B.) and Lille (Electricité de France).

(8) Non-control telephone traffic between stations, district offices, project groups, regional headquarters and day staffs at grid control centres and national control use the control networks subject to automatic disconnection by control traffic.

(9) Teleprinter service and facsimile transmission between national control and the area control rooms, Glasgow and Lille.

3.2. *Control of Grid Switchgear*

The control system relies on immediate control of grid switchgear by station operators, directly or by supervisory control on instruction from the grid control engineers. It also relies on delayed automatic reclosing of grid switchgear after transient line faults and automatic isolation of faulty transformers or feeders; grid transformers have on-load tap changing, usually with automatic voltage control.

3.3. *Telephone Facilities*

Each grid control area has been sub-divided into two districts (Fig. 3). Each station has telephone facilities in the associated district control room and, if it forms part of the supergrid, has full telephone and operational facilities (general indications, telemeters, telegraph and generation instruction) in the area control room as well.

Although they are larger, and have new telephone, instruction, indication and telemeter facilities, the new district and area control rooms (Fig. 4) are much the same as the existing control rooms; well-proved control facilities are still basic requirements.

'Control' telephones at supergrid stations call 'switching' and 'loading' engineers in area and district control rooms with priority over non-operational conversations, but only after 10 seconds of interrupted 'engaged' tone, during which time the call can be abandoned. After 10 seconds, the call proceeds, and the non-operational parties are automatically disconnected and given the 'engaged' tone. After 10 seconds of continuous tone, signifying a control conversation in progress, the call joins in the conversation with ringing tone to warn the conversing parties of the intrusion.

Emergency calls, made by dialling two digits, have immediate priority and are indicated by the station-calling lamp flickering and by continuous audible alarm. 'Head of queue' identification is provided for waiting calls, the station-busy lamp flashing alternately with the calling lamp. 'Area' as well as 'district' control engineers call the same 'control telephones' at supergrid stations. Calls from control engineers are distinguished by continuous ringing, whereas all other calls have the usual 'ring-ring/pause/ring-ring/pause' annunciation.

Non-operational conversations can be disconnected and given the busy tone by operating station keys on the main desk in the area control room. This operation also switches into service loudspeakers in the selected stations and in the local district control rooms to receive broadcasts from the desk microphone. In the same way, broadcasts from the national control centre will be received on loudspeakers in the area control rooms.

As some supergrid feeders extend through three control areas, area control engineers are able to key-call one another through intermediate control centres. 'Above-speech' tone dialling is used for all non-operational calls on control lines from control centres. These calls have no priority, but senior day staff at control centres are able to break in on non-operational conversations and ask for the control line. Frequency-modulated facsimile transmission between selected telephones has been provided between all control centres.

3.4. *Miscellaneous*

Digital generation instruction between zero and 999 MW for each generating station is provided on

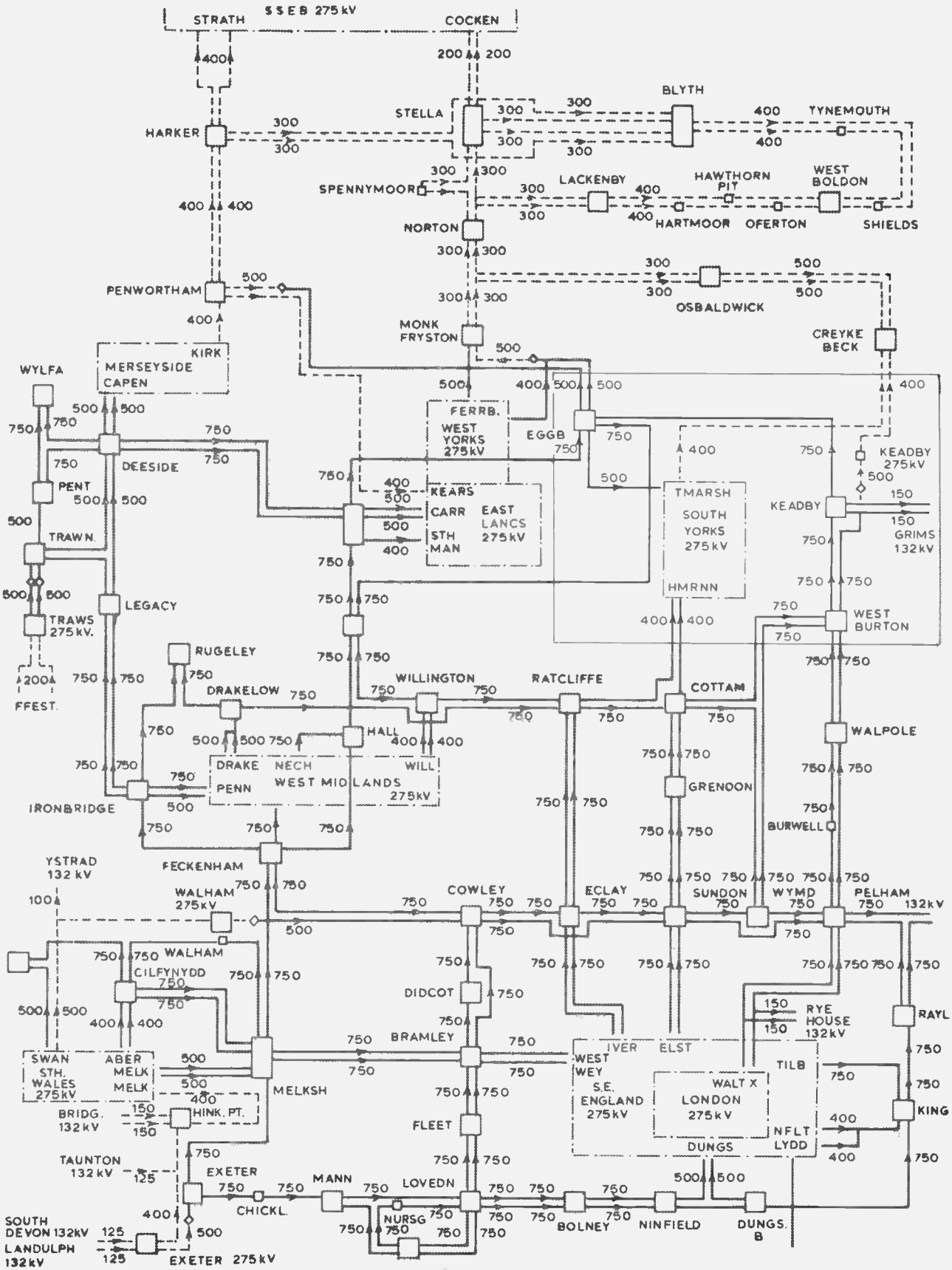

Fig. 4. National flow diagram as shown on the computer-storage display.

the control room loading desks by sets of rim operated decade switches.

Supergrid circuit breakers are automatically indicated on 1-inch mosaic system switching diagrams in both district and area control rooms with separate acknowledgment. Supergrid telemeter indications are displayed in both district and area control rooms on 6-inch tiled load flow diagrams. Telemetered indication of individual power station generation is displayed in the form of 3-figure readings (watts and reactive volt-amperes) by 'digivisors' on the loading desks. An analogue-to-digital converter successively converts d.c. telemeter analogues into 3-digit 'digivisor' readings.

Large 4-figure 'digivisor' indications are displayed of time, date, system time error, district/area generation, net transfer, demand and system frequency, the latter being derived from a shaft encoder driven by a self-balancing frequency indicator.

A 1-inch mosaic diagram of the entire supergrid system is provided in each area control room, together with line-end-open indications automatically updated from the national control centre to indicate the national supergrid running condition.

3.5. *National Control Centre*

The new national control centre requires 900 on-line telemeter readings and 4000 on-line indications of supergrid circuit breakers, overloads and line-end-open from the area control centres. It would be almost impossible to display these quantities with conventional feeder-flow telemeters, indication semaphores and lamps; the loading and switching diagrams would be so large that they could not be viewed intelligibly from operating desks in central positions. With conventional presentation, area and district control rooms can generally accommodate up to 200 dials and 2000 automatic indications.

Fortunately, the supervisory nature of national control, as distinct from the more direct area and district control of stations, permits the use of selective methods of display whereby only significant parts of the system need be displayed. This 'common-diagram' principle has been established for many years,[5] but there has always been a restriction of service, since only one part of the system could be on-line at a time, and it has always been difficult to indicate clearly and unambiguously switchgear numbers and feeder names.

3.5.1. Computer and display system

These disadvantages can now be largely overcome, by using cathode-ray tubes for display and a high-speed digital computer to scan the incoming signals from the area control centres (see Section 9.5) and, with stored diagram data, to generate the required pictures, and to route them to the selected display tube.

Three 2-position control desks are to be provided in the new national control room. Each desk will have four display tubes, and there will be others elsewhere in the building for program studies, display alterations, data setting-in and testing. It will be possible for 12 independent pictures to be displayed.

Even if it were possible, control room ergonomics preclude the showing of the whole supergrid system simultaneously on one tube. It has therefore been arranged to store the whole network as a complete mosaic picture in the computer store, and to steer the displayed area, so that any tube can show approximately 1/12 of the grid system (Fig. 4), complete with on-line power flows and any current-overload indications. Each control desk position will have a steering control and a set of self-illuminating control buttons for selection of tube, picture and data tabulation.

More detailed study will be possible using the same controls to select individual station diagrams showing switch positions, and generator and transformer power flows.

Other pictures and tabular lists of system conditions will also be displayed, e.g. the network voltage-profile, national and area generation and demand, area transfers, generator outputs, continuous group summations of up to any 20 feeders, automatic annunciation of switchgear operation and current overloads, etc.

Automatic indication of switchgear and network alarm conditions will be provided and the computers will automatically marshal the corresponding displays in readiness for detailed acceptance.

All on-line data will be stored at 1-minute intervals for up to 30 minutes, and at 5-minute intervals indefinitely, so that animated pictures of system conditions leading up to an incident can be permanently recorded for subsequent reproduction.

Many other facilities are to be provided by this novel equipment and new features are being planned. Continuous on-line security assessment is being provided for the entire supergrid system.

3.5.2. Security

The computers will be duplicated, each contributing its share to normal operation and each able automatically to carry the full work load with changed priorities in the event of failure.

The computer system will shut itself down safely should the stand-by diesel-alternator fail to restore power after 30 seconds of mains failure, and, when power is restored, it will check with the control areas to make sure that it is up to date before restoring service.

4. Communication Links

Only a few of the Generating Board's communication and signalling requirements, including data transmission, have required a transmission bandwidth greater than 3 kHz. Most signalling requirements are met by narrow band (120 Hz) tone channels or by metallic circuits for d.c. signal-line or direct comparison of a.c. fault currents.

The Generating Board has been able to satisfy its requirements by selective use of power line carrier, v.h.f. and u.h.f. radio, pilot cable and rented circuits.

4.1. *Power Line Carrier*

Power line carrier (p.l.c.) is transmitted phase-to-phase on 132, 275 and 400 kV power lines. At 400 kV the carrier line traps have to be capable of carrying 4000 A and of withstanding 60 000 A fault current. Power line carrier frequencies lie in the band 70–500 kHz, but there are considerable restrictions for continuous transmission in this band to avoid interference with aeronautical and marine navigation systems (Decca and radio beacons). A minimum separation of 4 kHz per 100 kHz is maintained between frequencies on adjacent lines. Greater separation is required between frequencies on lines which run in parallel. Power line carrier frequencies can be repeated when there are two or more power lines in series between the lines in question.

Most equipments are of the normally quiescent type but continuous carrier frequency shift equipments are now being used over any length of line, transmitting about 2 watts continuously and about 10 watts for the duration of the fault. Phase-comparison p.l.c. protection (Section 6.1.2) is usually restricted to lines of between 20 and 50 miles in length and is used occasionally on lines below 20 miles. Power line carrier installations are being specified less frequently because of their inflexibility and because of the tendency to tee connect power lines, giving rise to reflections at tee points and also because of the increasing number of instances where, for amenity reasons, a length of underground cable is inserted in the line. The effect of the cable is to introduce distortion and attenuation of the carrier signal.

One way of reducing dependence upon rented circuits (see Section 4.6) is to use more p.l.c. on the shorter feeders, but the cost of the outdoor coupling equipment and the line traps makes it an expensive solution. The reliability of power line carrier for protection signalling, however, still leaves something to be desired, and signal attenuation can be serious during icing conditions at the higher carrier frequencies.

4.2. *V.H.F.* and *U.H.F. Radio*

Single frequency common channel v.h.f. radio is used by the Board's mobile maintenance fleets and their base stations. It is also used in emergencies by major stations using code calling, should they lose the public as well as the private telephone service. Hilltop stations for the mobile fleets are controlled by u.h.f. links when reliable rented circuits cannot be provided. Single frequency v.h.f. radio on two other channels is used by health physics monitor cars in the districts around nuclear power stations. U.h.f. radio, hand portable and staff location, is used as required in power stations and for coal handling.

4.3. *Microwave Radio*

Because rented circuits are less expensive and are generally satisfactory, and because microwave transmission cannot be justified when only a few channels are required, microwave radio has not yet been used. Installations of short distance 1500 MHz microwave are being tried out to reinforce protection signalling by rented circuits between three stations of a future 5000 MW concentration, which includes 500 MW generators. Assuming Post Office consent, microwave transmission, preferably without relay stations, would be used in special circumstances requiring extreme security in difficult terrain (in flood areas or across estuaries), or requiring extremely high rate signalling, or where the cost might be economic for an exceptional route carrying heavy administration traffic. To reduce outage periods due to component failure, transmitters and receivers on high-security routes would be provided in duplicate.

4.4. *Catenary Cable or Insulated Earth Wire Transmission on Tower Line Routes*

This system of communication is not used by the C.E.G.B.

4.5. *Private Underground Cable*

Armoured pilot cables are reliable but high costs limit their general provision to short distances. The investment is lost should the requirement cease. Laid with power cables, they are subject to noise and induced voltages.

4.6. *Circuits Rented from General Post Office*

Circuits with a bandwidth between 300 Hz and 3 kHz are rented from the Post Office, with a surcharge if 4-wire end-to-end transmission is required. Most circuits rented by the C.E.G.B. are provided in ducted underground cable throughout. The rental of separately routed circuits is based on route mileage. Physical circuits for d.c. signalling can usually be obtained up to 20 miles. Non-physical circuits are derived by the Post Office from carrier transmissions over h.f. cable, coaxial cable or microwave radio.

Having regard to the complexities of the country-wide power system with its continually changing

configuration and the large number of stations, including the various control centres, there has been no practical alternative to the use of rented circuits. The C.E.G.B. rents more than 2000 circuits from the Post Office for control, telemetering, general indication, data transmission, telephony and protection signalling.

There were 2104 faults on the 2262 circuits rented in 1967. The average fault duration was 13·3 hours per circuit.

The use of rented circuits for power system control and protection over the last 35 years has demonstrated the following advantages:

(i) Without loss of investment unwanted circuits have been surrendered and new circuits rented to suit network development. Rented circuits have provided a ready means of keeping pace with the changing network requirements of the continually changing power system.

(ii) Throughout England and Wales, low-loss circuits have been made available by the Post Office over any distance and often at short notice.

(iii) Over the average distances involved, rented circuits have usually permitted the use of simple d.c. signalling equipment and are considerably cheaper than pilot cables, power line carrier systems or microwave installations.

(iv) Unlike p.l.c. installations, rented circuits are unaffected by the frequent diversion of power lines to suit system development.

(v) Being mostly underground and generally independent of the power system, rented circuits are generally immune from disturbances caused by power system interference, or atmospheric conditions, and do not require optical propagation paths or line-of-sight relay stations.

(vi) Apart from circuit testing and fault reporting by the Generating Board, rented circuits are maintained by the Post Office, who give priority treatment to faults on the Board's circuits and on occasion are able to make a replacement available during a repair outage.

(vii) Circuits over separate routes can be made available with separated outlet cables from major stations.

(viii) It has been possible to site grid control centres remote from cities, generating stations and grid stations.

5. Network Planning

By their very nature, rented telephone circuits cannot be as free from accidental interference as circuits in armoured cable, power line carrier or microwave channels.

Records taken over many years show the average circuit rented by the C.E.G.B. to be out of service from 13 to 15 hours a year. The probability of any two separately routed circuits being out of order at the same time can be ignored when adequate precautions are taken to avoid common cause failure.

By suitable reinforcement and by avoiding common cause failures, and with adequate district staff, a high standard of service essential for power system protection, control and operation has been obtained.

5.1. *Network Reinforcement*

5.1.1. Route diversity

With many exchanges and cables, the Post Office can generally route circuits in separate cables to provide satisfactory route diversity. In addition, each major station is connected to the Post Office cable system by two well-separated outlet cables and each grid control centre by at least four such cables over separate routes (Fig. 5).

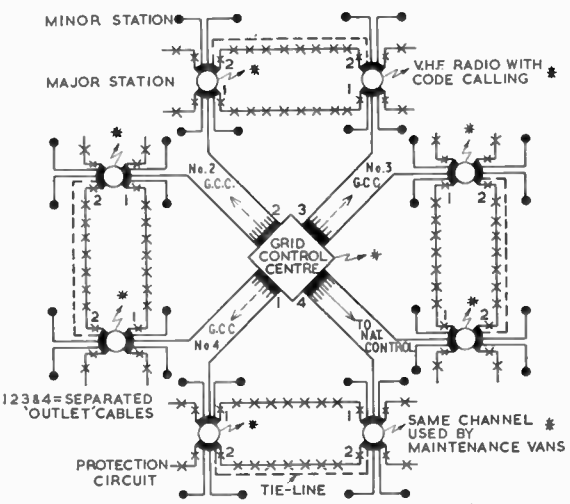

Fig. 5. Network security—diverse routing of telecommunication cables—duplicate circuits—stand-by tie lines and emergency v.h.f. radio.

5.1.2. Duplicated circuits

Supergrid protection systems are duplicated to obtain greater reliability (Section 6.6). Where the associated signalling channels are both rented circuits, each is routed in a separate P.O. cable.

5.1.3. Radial circuits and tie-lines

With an average failure rate of only 13 hours a year per circuit (Section 4.6), it would be an unwarranted expense to duplicate circuits used for communication, general indications and telemetering—the infrequent loss of these facilities from a station can be tolerated

if immediate communication is available over a stand-by route.

These conditions are met in radial networks where each major station has its own circuit to the control centre in one outlet cable for direct communication, general indications and telemetering, and has a tie-circuit in the other outlet cable to a neighbouring major station for indirect communication with the control centre where the radial circuits from the pair of major stations arrive in different outlet cables (Fig. 5). The tie-circuits are also used for local telephone traffic between the groups of minor stations based on the major stations, and permit independent group operation in an emergency.

In the same way, each grid control centre (Fig. 6) has its direct circuit to the national control centre in one outlet cable and a tie-circuit in a separate outlet cable to each of the neighbouring grid control centres for alternative and indirect communication with the national control centre. These tie-circuits are also used for inter-area telephony, general indications and telemetering, and for indirect data transmission to and from the national control centre in the event of direct circuit failure.

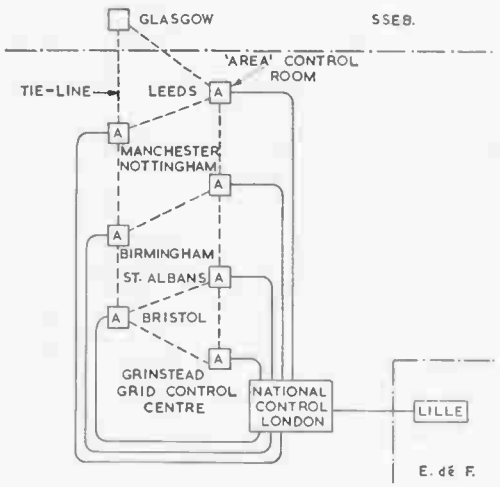

Fig. 6. National control network.

5.1.4. Parent-satellite operation

To economize in rented circuits, the more distant major stations can be connected in groups of two, but up to a maximum of four major stations. A group is served by a common line from the grid control centre to the nearest or most important station, and from this parent station by separate lines to each satellite station. Each station in the group is separately reinforced by having a tie-circuit to a neighbouring major station served by a separate line to the grid control centre (Fig. 7).

5.2. *Common-cause Failure*

The security planned into the communication networks by maximum route diversity would be illusory if precautions were not taken to prevent multiple failures resulting from common causes, such as flooding, loss of public power supplies, power system faults or concentrations of equipment.

5.2.1. Flooding

All communication and signalling equipment, including the associated power plant and cable terminations, should be installed well above recorded flood levels. The introduction of jelly-filled local cables and air-pressurized cables by the Post Office should remove any fear of widespread failure in areas prone to flooding.

5.2.2. Loss of public power supplies

As the control and protection of any power system must be independent of any supplies from that power system, the associated communication and signalling equipment must be energized from stand-by supplies when the mains fail. These can be float-charged batteries feeding d.c. direct to the equipment or to 'no-break' continuity sets which may be continuously-rotating alternators or static invertors. Interruption periods while self-starting diesel-alternators run up to speed cannot be tolerated where protection signalling is concerned.

5.2.3. Power system faults

The Post Office protect their plant from power system faults and prescribe effective isolation barriers, provided by the renter, to withstand excessive rise of earth potential from power system faults. Unfortunately, there can never be any guarantee that lightning will not induce transients into local circuits of sufficient intensity to break down terminal equipment or that power faults will not induce sufficient noise to maloperate or prevent protection tone signalling reception. The following precautions collectively appear to be effective in dealing with this phenomenon:

(i) Route rented circuits throughout in underground cable.

(ii) Reduce the inter-winding capacitance of line isolation transformers to a minimum.

(iii) Connect in series opposition across the station terminals of station line isolation transformers Zener diodes capable of dealing with heavy current transients.

(iv) Use a Post Office signalling earth for d.c. earth return signalling (Section 5.2.5).

(v) Use earth-free d.c. or 'fail safe' tone signals for protection signalling.

(vi) Use earth-free d.c. or continuously repeating coded tone signals for inter-tripping (Section 6.3.4.).

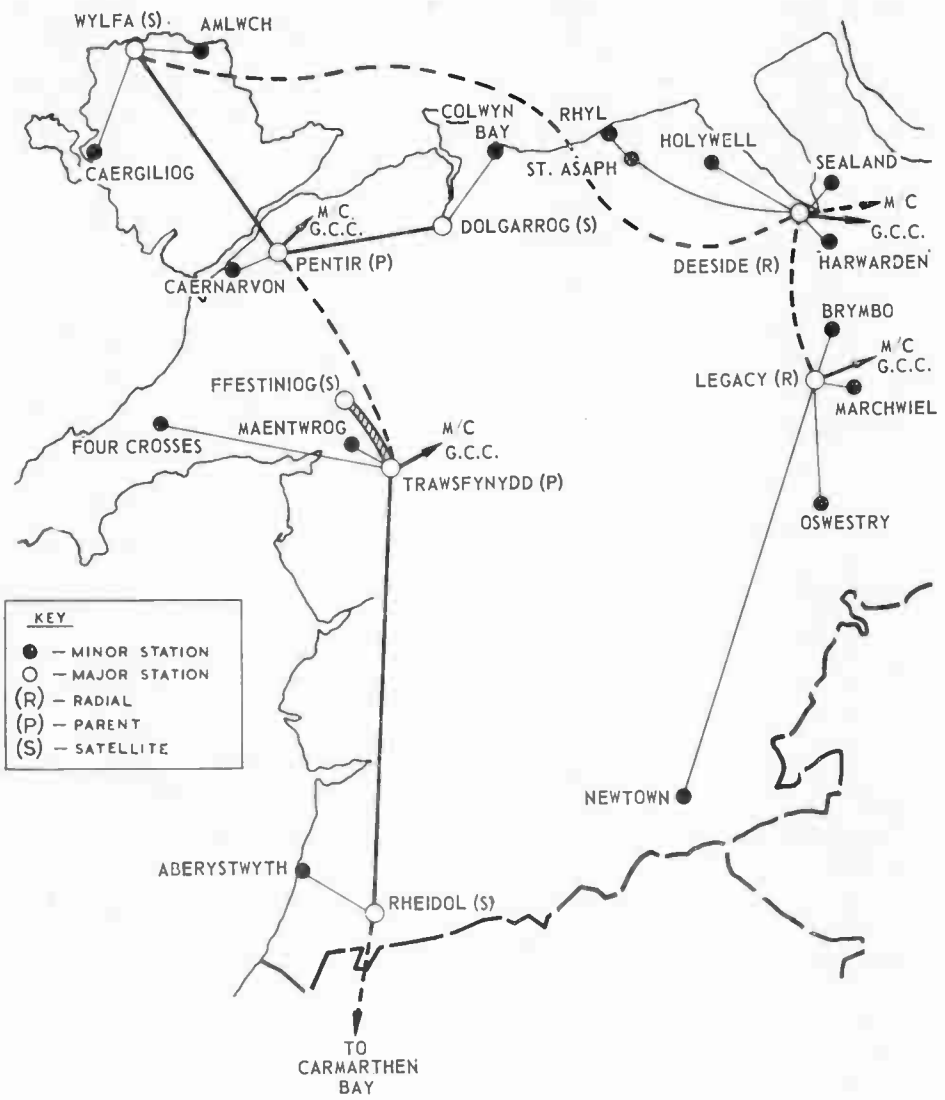

Fig. 7. North Wales portion of the Manchester grid control network.

5.2.4. Equipment concentration

The greatest weakness in any control network is at control centres where equipments and rented circuits for many stations are concentrated. The following precautions can be taken:

(i) The control centre and its contents should be fireproof.

(ii) All common equipment and power supplies should be well and generously engineered and provided in duplicate.

(iii) Each station equipment should have its own power feed for completely independent operation regardless of other station equipment at the control centre.

(iv) Route diversity should not be dependent on line amplifiers concentrated in local repeater stations. The Post Office are to transfer their local 'audio' line amplifiers to the grid control centres where high-security no-break power supplies are available.

5.2.5. Post Office signalling earth

Earth return d.c. phantom signalling has been in use for many years at all C.E.G.B. stations. It is simple, cheap and very reliable, and does not interfere with speech or tone signalling on 2-wire circuits.

Unfortunately, it depends on an insulated 'Post Office earth' wire at stations where the rise of station earth potential under power fault conditions has increased beyond 650 V and at 400 kV stations where there is out-of-balance a.c. interference with d.c. earth-return signalling and also at stations prone to lightning interference (Section 5.2.3). A failure of this remote earth connection at a major station would result in the

station and its dependent minor stations becoming isolated from each other and from the main control network. Although such failures are rare, major stations requiring Post Office signalling earth are being provided with two remote earth connections, one in each outlet cable (Section 5.1.1).

5.2.6. District staff

It has been necessary to have communication engineers experienced in Post Office work on call in the districts with adequate transmission testing instruments to detect and report faults promptly and to liaise with the Post Office engineers in speeding circuit restoration. This is followed up by regular scrutiny of fault records and consultations with the Post Office when necessary.

6. High-speed Protection of the Power System

The maximum fault level on the 132 kV grid system was 1500 MVA 20 years ago, when generation was 11 000 MW. Today, with total generation capacity at 38 500 MW, the maximum fault level on the 400 kV supergrid is 35 000 MVA, requiring large air blast circuit breakers to rupture currents of 60 000 amperes.

System faults used to be cleared in times between 0·25 and 1·0 second; today's severe system faults have to be cleared in 130 to 250 ms. These reduced times, which include up to 40 ms for fault detection and 80 ms for breaker tripping, would not be possible without high-speed signalling channels to ensure correct circuit breaker tripping.

6.1. *Protection Signalling Systems*

Power system protection is a study in itself, but for the purpose of this paper it is only necessary to know how different protection systems make use of signalling channels.

6.1.1. Current-balance protection

Current-balance protection uses a metallic channel (3000 Ω maximum) for the direct comparison of voltages derived from the fault current at each end of a feeder. In one system, if the voltages do not balance, current flows in the signalling channel and the feeder trips.

6.1.2. Phase comparison protection

Phase comparison protection is a system in which the ends of a healthy feeder, during a through fault, interchange signals over high speed power line carrier; A to B during positive half cycles of fault current, and B to A during negative half cycles. With a fault in the feeder, there is a reversal of flow at the end which was previously exporting power, and both ends send signals during the same half cycles. During the intervening half cycles, there are no signals and both ends trip.

6.1.3. Directional comparison protection

Power flowing from a feeder into a station denotes a healthy feeder and, when in excess on a through fault, is made to send a signal to prevent the other end from tripping where power is flowing into the feeder.

6.1.4. Directional distance protection

This technique not only protects its own feeder but also acts as back-up to the protection of adjacent feeders. In this system, stations affected by a fault detect the direction of the fault and locate it by zone:

1st zone: within the first 80% of the feeder length.
2nd zone: within the first feeder length plus 50% of the second feeder.

The 1st zone detector operates in 40 ms and trips the local breaker immediately; the 2nd trips the breaker if the fault persists after an adjustable delay between 0·2 and 0·8 second.

To obtain fast tripping on 'near end feeder' faults, the operated 1st zone detector at the 'near end' transmits a simple 'accelerate' signal to permit the waiting 2nd zone detector at the 'far end' to trip its circuit breaker immediately.

6.1.5. Intertripping protection

It is frequently necessary for faulty transmission plant or dangerous conditions at one station to be made safe by the tripping of a circuit breaker at a remote station. This is carried out by sending an 'intertripping' signal to the remote station. Intertripping signals are unconditional tripping commands which take no account of conditions at the remote stations. As such, they have to be coded to prevent maloperation by the receiving equipment from noise generated by power system disturbance and from any other interference that could affect the signalling channel.

6.2. *Signalling Channels*

The utilization of communication channels for protection signalling by the C.E.G.B. is:

8%	—	power line carrier (134 power lines)
fractional		
use in near future	—	microwave radio
2%	—	private cable
90%	—	rented Post Office circuits (1350)

6.3. *Protection Signalling Equipment*

Protection signalling systems must operate with 'one-shot' reliability after long periods of inactivity, and at no time—particularly in the case of intertripping—must the receiving equipment respond to spurious signals or channel interference.

Two signalling systems for distance protection acceleration are in general use over rented circuits—a 25 ms d.c. system, and a 50 ms tone system which uses an audio channel of 120 Hz bandwidth. Trip acceleration, directional blocking or unlocking is signalled by disconnection of tone, the tone being normally 'on' to monitor the channel and to guard against spurious operation from channel noise. The fastest speeds are obtained by direct point-to-point transmission avoiding channel filter delays at tandem stations. Two new signalling systems will shortly be available—a frequency shift tone system to provide a more positive accelerate signal and a 10 ms d.c. system.

Intertripping protection systems use coded signals to prevent spurious operation by channel interference which can be severe in the case of rented circuits. Two systems using tone signals and 3-step relay coding have been in use on rented circuits for many years; both have an excellent record of freedom from false operation—a single trip system with two tones and an overall time of 150 ms, and a two-trip selective system with three tones and a time of 120 ms. A single trip 35 ms tone system has recently been introduced. It has a simple frequency-shift signal protected by a wide band guard-channel to prevent spurious operation.

The development of a 35 ms single-tone multi-trip 12 bit 600 baud digital system is nearing completion, and two new intertripping systems are undergoing field trials:

(a) a two-trip selective 12 ms d.c. system for both-way intertripping of two separate feeders using three simultaneous d.c. signals over a metallic 4-wire circuit;

(b) a 35 ms single trip three-tone system.

In the new tone systems, so as to intertrip during the first interference-free period, the coded signals are repeated continuously until the fault is cleared.

6.4. *Use of Rented Circuits for Protection Signalling*

The National Grid has been protected successfully by rented circuits since 1934. Experience has made it necessary to take special precautions when rented circuits are used for protection signalling.

Protection signalling systems must have some form of testing or continuous monitoring to draw attention to Post Office line failures so that prompt remedial action can be taken or, as a last resort, the power system temporarily rearranged if there is no duplicate protection (Section 6.6).

It is prudent to transmit at maximum signal strength in case power faults create noise in the associated protection signalling channels. Post Office regulations limit the total power which may be transmitted to 200 μW within the frequency band 250–3000 Hz. This fixes tone transmitting levels between −7 dBm and −20 dBm depending upon the number of channels. If d.c. circuits are available, there is a strong case for d.c. rather than tone signalling in the presence of noise as Post Office regulations allow up to 5 W for d.c. signalling.

Power system faults can affect rented circuits by tripping off public power supplies to Post Office repeater stations. A momentary break in transmission in a 'tone-on' system would be sufficient to accelerate a waiting second zone detector at the wrong sub-station (Section 6.1.4) and possibly disconnect electricity over a wide area. It is, therefore, necessary when renting tone signalling circuits for system protection to specify continuous performance unaffected by electricity supply failure.

6.5. *Local Interference in High Voltage Stations*

Protection signalling equipment has also to be immune to severe noise and interference in high voltage stations affected by system disturbances. Transients greater than 4 kV have been detected on low voltage wiring and filters have to be inserted in external connections to prevent the destruction of transistor equipment.

In large high-voltage switching stations, the connections between the signalling equipment and the dispersed plant it protects are subject to considerable noise and interference. The security of these connecting circuits is to be substantially increased by 5 kV insulated high-speed interposing relays adjacent to the signalling equipment and double pole switching of substantial currents from the 110 V earth-free station battery.

6.6. *Duplication of Supergrid Feeder Protection Systems*

Supergrid feeder protection is duplicated throughout to obtain greater reliability. The associated protection signalling channels can be p.l.c., private cable, rented circuit or, where permitted, microwave, so long as they are physically separate and completely independent of each other.

7. Communication and Signalling

The 2000 or so communication links used in the control and protection of the National Grid are rarely exploited to their full capacity. There is very little traffic apart from telemetering. Signals are only transmitted when necessary. The signalling channels are normally quiescent.

7.1. *Speech Band*

Twenty years ago, when the average rented circuit cut off at 2400 Hz, speech was confined to the band between 400 and 2000 Hz to permit tone signalling below speech at 300 Hz for general indications and telephone calls, and above speech at 2220 and 2340 Hz for continuous telemetering. Speech reception was not noticeably degraded by filtering at 2000 Hz. The 300 Hz channel was only used when d.c. signalling was not available.

The practice continues today, except that speech is no longer restricted below 400 Hz. With rented circuits now cutting off above 3 kHz, tone signalling for general indications and telephone calls uses one of eight channels which are available at 120 Hz spacing above 2000 Hz.

The Board's latest general indicating and telemetering system, the Mk. II system, allows the speech band to be increased, as it requires only one tone signalling channel of 120 Hz bandwidth for 100 continuous telemeter readings (Section 9). Speech transmission on the new national control network will be raised to 2300 Hz (Fig. 6). Each link will still have six signalling channels above speech.

7.2. *Telephone Traffic*

Although control traffic for each major station and its dependent minor stations does not average more than one hour in 24, it is quite heavy during system disturbances and in the early morning and late afternoon, when the load on the power system is rapidly changing and grid switching operations are in progress. At other times, control traffic is quite light and non-control traffic is encouraged to make use of the control network subject to automatic disconnection by control traffic. Although this use can add one or two hours of traffic per office day to each major station and its dependent minor stations, single control circuits cannot cope with random traffic from large offices—the public system is less frustrating.

7.3. *Signalling Traffic*

General indication and telephone calling channels are normally quiescent. With trouble-free low-rate 10 pulse/s signalling, narrow band or d.c., it does not take more than two seconds to make any of 15 control calls or more than eight seconds to:

(i) select and update any of 10 groups of 40 indications,
(ii) send a 3-digit generation instruction or any of 16 visual telegraph instructions,
(iii) select and open or close any of 50 circuit breakers.

7.4. *General Indication and Telephone Calling Channels*

Each major station has a 'G.I.' (general indication) channel to each of its minor stations for remote control, general indications and telephone calls.

Each G.C.C. (Grid Control Centre) has a 'G.I.' channel to each of its major stations for general indications, tele-commands and telephone calls other than 'admin.' calls from the G.C.C. (Section 3.3.3).

The present National Control Centre (N.C.C.) has a 'G.I.' channel to each G.C.C. for general indications, tele-commands and telephone calls. The new N.C.C. will use the Mk. II system for these facilities (Section 9).

7.5. *'G.I.' Signalling*

Most minor stations and half of the major stations use earth return d.c. phantom signalling for 'G.I.' signalling, the remainder use tone signalling, some below but most above speech (Section 7.1).

The number of impulses transmitted in short uncoded trains conveys the selection information for control calls, call clearing and priority disconnections. Calls persist until answered, or for 60 seconds or so at unattended stations. The connection is held by the answering party and not by the 'G.I.' channel which is freed for other traffic as soon as the call is sent. Tandem connections are released by clearing signals sent over the 'G.I.' channel when the calling party clears.

Any of ten 3-digit generation instructors or ten 16-message instructors at a major station can be selectively updated by transmitting 20 impulses coded by pulse length '2-out-of-5 four times' from the G.C.C. An 'OK' impulse to the G.C.C. signifies that the new instruction has been correctly decoded and is being displayed.

Any of 50 circuit breakers at a minor station can be selected and opened or closed from its major station by a selection train of ten coded impulses and a 2 second operate impulse. The received impulses are subjected to impulse count and decoding checks.

Trains of impulses are used to transmit on/off general indications—one impulse for each indication, long for 'on' and short for 'off'. A prefix address, coded '2-out-of-5' by long impulses, selects from amongst 10 groups of 40 indications. Indication trains are only accepted when the total count is correct. An 'OK' impulse is then transmitted to the sending station to prevent repeat indication trains.

The provision of signal start equipment permits the minimum use of normally quiescent common service channels. This avoids continuous high-speed scanning of indications and unnecessary waste of bandwidth for high speed signalling channels. In one arrangement, signalling is started by a magnetic amplifier which responds to d.c. changes in a summating network controlled by 100 on/off condition signalling contacts.

8. Telemetering

Many different systems of telemetering were used to control the National Grid in the 25 years after 1932.[6] With the demand for more telemeters in the 1940s, telemetering systems which required a valuable signalling channel for each telemeter were superseded by multiplex systems which enabled single channels to serve up to 10 or more continuous readings. Impulse rate telemetering[7] became standard in 1957 when the Board's standardized system of communications, indications and telemetering was introduced.[8] The use of 50 baud start-stop time division multiplex transmission and cold-cathode 10-way electronic coder-senders and decoders also became standard.

In principle, impulses up to 80 a minute generated by rotating induction type measuring instruments are transmitted continuously from the out-stations to the control centres where thermionic converters, one for each reading, produce continuous direct voltage analogues in proportion to the corresponding impulse rates and with a time displacement of 15 seconds to operate indicating instruments and recorders. To conserve channels, each coder-sender at the out-stations scans the individual impulsing contacts of a group of 10 meters in 200 ms three times per second, transmitting the appropriate 20 ms signals as tone 'on' or 'off' depending upon the condition of the meter contacts. At the control centres, the continuously repeating start-stop 50 baud signal trains are decoded step by step to reconstitute the 10 meter impulses to operate the corresponding impulse rate converters.

The Board's control system has some 4000 impulse rate telemeters and more than 400 10-way multiplex systems in continuous operation. The average major station transmits 20 telemeter readings—some stations require 5 channels for 50 readings. A 15-way solid-state multiplex system has recently been introduced to supersede the 10-way system. The development of a solid-state impulse rate converter to supersede the thermionic converter has been completed.

Although more than adequate for area and district control, the standardized system cannot deal with the large number of telemeter readings and automatic indications which are to be transmitted from each area control centre to the new national control centre.

A version of the C.E.G.B.'s new Mk. II standardized system has been developed for the national control network, to transmit on a bandwidth of 120 Hz up to 100 continuous telemeter readings and 1000 point indications, together with signals for general telephone calling and supervision, telegraph instruction and check requests.

9. Mk. II Standardized System

The Mk. II standardized system is a large-capacity digital telemetering system, normally transmitting data paragraphs in cyclic order, each paragraph separately addressed and containing up to ten telemeter readings. It is also a large-capacity miscellaneous data transmission system, transmitting separately addressed paragraphs of numerical data. These paragraphs are only sent when required and in order of priority, and are interlaced one at a time between successive telemetering paragraphs. Telephone calls, circuit-breaker indications and statistical information are treated as miscellaneous data. The basic features of the new system are as follows.

9.1. *Line Transmission*

Line transmission requires a single narrow (120 Hz) channel for asynchronous transmission with 25 Hz amplitude modulation of the carrier to synchronize bit stepping. The amplitude modulation is removed for 100 ms to signal paragraph start. For bit intelligence, the carrier is frequency-modulated at 50 bauds in step with the 25 Hz modulation.

9.2. *Telemetering Transmission*

Each telemetering paragraph contains up to 11 words with no spacing between words. The first word is the address, the second word the first telemeter reading, and so on.

Each word of fifteen 20 ms bits is marked 2 or 3 out-of-5 three times; 2-out-of-5 for import readings and 3-out-of-5 for export readings and for address words. Each reading can be from 000 to 999, and, although there can be 1000 paragraphs, these are being limited to 100. Telemeter readings are transmitted by cyclic repetition. Fast response readings can be transmitted more frequently than slow response readings.

By sending each telemeter reading in 0·3 second, better use is made of the 50 baud telemeter signalling channel than with standard pulse rate time-division multiplex, in which a separate channel is needed for ten readings, and a response time of 15 seconds is given. The Mk. II system can send approximately 50 readings on a single channel with a similar response characteristic.

9.3. *Analogue-to-Digital Conversion*

At the area control centres, analogue-to-digital converters (a.d.c.) are successively connected, one word in advance of line transmission, by 2-pole reed relays to d.c. analogues derived from the 0–75 V outputs of the thermionic converters[7], which are responding to the incoming impulse rates received from the stations.

To simplify summation and display at the national control centre, scaling resistors in the individual analogue circuits enable the a.d.c. to count directly in megawatts, megavars, amperes and volts, etc. in '2- (or 3) out-of-5' code, depending on the polarity of the analogues being scanned.

9.4. *Miscellaneous Data Transmission*

Single paragraphs of miscellaneous data waiting to be transmitted are sent interlaced between successive telemetric paragraphs. With telephone calls, telegraph instructions and acknowledgment and request checks having priority over general point indications (switchgear, line-end-open and current overloads), any of these will interrupt telemeter transmission at the first 100 ms inter-paragraph pause, and a paragraph of miscellaneous data will be transmitted. The address word is coded three times 2-out-of-5; then follow up to 10 miscellaneous data words, the first 10 bits of each word being marked with 10 on/off indications and the last 5 bits coded 2-out-of-5 to signal the total number of random marks in the first 10 bits. The address word of a miscellaneous data paragraph instructs the receiving station to decode accordingly. Telemeter transmission then proceeds from the position in the cycle where it was interrupted.

9.5. *Reception of Signals*

Continuous error detection rejects paragraphs received incorrectly owing to transmission interference. At the national control centre, each word is decoded and, if correct, electronically updates the duplicate computers of the central processor, each one separately (Section 3.5.1).

Word data are stored on sets of relays for telephone calling, telegraph acknowledgment, check request and line-end-open indications.

At the area control centres, word data are stored on sets of relays for telephone calling and supervision, telegraph instruction, check requests and indications of line-end-open (Section 3.4.4).

9.6. *Check Requests*

Check requests are transmitted as point signals in a miscellaneous data paragraph. There are two types of check request: 'last check' and 'all check'. 'Last check' requires any miscellaneous data transmitted in the last 15 seconds to be repeated. 'Last check' requests are made automatically whenever a faulty word is received, or transmission is briefly interrupted or one of the computers fails to store a word correctly. 'All check' requests are made automatically on resumption of transmission after a failure of more than 10 seconds, and at any time manually to update or check indications.

10. Conclusion

The continually evolving control system of the National Grid owes much to the foresight of those who created the original Grid Control Centres and National Control Centre in the early 1930s—who introduced centralized display of on-line data from power stations and grid stations using normal grade communication links rented from the Post Office and who used such links to protect the power system.

The security of the control system is based on maximum route diversity of radial communication links reinforced by orbital links between stations and between control centres. Protection signalling is reinforced by duplicate links over separate routes, 1350 communication links are used for high speed protection of the power system.

The development of the control system has kept pace with the continually expanding power system and is well able to integrate with sophisticated aids to control, such as computer controlled c.r.t. display systems.

11. Acknowledgments

The author wishes to thank the Central Electricity Generating Board for permission to present the paper.

12. References

1. Peattie, J. D., 'Control rooms and control equipment of the Grid system', *J. Instn Elect. Engrs*, **81**, p. 607, November 1937.
2. Cooper, A. R., 'Load dispatching and the reasons for it, with special reference to the British Grid system', *J.I.E.E.*, **95**, Part II, p. 713, December 1948.
3. Gunning, P. F., 'Standardization of control facilities for the British Grid: communications, indications and telemetering', *Proc. I.E.E.*, **105A**, pp. 554–64, December 1958.
4. Pulsford, H. E. and Gunning, P. F., 'Developments in power system control', *Proc. I.E.E.*, **114**, pp. 1139–48, August 1967.
5. Kidd, W. and McWhirter, E. M. A., 'Operational control of electricity supply systems', *J.I.E.E.*, **92**, Part II, pp. 311–26, August 1945.
6. Gunning, P. F., 'Thirty Years of Grid Telemetering', International Telemetering Conference, London, 1963.
7. Dunn, R. H. and Chambers, C. H., 'Telemetering for system operation', *Proc. I.E.E.*, **100**, Part 1, p. 39, October 1952. (I.E.E. Paper No. 1400M.)
8. Burns, G. A., Fletcher, F., Chambers, C. H. and Gunning, P. F., 'The development of communication, indication and telemetering equipment for the British Grid', *Proc. I.E.E.*, **105A**, pp. 565–74, December 1958.

Manuscript received by the Institution on 23rd May 1968.
(Paper No. 1270/Com. 18.)

U.D.C. 512.83:621.372.542.2

The Recurrent-Continuant Method of Transfer Function Synthesis

By

JAMES G. HOLBROOK,
B.Sc., M.Sc., C.Eng., M.I.E.R.E.†

Summary: It is shown that the ratio of input voltage to output voltage for any passive ladder type low-pass filter network is always a polynomial in the complex frequency s. This polynomial can always be written by inspection as a single determinant in the form of a *recurrent*. The recurrent determinant is then converted by elementary manipulation into an alternate form known as a *continuant*. The transfer function of any passive ladder type low-pass filter network can also be written by inspection as a single determinant in continuant form. The synthesis of such networks is thus reduced to the simple procedure of writing the given transfer function in recurrent form by inspection, use of simple arithmetic operations to change the recurrent into continuant form, and reading the numerical values of the network elements directly from the continuant.

1. Introduction

A new network synthesis technique, called the *recurrent-continuant* method, is presented in this paper. One advantage of this new method is its extreme simplicity, since almost no formal training in network synthesis is required to understand the concept. The procedure is so direct that it bears no resemblance to any previous methods of which the writer is aware. Another advantage is the ease with which many network variations can be made to appear almost by inspection, each having a common transfer function. The method is perfectly suitable for solution by hand as well as by a computer program, since only elementary arithmetic operations are involved.

The discussion is limited to active and passive ladder networks, but this is not a very severe restriction, as almost all practical networks use the ladder form in one way or another. Only low-pass transfer functions are discussed, since the writer has shown elsewhere[1] that high-pass, band-pass, and band-rejection networks are only simple modifications of the low-pass prototype network.

2. The Network Continuant

The ladder network shown in Fig. 1 has all of its series elements given as impedances Z and all shunt elements labelled as admittances Y. Within the network, only currents through the impedances and voltages across the admittances are labelled. If one uses Kirchhoff's voltage and current laws alternately, starting at the input, the set of simultaneous equations (1) follows. We note that in this form, the variable in successive columns alternates between current and voltage.

$$\left.\begin{aligned} e_{in} &= Z_1 i_1 + e_2 + 0 + 0 \\ 0 &= -i_1 + Y_2 e_2 + i_3 + 0 \\ 0 &= 0 - e_2 + Z_3 i_3 + e_0 \\ 0 &= 0 + 0 - i_3 + Y_4 e_0 \end{aligned}\right\} \quad \ldots\ldots(1)$$

The set of equations (1) is solved by determinants in the usual way, so that e_0 becomes

$$e_0 = \frac{\begin{vmatrix} Z_1 & 1 & 0 & e_{in} \\ -1 & Y_2 & 1 & 0 \\ 0 & -1 & Z_3 & 0 \\ 0 & 0 & -1 & 0 \end{vmatrix}}{\begin{vmatrix} Z_1 & 1 & 0 & 0 \\ -1 & Y_2 & 1 & 0 \\ 0 & -1 & Z_3 & 1 \\ 0 & 0 & -1 & Y_4 \end{vmatrix}} \quad \ldots\ldots(2)$$

Since e_{in} is the only term in the last column, it is easy to expand the numerator by minors along the last column. The single co-factor of e_{in} is always -1, and therefore the entire numerator is always equal to e_{in} when the original equations are in the form of (1).

The voltage transfer function for Fig. 1 is normally written as e_0/e_{in}. However, in this paper we will use the reciprocal for convenience. Equation (2) then becomes

$$\frac{e_{in}}{e_0} = \begin{vmatrix} Z_1 & 1 & 0 & 0 \\ -1 & Y_2 & 1 & 0 \\ 0 & -1 & Z_3 & 1 \\ 0 & 0 & -1 & Y_4 \end{vmatrix} \quad \ldots\ldots(3)$$

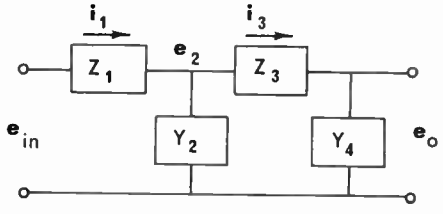

Fig. 1. Basic ladder network.

† Research Fellow, Department of Electronics, University of Southampton.

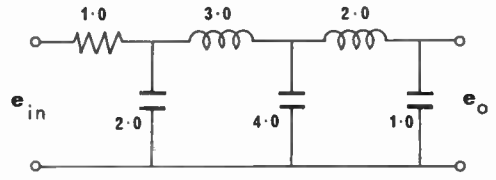

Fig. 2. Example ladder network.

It is easy to see that the ladder network of Fig. 1 can be extended to any length, and that the transfer ratio in (3) can be written by inspection, since the network impedances and admittances appear only in the main diagonal, and progress alternately from Z_1 to Y_n.

The determinant (3) is somewhat special, in that the variables occur only in the main diagonal. The lower adjacent diagonal consists only of -1 elements, while the upper adjacent diagonal is made up only of $+1$ elements. All other elements of the determinant are zeros. Determinants which have this special form are called *continuants*.

As an example to show the ease of obtaining the input-output voltage ratio by use of the continuant, we look at the network in Fig. 2 and write the continuant (4) by inspection. The values of the elements are in ohms, henrys, and farads.

$$\frac{e_{in}}{e_0} = \begin{vmatrix} 1 & 1 & 0 & 0 & 0 & 0 \\ -1 & 2s & 1 & 0 & 0 & 0 \\ 0 & -1 & 3s & 1 & 0 & 0 \\ 0 & 0 & -1 & 4s & 1 & 0 \\ 0 & 0 & 0 & -1 & 2s & 1 \\ 0 & 0 & 0 & 0 & -1 & s \end{vmatrix} \quad \text{.....(4)}$$

In the reverse situation, if the continuant (4) had been given, there would be no difficulty in drawing the network, and in writing in the numerical values for all the network elements directly from the main diagonal of the continuant. The continuant notation is not restricted to the low-pass case only, as (3) is completely general and applies to any linear, passive, ladder network.

For completeness, it is observed that the dual network corresponding to Fig. 1 and the set of equations (1) will have a shunt admittance as the first network element. Equations for the dual network will have exactly the same form as the set (1), except that all quantities are duals. The corresponding network continuant is shown in (5), although no use of this will be made in this paper.

$$\frac{i_{in}}{i_0} = \begin{vmatrix} Y_1 & 1 & 0 & 0 \\ -1 & Z_2 & 1 & 0 \\ 0 & -1 & Y_3 & 1 \\ 0 & 0 & -1 & Z_4 \end{vmatrix} \quad \text{.....(5)}$$

3. The Recurrent

We now leave the network and its continuant temporarily to examine the low-pass transfer polynomial. In any low-pass ladder network, the ratio e_{in}/e_0 will be a simple polynomial in s with constant coefficients. As a typical example, one might have the 5th-order low-pass network, where the polynomial is

$$\frac{e_{in}}{e_0} = a_5 s^5 + a_4 s^4 + a_3 s^3 + a_2 s^2 + a_1 s + 1 \quad \text{.....(6)}$$

It is known that the numerical coefficients of (6) will completely determine a set of values for the resistors, inductors and capacitors which make up the synthesized network. Further, it is known that the network is normally analysed by writing a set of equations which are usually solved by determinants as a ratio, and that the resulting voltage transfer function can even be written easily by inspection as a single special determinant called a continuant.

$$\frac{e_{in}}{e_0} = \begin{vmatrix} a_5 & a_4 & a_3 & a_2 & a_1 & a_0 \\ -1 & s & 0 & 0 & 0 & 0 \\ 0 & -1 & s & 0 & 0 & 0 \\ 0 & 0 & -1 & s & 0 & 0 \\ 0 & 0 & 0 & -1 & s & 0 \\ 0 & 0 & 0 & 0 & -1 & s \end{vmatrix} \quad \text{.....(7)}$$

A polynomial such as (6) can always be written in the determinant form shown in (7). One can write this determinant by inspection by remembering that the coefficients of the given polynomial make up the first row, the main diagonal (except for the first element) consists of the polynomial variable s, the lower adjacent diagonal is made up entirely of -1 elements, and all other elements are zero. This special form of determinant is called a *recurrent*. It will be seen by inspection that the recurrent can easily be extended to represent a polynomial of any order. The term a_0 normally equals unity.

4. Recurrent to Continuant Conversion

The key step in this method of network synthesis lies in changing the recurrent determinant, which represents the given transfer polynomial, into the continuant determinant which represents the physical network. The conversion process requires only elementary arithmetic operations on the determinant, and once the technique is learned is much easier to perform than to describe. The following procedure appears to require the least number of non-redundant steps.

To illustrate the method, we will use the 5th-order polynomial in (6), whose recurrent is given in (7). It

will be clear from what follows, however, that the procedure is applicable to recurrents of any order.

We begin by observing that if we divide the first column by a_5, and then multiply the second row by a_5, the determinant remains unchanged in value. When this has been done, the second column is divided by a_4 and the third row is multiplied by a_4. Although the elements have been rearranged, the determinant remains unchanged by this operation on columns and rows. The steps thus far have reduced the first two elements in the first row to unity, and new elements begin to appear elsewhere. As new elements appear, new letters will be assigned for the numerical coefficients, and double subscripts will indicate the row and column. At this point, the determinant has the form

$$\frac{e_{in}}{e_0} = \begin{vmatrix} 1 & 1 & a_3 & a_2 & a_1 & a_0 \\ -1 & b_{22}s & 0 & 0 & 0 & 0 \\ 0 & -1 & b_{33}s & 0 & 0 & 0 \\ 0 & 0 & -1 & s & 0 & 0 \\ 0 & 0 & 0 & -1 & s & 0 \\ 0 & 0 & 0 & 0 & -1 & s \end{vmatrix} \quad \ldots\ldots (8)$$

All remaining a elements in the first row are now reduced to zero as follows:

Multiply column one by $-a_3$, add to column three.

Multiply column one by $-a_1$, add to column five.

Continue with column one in this way until all *odd* columns have zeros for the first row elements.

Multiply column two by $-a_2$, add to column four.

Multiply column two by $-a_0$, add to column six.

Continue using column two in this manner until all *even* columns remaining have zeros for the first row elements. We now have the form

$$\frac{e_{in}}{e_0} = \begin{vmatrix} 1 & 1 & 0 & 0 & 0 & 0 \\ -1 & b_{22}s & b_{23} & b_{24}s & b_{25} & b_{26}s \\ 0 & -1 & b_{33}s & b_{34} & 0 & b_{36} \\ 0 & 0 & -1 & s & 0 & 0 \\ 0 & 0 & 0 & -1 & s & 0 \\ 0 & 0 & 0 & 0 & -1 & s \end{vmatrix} \quad \ldots\ldots (9)$$

The unwanted elements $b_{24}s$, $b_{26}s$, are cleared from the second row for the fourth and all higher *even* columns.

Multiply row four by $-b_{24}$, add to row two.

Multiply row six by $-b_{26}$, add to row two.

For higher order determinants, continue these steps with *even* order rows until all s terms except $b_{22}s$ in the second row are zero. The determinant now appears as

$$\frac{e_{in}}{e_0} = \begin{vmatrix} 1 & 1 & 0 & 0 & 0 & 0 \\ -1 & b_{22}s & c_{23} & 0 & c_{25} & 0 \\ 0 & -1 & b_{33}s & b_{34} & 0 & b_{36} \\ 0 & 0 & -1 & s & 0 & 0 \\ 0 & 0 & 0 & -1 & s & 0 \\ 0 & 0 & 0 & 0 & -1 & s \end{vmatrix} \quad \ldots\ldots (10)$$

The remaining unwanted terms in the second row are now reduced to zero in the fifth and all higher *odd* columns. In this example only c_{25} remains.

Multiply column three by $-c_{25}/c_{23}$, add to column five.

Use column three until all *odd* columns from column five onward have zeros for the second row elements. The determinant now takes the form

$$\frac{e_{in}}{e_0} = \begin{vmatrix} 1 & 1 & 0 & 0 & 0 & 0 \\ -1 & b_{22}s & c_{23} & 0 & 0 & 0 \\ 0 & -1 & b_{33}s & b_{34} & c_{35}s & b_{36} \\ 0 & 0 & -1 & s & c_{45} & 0 \\ 0 & 0 & 0 & -1 & s & 0 \\ 0 & 0 & 0 & 0 & -1 & s \end{vmatrix} \quad \ldots\ldots (11)$$

The remaining steps repeat the previous plan, and must be done in the exact indicated order.

Multiply row five by $-c_{35}$, add to row three.

Continue until all *odd* columns from column five onward have zeros for the third row elements.

Column four is multiplied by $-b_{36}/c_{34}$, and added to column six. Third row elements in all *even* columns from six and higher are reduced to zero in this sequence.

Finally, in the present example, row six is multiplied by the proper constant and added to row four. The last three steps have not been illustrated to conserve space. It should be clear however, that the determinant now has the form

$$\frac{e_{in}}{e_0} = \begin{vmatrix} 1 & 1 & 0 & 0 & 0 & 0 \\ -1 & b_{22}s & c_{23} & 0 & 0 & 0 \\ 0 & -1 & b_{33}s & c_{34} & 0 & 0 \\ 0 & 0 & -1 & s & d_{45} & 0 \\ 0 & 0 & 0 & -1 & s & b_{56} \\ 0 & 0 & 0 & 0 & -1 & s \end{vmatrix} \quad \ldots\ldots (12)$$

We see that (12) now has the form of the *continuant*, except that the upper adjacent diagonal does not consist of the required +1 elements. The upper diagonal elements can all be reduced to unity by the remaining almost trivial steps.

Divide row five by b_{56}, multiply column four by b_{56}.

Divide row four by d_{45}, multiply column three by d_{45}.

Divide row three by d_{34}, multiply column two by d_{34}.

Divide row two by d_{23}, multiply column one by d_{23}.

When this is done, we can return to a single subscript notation and show the final continuant as

$$\frac{e_{in}}{e_0} = \begin{vmatrix} b_1 & 1 & 0 & 0 & 0 & 0 \\ -1 & b_2 s & 1 & 0 & 0 & 0 \\ 0 & -1 & b_3 s & 1 & 0 & 0 \\ 0 & 0 & -1 & b_4 s & 1 & 0 \\ 0 & 0 & 0 & -1 & b_5 s & 1 \\ 0 & 0 & 0 & 0 & -1 & s \end{vmatrix} \quad \ldots\ldots(13)$$

Equation (13) displays the resistor, inductor, and capacitor values directly, as is evident by comparison with (4) and Fig. 2.

The space required to explain the recurrent to continuant conversion process is greater than needed to actually do the job once the technique has been established. To be certain that the complexity of the explanation does not mask the extreme simplicity of the process, we will synthesize one polynomial as a brief numerical illustration.

5. The 3rd-order Polynomial

Let us choose the 3rd-order maximally-flat, or *Butterworth* function as an example that is just complex enough not to be trivial, and yet adequate to illustrate the new synthesis method clearly. The polynomial is given as

$$\frac{e_{in}}{e_0} = s^3 + 2s^2 + 2s + 1 \quad \ldots\ldots(14)$$

We write the recurrent immediately by inspection as

$$\frac{e_{in}}{e_0} = \begin{vmatrix} 1 & 2 & 2 & 1 \\ -1 & s & 0 & 0 \\ 0 & -1 & s & 0 \\ 0 & 0 & -1 & s \end{vmatrix} \quad \ldots\ldots(15)$$

Following the steps given in Section 4, since a_{11} is already unity, divide column two by 2, and then multiply row three by 2. This gives

$$\frac{e_{in}}{e_0} = \begin{vmatrix} 1 & 1 & 2 & 1 \\ -1 & \frac{1}{2}s & 0 & 0 \\ 0 & -1 & 2s & 0 \\ 0 & 0 & -1 & s \end{vmatrix} \quad \ldots\ldots(16)$$

Multiply column one by -2, add to column three.

Multiply column two by -1, add to column four.

$$\frac{e_{in}}{e_0} = \begin{vmatrix} 1 & 1 & 0 & 0 \\ -1 & \frac{1}{2}s & 2 & -\frac{1}{2}s \\ 0 & -1 & 2s & 1 \\ 0 & 0 & -1 & s \end{vmatrix} \quad \ldots\ldots(17)$$

Multiply row four by $\frac{1}{2}$, add to row two.

$$\frac{e_{in}}{e_0} = \begin{vmatrix} 1 & 1 & 0 & 0 \\ -1 & \frac{1}{2}s & \frac{3}{2} & 0 \\ 0 & -1 & 2s & 1 \\ 0 & 0 & -1 & s \end{vmatrix} \quad \ldots\ldots(18)$$

Convert the upper adjacent diagonal to unity values by dividing row two by 3/2 and multiplying column one by 3/2.

$$\frac{e_{in}}{e_0} = \begin{vmatrix} \frac{3}{2} & 1 & 0 & 0 \\ -1 & \frac{1}{3}s & 1 & 0 \\ 0 & -1 & 2s & 1 \\ 0 & 0 & -1 & s \end{vmatrix} \quad \ldots\ldots(19)$$

The continuant (19) shows the network element values explicitly and the network is shown in Fig. 3. The polynomial has been synthesized directly, using the determinant as the connecting link between the polynomial coefficients and the network element values.

6. Synthesis of Even-order Polynomials

If the given polynomial is *even*-order, there is one minor point which should be mentioned. It can be clarified by looking at the simple 2nd-order polynomial

$$\frac{e_{in}}{e_0} = s^2 + \sqrt{2}s + 1 \quad \ldots\ldots(20)$$

By inspection, the recurrent is

$$\frac{e_{in}}{e_0} = \begin{vmatrix} 1 & \sqrt{2} & 1 \\ -1 & s & 0 \\ 0 & -1 & s \end{vmatrix} \quad \ldots\ldots(21)$$

Multiply column one by -1, add to column three. Then divide column two by $\sqrt{2}$ and multiply row three by $\sqrt{2}$. The resulting continuant is

$$\frac{e_{in}}{e_0} = \begin{vmatrix} 1 & 1 & 0 \\ -1 & \frac{1}{\sqrt{2}}s & 1 \\ 0 & -1 & \sqrt{2}s \end{vmatrix} \quad \ldots\ldots(22)$$

Now before trying to draw the corresponding network, we observe that any *odd*-order continuant such as this one should be simplified by one order by simply adding row one to row two. That is,

$$\frac{e_{in}}{e_0} = \begin{vmatrix} (1+\frac{1}{\sqrt{2}}s) & 1 \\ -1 & \sqrt{2}s \end{vmatrix} \quad \ldots\ldots(23)$$

The element a_{11} is the first series impedance, which in this simple case is the sum of a 1 Ω resistor and 0·707 H inductor. The element a_{22} is the shunt admittance, a 1·414 F capacitor.

7. Alternate Networks from the Continuant

One of the advantages of the recurrent-continuant synthesis method is that the continuant itself may be converted easily into several forms, each form representing a different network configuration. A complete discussion of this topic is well outside the scope of this paper. We shall choose only one example therefore, which has already been partially

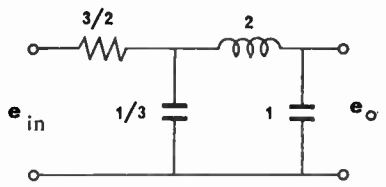

Fig. 3. First-form network derived from basic continuant.

worked, to show the variety of network forms which may be extracted from the basic continuant. The polynomial (14) has already been shown in continuant form (19), and Fig. 3 shows what may be called the *first form* of this network.

The writer is not aware of its previous use in any reference work, but it is easy to prove by elementary determinant manipulations that the following rule is completely general for any continuant:

> *The main diagonal of any continuant can always be reversed end-for-end without altering the value of the continuant.*

When this rule is applied to (19), the continuant takes the form

$$\frac{e_{in}}{e_0} = \begin{vmatrix} s & 1 & 0 & 0 \\ -1 & 2s & 1 & 0 \\ 0 & -1 & \frac{1}{3}s & 1 \\ 0 & 0 & -1 & \frac{3}{2} \end{vmatrix} \qquad \text{.....(24)}$$

The *second form* of the network is shown in Fig. 4(a).

The above rule is easily developed. Exchange first and last columns, then exchange second and penultimate columns, etc. When all columns have been exchanged in this manner, perform the same operations on rows. It will be observed that the -1 elements move from the lower to the upper adjacent diagonal as a result of these exchanges, but this does not affect the value of the continuant. In fact, the signs of the adjacent diagonals may be reversed at any time by merely dividing all *odd* rows by -1 and then multiplying all *odd* columns by -1.

Starting again with the original continuant (19), two new networks are revealed by the following steps: Exchange row one with row two, row three with row four, then exchange column one with column two, and column three with column four. When this has been done, it is seen that the $\frac{3}{2}\,\Omega$ resistive element has moved along the main diagonal from position a_{11} to the new position a_{22}.

Unfortunately, in this exchange scheme some of the adjacent diagonal elements are scattered, and it is usually not possible to return them to their normal places by inspection alone. It requires only a small amount of manipulation to reform the continuant however, which is

$$\frac{e_{in}}{e_0} = \begin{vmatrix} s & 1 & 0 & 0 \\ -1 & 2 & 1 & 0 \\ 0 & -1 & \frac{1}{3}s & 1 \\ 0 & 0 & -1 & \frac{3}{2}s \end{vmatrix} \qquad \text{.....(25)}$$

Equation (25) can easily be checked by direct expansion and comparison with (14). One must take care to distinguish reciprocal ohms (siemens) from ohms. The *third form* of the network is shown in Fig. 4(b).

No additional effort is required to find the *fourth form* of the network, as the main diagonal in (25) can be reversed end for end by inspection to give the final network shown in Fig. 4(c), which ends this example.

A closing observation about recurrents should perhaps make the point that the s elements along the main diagonal such as in (7) can always be separated by inserting dummy rows and columns which are made up entirely of zeros, except that a $+1$ is used at the intersection of the dummy row and column. This operation can be applied any number of times to any recurrent without changing its value, since it is equivalent to multiplying the recurrent by unity. With the s elements separated by the $+1$ elements, it is clear that the resulting continuant will require only *one*, rather than two reactance types. Polynomials such as

$$\frac{e_{in}}{e_0} = s^3 + 5s^2 + 6s + 1 \qquad \text{.....(26)}$$

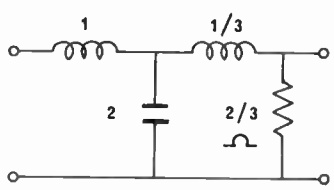

(a) Second-form network.

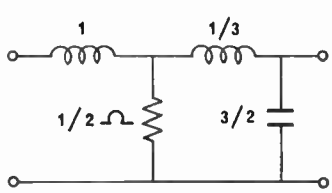

(b) Third-form network.

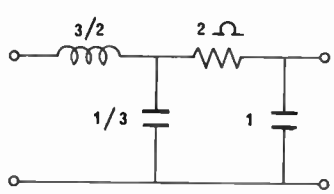

(c) Fourth-form network.

Fig. 4.

which have only negative real roots, can be synthesized by the recurrent-to-continuant process to have any of the n forms contained in the normal $n \times n$ continuant; or alternately, the s elements in the basic recurrent can be separated so that only a single reactance network continuant results. If (26) is synthesized in this way, the continuant is

$$\frac{e_{in}}{e_0} = \begin{vmatrix} 1 & 1 & 0 & 0 & 0 & 0 \\ -1 & s & 1 & 0 & 0 & 0 \\ 0 & -1 & 1 & 1 & 0 & 0 \\ 0 & 0 & -1 & s & 1 & 0 \\ 0 & 0 & 0 & -1 & 1 & 1 \\ 0 & 0 & 0 & 0 & -1 & s \end{vmatrix} \quad \text{.....(27)}$$

which results in the three-equal-section RC network that was popular in RC oscillators *circa* 1940. Needless to say, if the given polynomial has any complex roots, some of the main diagonal elements in this type of continuant will be negative, so unless prepared to use negative impedance converters, one must go back to the normal continuant for the general case.

8. Active Continuants

Many practical ladder networks use voltage feedback from the output to some or all of the internal admittance elements. Figure 5 shows a dependent voltage generator for each admittance. The amplifiers are assumed to have zero output impedance, and to have individually adjustable gains A_2, A_4, etc. This arrangement is particularly useful for generating high-order polynomials when using only resistance for Z and capacitance for Y, especially at frequencies well below 1 Hz.[2]

Analysis of Fig. 5 by conventional methods is easy enough, but could hardly be done 'by inspection'. It seems worthwhile, therefore, to extend the idea of the continuant to include the active ladder network, so that the transfer polynomial can be written by inspection.

If the Kirchhoff equations for Fig. 5 are written in mixed form as in the beginning of Section 2, the equations will be exactly the same as the set (1), except that all equations which contain the admittance Y_n will also have the term $-A_n Y_n e_0$ added at the end. This fact can be used as the basis for the following simple rule for writing the continuant of Fig. 5 by inspection:

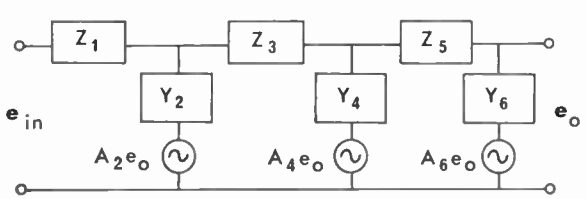

Fig. 5. Practical ladder network containing dependent voltage generators.

First, assume that the gain of each amplifier is zero, and write the normal continuant by inspection. The result will be the same as (3), but extended to include Z_5 and Y_6. Thus far nothing is new.

Second, in each *even* row, where Y_n appears, add the term $-A_n Y_n$ at the intersection of that row and the *last* column.

$$\frac{e_{in}}{e_0} = \begin{vmatrix} Z_1 & 1 & 0 & 0 & 0 & 0 \\ -1 & Y_2 & 1 & 0 & 0 & -A_2 Y_2 \\ 0 & -1 & Z_3 & 1 & 0 & 0 \\ 0 & 0 & -1 & Y_4 & 1 & -A_4 Y_4 \\ 0 & 0 & 0 & -1 & Z_5 & 1 \\ 0 & 0 & 0 & 0 & -1 & Y_6(1-A_6) \end{vmatrix} \quad \text{.....(28)}$$

Using this rule, the continuant for this type of active ladder network is written easily by inspection. If not all of the generators are present, the intersection of the corresponding row with the last column merely remains zero, as in the passive case.

The two most obvious uses for the active continuant are for quickly writing the polynomial of a given network, and for synthesis starting from the single-reactance type recurrent discussed previously. It will be obvious by now that whenever such a recurrent can be manipulated into the form of (28), then it is a simple matter to draw the network and feedback arrangement required for the synthesis.

9. Conclusions

A new approach to network synthesis has been developed, which links the coefficients of a given transfer polynomial directly to the network element values by means of the special recurrent-continuant determinant transformation. Several interesting properties of the continuant[3] have been discussed, and examples have shown ways of extracting a variety of network forms from one original continuant. A simple rule has been given for writing the continuant of active ladder networks by inspection. It is hoped that this paper may prove useful to others who are interested in this subject.

10. Acknowledgments

The writer is from California, living in England temporarily. He would like to thank Professor W. A. Gambling and Dr. T. H. Wilmshurst of the University of Southampton for their careful checking of the manuscript both for technical accuracy and for readability.

11. References and Bibliography

1. Holbrook, James G., 'Laplace Transforms for Electronic Engineers', 2nd edn. (Pergamon, New York and London, 1966).

2. Bloodworth, G. G. and Nesbitt, N. R. S., 'Active filters operating below 1 Hz', *Trans. Inst. Elect. Electronics Engrs on Instrumentation and Measurement*, **IM-16**, pp. 115–20, June 1967.
3. Storch, Leo, 'Continuants—a superior tool in the analysis of ladder networks', *Trans. Inst. Elect. Electronics Engrs on Circuit Theory*, **CT-12**, No. 3, pp. 444–6, September 1965.
4. Weinberg, Louis, 'Network Analysis and Synthesis', (McGraw-Hill, New York, 1962). Excellent textbook and reference on passive synthesis techniques.
5. Ghausi, M. S., 'Principles and Design of Linear Active Circuits', (McGraw-Hill, New York, 1965). An excellent text and reference work on active synthesis.

Manuscript first received by the Institution on 3rd January 1969 and in final form on 5th March 1969. (Paper No. 1271/CC52.)

Contributors to this Issue

A. C. Ferguson is a graduate of the University of Strathclyde. He is at present manager of research and development with W. & T. Avery Ltd., whom he joined in 1962; his work is concerned with weighing and materials testing. After obtaining his degree he served a graduate apprenticeship with The General Electric Company. Between 1958 and 1963 he was employed by Rank Pullin Controls as a systems engineer responsible for the development of telemetry systems for use in oil refineries.

S. C. Majumdar received his B.Sc. degree in physics from Calcutta University in 1957 and his M.Sc.(Tech.) in Radio Physics and Electronics from the same University in 1960. He joined the Saha Institute of Nuclear Physics, Calcutta, in 1961 as a Research Assistant and worked on transport phenomena in semiconductors for about a year, during which period he published two papers. In 1962 Mr. Majumdar joined the Civil Aviation Department and is now a Senior Technical Officer, working as engineer-in-charge of flight inspection of a variety of radio navigation aids. Since 1964 he has been engaged in research on tropospheric propagation beyond radio horizon and has already published five papers on this subject. One of these gained him an award from the Institution of Telecommunication Engineers (India).

Other Recent Contributors

Prof. Marc C. Vanwormhoudt graduated at the University of Ghent in 1955 with a degree in electronics engineering. He received his M.Sc. and Ph.D. degrees in 1956 and 1961 from the Massachusetts Institute of Technology. He was in succession assistant and associate professor at the University of Ghent and was appointed to a chair in 1967. Professor Vanwormhoudt's prime interest is statistical communication theory and noise.

Daniël H. J. Baert received his engineering diploma in electronics engineering in 1963 at the State University of Ghent. He is at present an assistant in the Laboratory of Electronics and Metrology of the University and is mainly concerned with the investigation of radio frequency interference caused by h.f. furnaces and the development of thyristor r.f. interference filters.

The joint paper by Professor Vanwormhoudt and Mr. Baert on 'Frequency-dependence of a Balun Evaluated by a Frequency Transformation' was published in the July issue.

Joint Conference on 'Industrial Ultrasonics'

Organized by The Institution of Electronic and Radio Engineers
with the association of
The Institution of Electrical Engineers (Electronics Division), The Institute of Physics and The Physical Society, The Institute of Electrical and Electronics Engineers (United Kingdom and Republic of Ireland Section), The British Acoustical Society, and The Non-Destructive Testing Society of Great Britain.

University of Technology, Loughborough—23rd to 25th September 1969

PROVISIONAL PROGRAMME

Tuesday, 23rd September. 10.30 a.m. to 12.30 p.m.

Opening by MAJOR GENERAL SIR LEONARD ATKINSON, K.B.E., *President of the I.E.R.E.*

Session on 'HIGH POWER APPLICATIONS'

Chairman: W. V. RICHINGS

'High Power Ultrasonics in Industry—a Review,' A. E. CRAWFORD, *Radyne Limited.*

'High Power Ultrasonic Equipment for Assembling Rigid Thermoplastic Components,' R. D. STAFFORD, *Dawe Instruments Limited.*

'Ultrasonic Textile Thread Welder,' A. E. CRAWFORD, *Radyne Limited.*

'The Ultrasonic Atomizer—Its Development and Applications,' C. H. BRADBURY and D. S. WILLMER, *Simms Group Research and Development Limited.*

2 p.m. to 5.30 p.m.

Session on 'ANALYSIS OF PROPERTIES OF MATERIALS'

Chairman: PROFESSOR L. KAY

'Measurement of Grain Size Using Ultrasonics,' E. E. ALDRIDGE, *Atomic Energy Research Establishment, Harwell.*

'Statistical Treatment of Ultrasonic Scatter Signals,' H. G. TATTERSALL, *Non-Destructive Testing Centre, Harwell.*

'High Resolution Ultrasonic Testing,' J. SZILARD and G. SCRUTON, *University of Technology, Loughborough.*

'Measurements on Austenitic Steels,' MRS. R. M. MURRAY and J. D. LAVENDER, *Steel Castings Research Association.*

'The Measurement of the Elasticity and Ultrasonic Wave Velocities in Steel,' E. H. F. DATE, M. ATKINS and G. V. BEATON, *British Steel Corporation.*

'Ultrasonic Detection of Gas Bubbles in Liquids,' V. G. WELSBY, *University of Birmingham.*

Wednesday, 24th September. 9 a.m. to 12.30 p.m.: 2 p.m. to 3 p.m.

Session on 'NON-DESTRUCTIVE TESTING'

Chairman: P. D. HANSTEAD

'Application of a Phased Array to Ultrasonic Flaw Detection in Tubes,' K. R. WHITTINGTON and B. D. COX, *Tube Investments Research Laboratories.*

'The Ultrasonic Reflection from Small Surface Cracks and the Problems Associated with Reference Defects when Examining Tubes and Bars,' R. FRIELINGHAUS, J. KRAUTKRAMER and U. SCHLENGERMANN, *Dr. J. u. H. Krautkramer gesellschaft fur Elektrophysik, Cologne.*

'A High Speed Ultrasonic Testing Machine,' G. KYTE and K. R. WHITTINGTON, *Tube Investments Research Laboratories.*

'The Ultrasonic Examination of Marine Boiler Tubes *in situ*,' C. J. HOLMAN, *D.G. Ships, Ministry of Defence.*

'Ultrasonic Evaluation of Tube Wastage in Marine Boilers,' B. F. PETERS, J. A. O'MALIA and B. W. GREENWOOD, *Defence Research Board, Canada.*

Joint Conference on 'Industrial Ultrasonics'—continued

'Finding Defects in Rubber or Plastic Behind a Metal Plate,' F. LAM and DR. J. SZILARD, *University of Technology, Loughborough.*

'Development of Inspection Systems for Fast Reactors,' J. R. FOTHERGILL and I. D. MACLEOD, *U.K.A.E.A. Reactor Engineering Laboratory.*

3.30 p.m. to 5.30 p.m.

Session on 'TRANSDUCERS'

Chairman: A. E. CRAWFORD

'The Behaviour of Magnetostrictive Transducers Prepared for Commercial Use,' A. GRANGE, *Ultrasonics Limited* and B. BROWN, *University of Salford.*

'A Computer Program for the Analysis of the Circle Diagram of an Ultrasonic Transducer,' D. G. J. FANSHAWE, *Mullard Research Laboratories.*

'The Development of Transducers for Metal Working Processes,' A. GRANGE, *Ultrasonics Limited.*

'An Acoustic Bulk-Surface-Wave Transducer,' R. F. HUMPHRYES, *University College London.*

Thursday, 25th September. 9 a.m. to 12.30 p.m.

Session on 'IMAGING'

Chairman: PROFESSOR J. W. R. GRIFFITHS

'A Different Approach to Ultrasonic Holography', P. C. CALVERT, *University of Technology, Loughborough.*

'Progress in Ultrasonic Holography at Harwell,' E. E. ALDRIDGE, A. B. CLARE and D. A. SHEPHERD, *Atomic Energy Research Establishment.*

'The Visualization of Ultrasound in Solids,' J. H. GUNTON and D. M. MARCH, *Tube Investments Research Laboratories.*

'Ultrasonic Imaging in Solids,' PROFESSOR L. KAY, *University of Canterbury, New Zealand.*

'Developments in Real-Time Ultrasonic Imaging by Bragg Diffraction,' C. WADE, J. LANDRY and J. POWERS, *University of California.*

'Electronic Scanning of Ultrasonic Beams,' S. GERGELY, *Lanchester College of Technology.*

2 p.m. to 5 p.m.

Session on 'INSTRUMENTS'

Chairman: J. BLITZ

'Absolute Ultrasonic Intensity Measurements at Megahertz Frequencies,' J. BLITZ, *Brunel University.*

'Ultrasonic Position Sensing for Automatic Control,' PROFESSOR L. KAY, *University of Canterbury, New Zealand.*

'Two-phase Flow Profile Information by Analysis of Sound Reflected from Moving Interfaces,' T. E. EVANS, *University of Sussex.*

'An Ultrasonic Position Plotter for Ship Models,' D. V. BLAKE, M. D. W. COLLARD and W. WILSON, *National Physical Laboratory, Teddington.*

'Use of Ultrasonics in Electrical Fault Detection,' R. N. BASU, *Vanguard Services, Stuttgart, Germany.*

The cost of the conference to members of the sponsoring bodies is £21 (non-members £24). This charge includes the preprint volume, accommodation, all meals and the Conference Reception and Dinner.

Registration forms are now available from the Conference Registrar, The Institution of Electronic and Radio Engineers, 9 Bedford Square, London, W.C.1 (Telephone 01-580 8443, ext. 3). An application form will be found at the end of this issue of the Journal.

U.D.C. 519.2:621.396.677

Pseudo-random Selection of Elements in a Multi-element Array

By

G. B. COOK, B.E.(Hons.)†

AND

D. A. H. JOHNSON, M.Sc., M.N.Z.I.E., C.Eng., M.I.E.E.‡

Presented at the Second New Zealand Electronics Convention (NELCON II) organized by the New Zealand Section of the Institution and the New Zealand Electronics Institute and held in Auckland in August 1968.

Summary: Simple random number generators using integrated circuit shift registers are being employed to make random selections of points on multi-element (12 000 array points) ultrasonic planar transducers.

The transducer is a 2-in (5·1 cm) diameter piezoelectric plate used to detect the scattered acoustic field caused by an object placed in an ultrasonic field. The transducer is digitally scanned to enable information from discrete points to be encoded for image reconstruction by computer processing. For unambiguous reconstruction, point spacing of one half-wavelength is required. This would require 12 000 sample points, and processing this information would be unwieldy. Removing the points randomly according to a specific density distribution enables up to 95% of the points to be removed with little deterioration in transducer performance.

Computer simulations of the thinned array have been completed and these confirm that the transducer directivity patterns are satisfactory in the far-field and focused near-field.

1. Ultrasonic Image Convertors

The use of ultrasonic radiation to study the interior of visually-opaque objects is well established. The acoustic field distribution may be recorded by the use of single or multiple transducers. The transducer may be small (only a few wavelengths in diameter) and scanned mechanically over an aperture viewing the region of interest, or large and scanned electronically.

The sensitivity of 'small' transducers increases with their size. However, the physical size of the transducer limits the minimum usable wavelength to a value comparable to its own dimensions, as unambiguous field reconstruction requires independent samples to be taken at half-wavelength intervals.

A 'large' transducer, many wavelengths in diameter, was first proposed by Sokolov.[1] It employs a thin slab of piezo-electric material, which when subjected to an acoustic field incident on one of its large faces, responds with a voltage distribution proportional to the instantaneous value of the field at that point. This electrical reproduction of the acoustic field may be read off by scanning the piezoelectric plate in a manner similar to that of a television camera-tube. The ultimate fineness of aperture sampling is now limited only by the focus of the electron beam. Most acoustic-electrical tubes[2] use the transducer plate as part of the vacuum envelope for the electron beam. This imposes a large static stress on the plate. Progressively thinner plates are required at higher frequencies,[3] thus restricting the ratio of aperture size to wavelength and hence the image resolution available.

A majority of conventional ultrasonic imaging systems use shadow casting techniques as the applications of practical acoustic lenses are limited. We are actively engaged in the application of a digital computer to the problem of signal processing the data recorded from the conversion tube. Optical reconstruction has been considered but the inherent limitations of wavelength disparity[4] and alignment problems in the optical processors[5] make this technique seem impractical.

2. Aperture Sampling

Ultimate resolution requires that the sample points be at half-wavelength spacing or less (in steel, the wavelength is 1·22 mm at 5 MHz). Over 12 000 points are involved on a 2-inch (5·1 cm) diameter aperture transducer, and if all these points were sampled the handling of the data would be a mammoth task. Fortunately, substantial reduction in the number of points sampled can be made with little loss in resolution, and without creating secondary principal

† Formerly at the Department of Electrical Engineering, University of Canterbury, Christchurch, New Zealand; now with the New Zealand Post Office, E-in-C's Office (Radio Section), Wellington.

‡ Formerly at the Department of Electrical Engineering, University of Canterbury, New Zealand; now at the University of Melbourne.

maxima. This technique[6] involves selection of points with random spacing but with a prescribed density function, usually one which tapers from the centre to the edge of the aperture. It is related to methods of approximating an amplitude taper in multi-element antenna arrays with equally-excited elements. This technique enables desirable radiation patterns (e.g. narrow beamwidth and low side-lobes) to be obtained without an amplitude taper across the aperture, and with a reduced number of elements.[7-11]

The method we are employing is similar to that of Skolnik[6] in that the selection of points is performed statistically by using a model amplitude taper as the probability density function for specifying the location of elements. At each array point, a distance r from the aperture centre, the magnitude of the model amplitude taper $A(r)$ is computed and normalized such that maximum $A(r) = 1$. This is modified by a factor k and then compared to a random number N in the range 0 to 1. The array point is sampled only if

$$kA(r) \geqslant N, \quad 0 \leqslant k \leqslant 1 \qquad \ldots\ldots(1)$$

The value of k controls the number of elements remaining in the thinned array (a 'thinned' array is one that contains fewer elements than a 'filled' array of equally-spaced elements at half-wavelength intervals). The statistical properties of the array are controlled by the random numbers represented by N.

The individual sample points are assumed to be located only at the intersections of a square grid with a spacing of a half-wavelength. These sample points may be scanned with an electron beam by applying a step voltage to the deflection plates of the acoustic-electrical tube. The density tapering of the array points should be carried out before any information is recorded so as to reduce the storage of data. The sample points may be selected during a scan of the transducer and the decision of whether or not to sample an array point can be made whilst the scanning beam is resting on that point. Thus, the decision to sample, or not to sample, can be made by generating analogue voltages proportional to $kA(r)$ and N, and determining with a comparator when $kA(r) \geqslant N$ (Fig. 1).

The geometry of the array is shown in Fig. 2. At each array point voltages $V(x)$ and $V(y)$, proportional to the x and y co-ordinates respectively, are generated.

3. Amplitude Taper Generator

The choice of a suitable amplitude taper on which to model the density taper requires some consideration. Previous work[6-9] on the density tapering of multi-element antenna arrays has shown that the near-in side-lobes are determined by the model taper, whilst the side-lobes in the region removed from the main beam are determined by the statistical removal of the elements. But for extreme thinning (about 90% of the elements removed) the near-in side-lobe level is also determined more by the statistical removal of the elements than by the model taper. Thus, for extreme thinning, a model taper can be chosen more for ease of generation than for optimization of side-lobe level and beamwidth.

The model taper chosen is of the form

$$A(r) = 1 - 0{\cdot}8r, \quad 0 \leqslant r \leqslant 1$$

where r is the distance of a point from the aperture centre. This function takes the form of a cone-on-a-pedestal.

The analogue function generator consists of a passive section[12] to form $V(r) = (V(x)^2 + V(y)^2)^{\frac{1}{2}}$ and an operational amplifier to modify the function to be in the form

$$kA(r) = k(1 - 0{\cdot}8V(r)).$$

$V(r)$ is a voltage proportional to r.

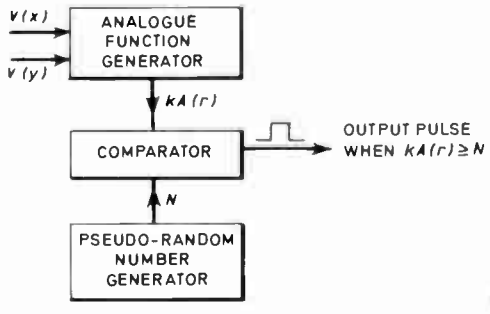

Fig. 1. Schematic of pseudo-random aperture sampling.

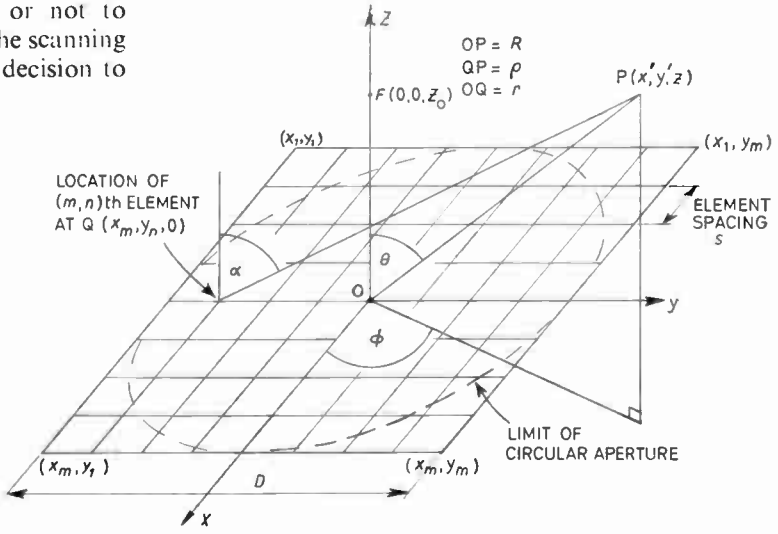

Fig. 2. Geometry of an $M \times M$ element array.

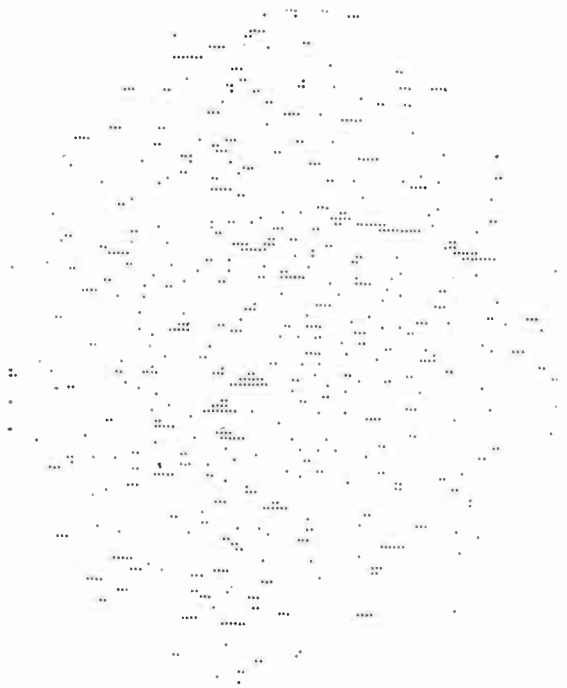

Fig. 3. Location of the elements for 94% thinning. A 15-stage feedback shift register with decoding from 6 adjacent stages is used to generate the random numbers.

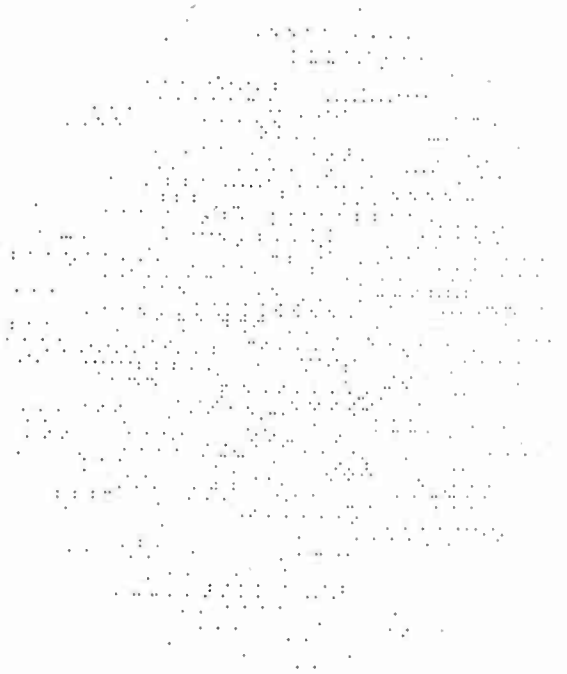

Fig. 4. Location of the elements for 94% thinning. A 20-stage feedback shift register and 6 stage decode with inputs from every fourth stage is used to generate the random numbers.

4. Random Number Generator

The random numbers are generated by an n-stage feedback shift register connected to generate a maximum length sequence (a pseudo-random sequence). The maximum length sequence consists of all the combinations of '1's and '0's in the n-stages of the shift register (with the exception of the all '0's state). The sequence length is thus $L = 2^n - 1$. The binary weighted sum of m of the shift register stages is a set of virtually random numbers occurring with equal probability,[13] and lying in the range 0 and $2^m - 1$. The set is repeated after L cycles.

An alternative method of generating random numbers involves polarity sampling of n independent noise generators. This method, while producing absolutely random numbers without any periodicity, is considerably more difficult to instrument.

The pseudo-random sequence generator was chosen because of the ease of construction. By choosing a sequence of length somewhat greater than the number of sample points, no difficulty arises due to the periodicity. Moreover, the numbers are deterministic and the designer is free to specify whether the same set of sample points be selected over successive scans, or whether independent random selections be made.

As a result of computer simulations it was found that a 20-stage feedback shift register with a 6-stage digital-to-analogue decoder with inputs from every fourth stage proved satisfactory. Various combinations of shift register length and decode matrix were simulated and it was found that the effect of short length shift registers (less than about 15 stages) and of decoding adjacent stages produced density tapers that had some apparent uniformity (Fig. 3). Longer length shift registers with every third or fourth stage decoded practically eliminated this lack of randomness (Fig. 4). Altering the decoding from adjacent stages to every second or third stage modifies the power spectrum of the decoded signal, by suppressing the low frequency components, and increasing the high frequency components.[13] This property of decoded feedback shift registers would seem to explain the different density tapers produced with changed decoding.

The feedback shift register has been constructed using integrated circuit J–K flip-flops and NOR gates. The digital-to-analogue decoder employs a resistor ladder network and discrete component transistor switches.

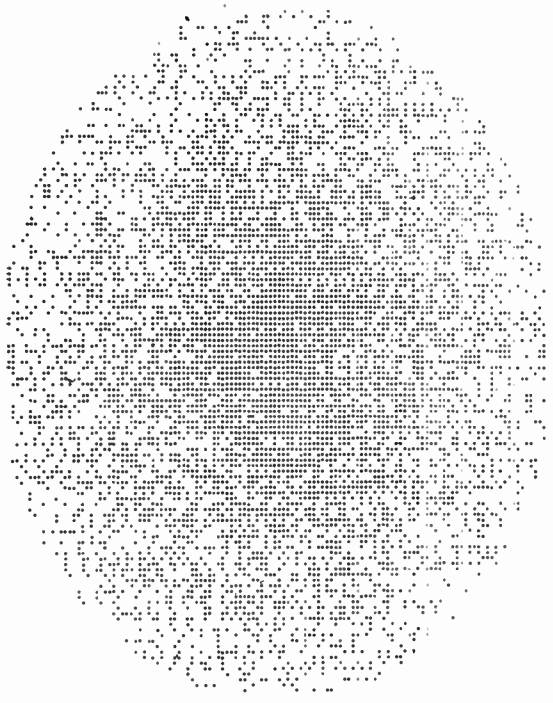

Fig. 5. Location of the elements for 'natural thinning'. The random number generator is the same as that used for Fig. 4.

5. Computer Simulation

The technique used to determine the position of elements in the thinned array was simulated in a digital computer. The method of determining $A(r)$ and N for each array point was followed exactly, and the results show the position of the elements in the thinned array (Figs. 3, 4 and 5). Theoretical radiation patterns in the near- and far-field were also computed for arrays with various degrees of thinning.

The basic aperture is a square of side $63{\cdot}5\lambda$ (where λ = wavelength), with individual elements located only at the intersections of the square grid and within the inscribed circle (Fig. 2). The grid spacing is taken to be $\lambda/2$. This square aperture would contain 16 384 elements if completely filled. The field patterns are calculated for the circular aperture (Fig. 2) which has 12 708 elements if completely filled.

The piezoelectric transducer responds only to components of stress normal to its surface. For an aperture element at point Q (Fig. 2), the response is proportional to $\cos^2\alpha$. Assuming the elements to have a $\cos^2\alpha$ characteristic and neglecting mutual coupling, the field $E(x', y', z)$ at P due to the element at Q is given by:[14]

$$E(x', y', z) = \frac{1}{\rho}\exp(j\beta\rho)\cos^2\alpha \qquad .....(2)$$

where

$$\rho = \sqrt{(x_m - x')^2 + (y_n - y')^2 + z^2}$$

$$\beta = \frac{2\pi}{\lambda}$$

x_m and y_n are integral values of $\lambda/2$.

Now,

$$\begin{aligned} x' &= R\sin\theta\cos\varphi \\ y' &= R\sin\theta\sin\varphi \\ z &= R\cos\theta \end{aligned} \qquad .....(3)$$

Thus

$$\rho = \sqrt{x_m^2 + y_n^2 + z^2/\cos^2\theta - 2z\tan\theta(x_m\cos\varphi + y_n\sin\varphi)} \qquad .....(4)$$

Substituting for ρ, and applying the far-field approximations, the total far-field intensity of the statistically-designed array is

$$E(\theta, \varphi) = \sum_{m=1}^{M}\sum_{n=1}^{M} F(x_m, y_n)\cos^2\alpha \times \times \exp(j\beta\sin\theta(x_m\cos\varphi + y_n\sin\varphi)) \qquad .....(5)$$

$F(x_m, y_n)$ takes the value 1 when an array point is at (x_m, y_n) and 0 when it is not. The function $F(x_m, y_n)$ thus completely specifies the distribution of sampling points and is determined as previously described.

The antenna may be focused in the near-field by applying a phase taper across the aperture, so that the wavefronts from each aperture point all arrive at the focal point in phase. This focusing will be carried out during the image reconstruction in a digital computer.

For an aperture focused at a point F on the z-axis, the aperture illumination is

$$f(x_m, y_n) = F(x_m, y_n)\exp(j\beta(z_0 - \sqrt{x_m^2 + y_n^2 + z_0^2})) \qquad .....(6)$$

where the exponential term is the phase distribution necessary for focusing the aperture.

Thus, for an aperture focused in the near-field

$$E(\theta, \varphi) = \sum_{m=1}^{M}\sum_{n=1}^{M} F(x_m, y_n)\cos^2\alpha \times \times \frac{1}{\rho}\exp(j\beta(\rho + z_0 - \sqrt{x_m^2 + y_n^2 + z_0^2})) \qquad .....(7)$$

6. Results

6.1. *Aperture Element Distributions*

Different aperture element distributions are shown in Figs. 3, 4 and 5. The fraction of elements removed has been calculated with respect to the number of elements in the filled circular aperture.

The effect of modifying the random number generator is demonstrated in Figs. 3 and 4. Both patterns are for 94% thinning (i.e. 6% of the original points remaining in the aperture).

The element positions in a 'naturally-thinned' array are shown in Fig. 5. 'Naturally-thinned' arrays are those for which $k = 1$. The random numbers are generated by using a 20-stage feed-back shift register with every fourth stage decoded.

Although the basic aperture is a circle (Fig. 2), the aperture distributions shown in Figs. 3, 4 and 5 are elliptical due to line printer limitations.

The density tapered arrays represented by Figs. 4 and 5 were used in the calculation of radiation patterns.

6.2. *Far-field Radiation Patterns*

Figure 6 shows two far-field radiation patterns for natural and 94% thinning. These were calculated using eqn. (5). It is worth noting here that two properties of the model array (i.e. an equivalent filled array with an amplitude taper of the form $A(r) = 1-0{\cdot}8r$) are a half-power beamwidth of 0·018 radians and a first side-lobe 27 dB down from the main-lobe.

Table 1 summarizes the properties of the two patterns shown in Fig. 6. The results indicate that the far-field beamwidth of the thinned array is the same as that of the model array, whilst the maximum side-lobe is about 9 to 13 dB above the predicted statistical average. A number of other field patterns for various degrees of thinning, different tapers and different values of φ have also been computed. These included eight independent patterns for the 94% thinned array, calculated from three independent designs and various values of φ. The maximum side-lobe of these eight patterns was -19 dB below the main-lobe. The results confirm that the pseudo-random design method for thinning arrays achieves radiation patterns with narrow beamwidth and good side-lobe behaviour, with as much as 94% thinning.

A major objection to the severe thinning of radar arrays is the resulting loss in directive gain, as this is proportional to the number of elements (if the average spacing is large). The directive gain of a radar array is important as the signal/noise ratio in the medium may be very low. However, the signal from the ultrasonic transducer will be sufficiently strong to enable the array points to be severely thinned.

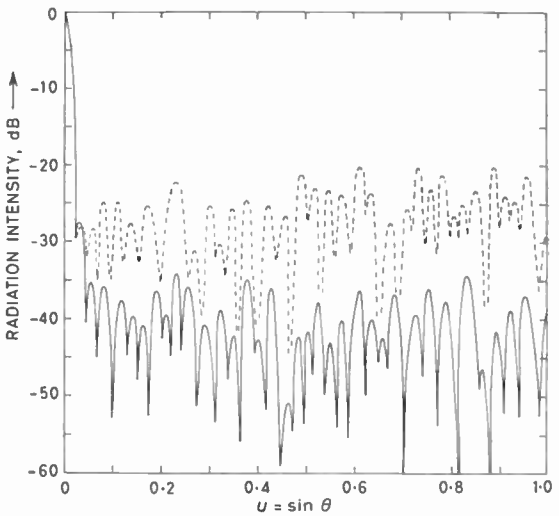

Fig. 6. Computed far-field radiation patterns of a density-tapered array for $\varphi = 0°$.
——— 'natural thinning' (52% thinning).
– – – – 94% thinning.

The near-field patterns of an aperture focused in the far field are shown in Fig. 7. This shows the deterioration of the pattern as the distance from the aperture decreases. However, the field pattern on a plane 768 wavelengths from the aperture still retains a distinct main-lobe and side-lobes below -14 dB, even though it is well inside the Fresnel zone. This demonstrates that the boundary between the 'far' region and the Fresnel region (usually taken as $2D^2/\lambda$, in this case 8064λ) is not sharply defined.

6.3. *Near-field Radiation Patterns*

The radiation patterns of an aperture focused in the near-field were found by using eqn. (7). Some of the results are shown in Fig. 8 and Table 2. All the results are taken for 94% thinning (or 776 array points) and the patterns shown are taken on the focal plane of the focused array.

The near-field radiation patterns of the thinned array retain a narrow beamwidth and low side-lobes. The half-power beamwidth is seen to increase as the

Table 1

Characteristics of the far-field patterns

Thinning	Number of elements	Maximum side-lobe (dB)	Average side-lobe (dB) predicted (by Skolnik)	Average side-lobe (dB) actual	Half-power beamwidth (Δu) model	Half-power beamwidth (Δu) actual
Natural	6082	−27	−40·7	−43	0·018	0·018
94%	766	−20	−29·1	−30	0·018	0·018

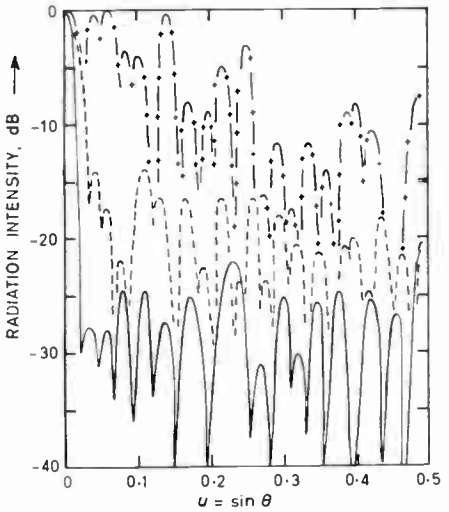

Fig. 7. Computed radiation patterns of a density tapered array with 94% thinning and $\varphi = 0°$. The aperture is focused at infinity and the patterns calculated on planes, a distance z from the aperture.

——— $z = \infty$
– – – – $z = 768\lambda$
—+— $z = 256\lambda$

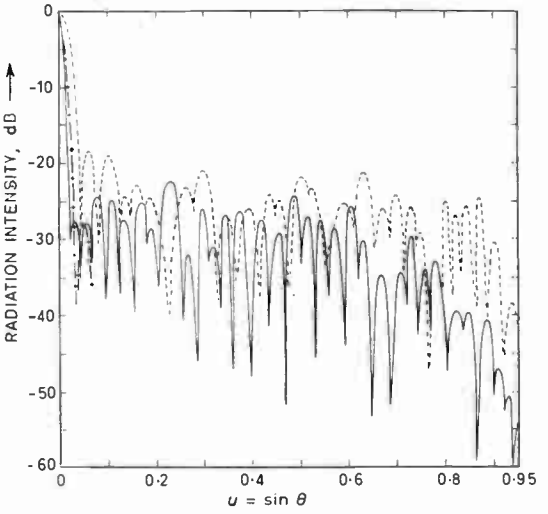

Fig. 8. Computed near field radiation patterns of a density tapered array with 94% thinning and $\varphi = 0°$. The array is focused in the near-field and the patterns are taken on the focal plane.

——— focal distance = 8192λ
—+— focal distance = 64λ
– – – – focal distance = 16λ

focal distance becomes small but the resolution in the image plane is not impaired because the half-power beamwidth is an angular measure.

The results indicate that a severely-thinned array can still have good radiation patterns when focused as near as a quarter of the aperture diameter from the centre of the aperture.

7. Conclusion

The technique of density tapering a planar array of antenna elements is well established. Previous investigations have been concerned with the actual positioning of elements in the thinned array. When this has been done and the array built, the aperture element distribution is fixed.

However, with the ultrasonic transducer the investigator has access to all the sample points (which can be regarded as antenna elements) and the problem is to reduce the processing of data from the transducer. This can be achieved by thinning the sample points. Thus there can be flexibility in choosing a specific sample point distribution which can be altered if required. The pseudo-random thinning of sample points enables this to be done and is both cheap and easy to implement.

The results show that the pseudo-random thinning of sample points generates arrays which have satisfactory radiation patterns.

8. References

1. Sokolov, S., British Patent No. 477139, 1937. U.S.A. Patent No. 2164125, 1939.
2. MacKay, R. S., (Ed.), 'Ultrasonic Imaging', Mine Advisory Committee, National Academy of Sciences, National Research Council, (U.S.) Report No. AD621-372, April 1965.

Table 2

Characteristics of the near-field patterns

Focal distance (λ)	Maximum side-lobe (dB)	Average side-lobe (dB) predicted (by Skolnik)	actual	Half-power beamwidth (Δu) model	actual
8192	−22·5	−29·1	−34	0·018	0·018
64	−23·5	−29·1	−34	0·018	0·020
16	−18·5	−29·1	−30	0·018	0·038

3. Smyth, C. N., Poynton, F. J. and Sayers, J. F., 'The ultrasound image camera', *Proc. Instn Elect. Engrs*, **110**, pp. 16–28, January 1963.

4. Maginness, M. G., 'Comment on nonoptical holography', *Proc. Inst. Elect. Electronics Engrs*, **55**, pp. 2050–1, November 1967 (Letters).

5. Deschamps, G. A., 'Some remarks on radio frequency holography', *Proc. I.E.E.E.*, **55**, pp. 570–1, April 1967 (Letters).

6. Skolnik, M. I., Sherman, J. W. and Ogg, F. C. Jr., 'Statistically designed density-tapered arrays', *I.E.E.E. Trans. on Antennas and Propagation*, **AP-12**, pp. 408–17, July 1964.

7. Willey, R. E., 'Space tapering of linear and planar arrays', *I.R.E. Trans.*, **AP-10**, pp. 369–77, July 1962.

8. Lo, Y. T., 'A mathematical theory of antenna arrays with randomly spaced elements', *I.E.E.E. Trans.*, **AP-12**, pp. pp. 257–68, May 1964.

9. Ishimaru, A. and Chen, Y. S., 'Thinning and broadbanding antenna arrays by unequal spacings', *I.E.E.E. Trans.*, **AP-13**, pp. 34–42, January 1965.

10. Lo, Y. T. and Lee, S. W., 'A study of space-tapered arrays', *I.E.E.E. Trans.*, **AP-14**, pp. 22–30, January 1966.

11. Ogg, F. C. Jr., 'Steerable array radars', *I.R.E. Trans. on Military Electronics*, **MIL-5**, pp. 80–94, April 1961.

12. Stern, T. E. and Lerner, R. M., 'A circuit for the square root of the sum of the squares', *Proc. I.E.E.E.*, **51**, pp. 593–6, April 1963.

13. Davio, M., 'Random and pseudorandom number generators', *Electronic Engineering*, **38**, pp. 558–9, September 1967.

14. Silver, S., 'Microwave Theory and Design', Chapter 3, p. 79 (M.I.T. Radiation Series, McGraw-Hill, 1949).

Manuscript first received by the Institution on 23rd October 1968, and in final form on 3rd March 1969. (Paper No. 1272/Com. 19.)

Contributors to this Issue

Joram Agar (M. 1962, G. 1957) is founder and managing director of Joram Agar and Company Limited, who specialize in industrial instrumentation. He received his early technical training in communications and radar while serving with the Israeli Navy; in 1961 he completed post-graduate studies for the Diploma in Engineering of the University of Surrey, achieving distinction in control engineering. From 1959 to 1967 he was a research and development engineer with the Solartron Electronic Group. Mr. Agar has been a member of the Institution's Instrumentation and Control Group Committee since its formation in 1967, and he served on the Organizing Committee for the recent conference on 'Digital Methods of Measurement'. He has written several papers and articles including two which have appeared in *The Radio and Electronic Engineer*.

James G. Holbrook (M. 1968) entered electronics via amateur radio and the U.S. Air Force some thirty years ago. He then worked in broadcasting and with the Federal Communications Commission. He received his B.Sc. degree from the Milwaukee School of Engineering in 1952. Before coming to the University of Southampton in 1968 for a three-year stay as Research Fellow, he was a Senior Engineer with Varian Associates in Palo Alto, California, and prior to this was a research scientist for six years with Lockheed Missiles and Space Company. His work at Southampton, and for the past five years, has been in the field of electron-spin-resonance. Mr. Holbrook received his M.Sc. degree in 1962 from the University of Santa Clara. He holds two patents on oscillator circuits and phase detectors, and is author of a book on Laplace Transforms.

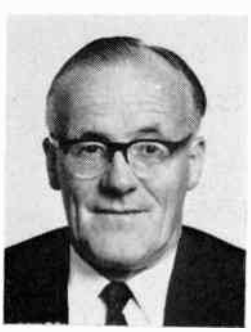

P. F. Gunning received his technical education at Liverpool Institute and joined the Automatic Telephone Manufacturing Company in 1926. In the early 30s he was concerned with the design of general communication, supervisory control and telemetering projects for the electrical power industry at home and abroad. In 1934 he joined the Central Electricity Board as Telecommunications Engineer for the North West England District. When the Industry was nationalized in 1948 he was appointed Headquarters Telecommunications Engineer with the C.E.G.B. With the help of the telephone manufacturers he developed and introduced the 'standardized system' of telecommunication telemetering, limited selective control and general indications as used extensively by the C.E.G.B. and S.S.E.B. in power stations, grid stations and control centres. Later he developed and introduced delayed automatic reclosing for the 132 kV system and protection acceleration for the 275 and 400 kV supergrid. Since 1963 he has been responsible for the design, development and construction of the C.E.G.B.'s 3-tier control project. As an authority on power supply telecommunications, he has presented papers and lectured to different institutions in this country and abroad.

U.D.C. 621.317.39:621.376.3

Frequency Modulating Transducers

By

J. AGAR,

Dipl. Eng., M.I.M.C., C.Eng.,
M.I.E.R.E.†

Presented at a meeting of the Institution's Instrumentation and Control Group in London on 26th November 1968.

Summary: Frequency modulating (f.m.) transducers are instruments whose output frequency is proportional to the measured physical parameter, such as flow (turbine flow meter), radiation (Geiger counter), pressure, density etc. The paper deals with the advantages of using f.m. in process plants and describes some f.m. instruments which measure flow, pressure, temperature and density.

1. The Advantages of Using F.M. in Plants

The advantages of frequency modulating transducers from the process control view-point are as follows:

(i) Overcoming loss of information due to series and shunt resistances of conductors

The loss of signal over long distances in the conventional current-transmitting systems presents a severe problem and dictates the use of high-quality cables. In civil engineering, where many points of strain have to be monitored in pressure vessels, sky-scraper foundations, bridges, etc., hundreds of strain-gauges are buried in the concrete and economics dictates that only cheap cables can be used. Reliable information may have to be transmitted for a period of a few decades at least and f.m. was the only satisfactory solution found. The same applies to pressure transducers which are buried in the ground to measure the pore-water pressure of the soil in order to determine slope stability and the stability of buildings on clay. The actual transducers used in these cases are described later.

In oceanography, the problems are even more severe, and again, f.m. was found to overcome the problem of loss of information due to sea-moisture decreasing the cable insulation. When f.m. is used, the signal can deteriorate in strength from an initial value of a few volts right down to a few millivolts, since as long as the signal can be amplified and squared no information is lost.

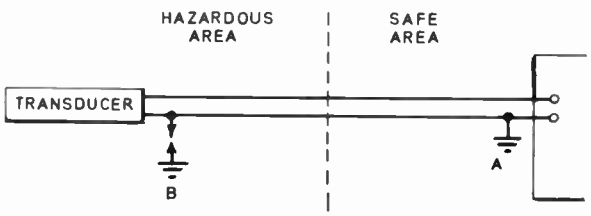

Fig. 1. Hazard caused by earth potentials.

† Joram Agar & Co. Ltd., 2 Knoll Close, Fleet, Hants.

(ii) Avoidance of mains interference

The carrier frequency of the transducers is selected such that it is a few times higher than the mains frequency (from 8 times upwards). This means that by using standard commercially available low-pass and band-pass filters (to I.R.I.G. specification), unwanted common-mode and series-mode pickup can be rejected with great ease.

(iii) Use of one pair of wires to transmit power and receive information from many transducers

This is a well-known technique in telephony, where power lines are used to carry many conversations simultaneously. At present, the 'live-zero' (4–20 mA and 10–50 mA) amplitude modulated (a.m.) current-signal transmission enables power and signal to be transmitted over one channel only. This is due to its d.c. nature, hence isolation is impossible; while with f.m., by using transformers and band-pass filters, isolation of one channel from another, and of the power from signals, is easily achieved. Equipment developed for telephony can be applied to process control.

(iv) Improvement in intrinsic safety

Normally, f.m. transducers require only a few milliwatts to drive them, compared in some cases with a few tens of watts for conventional instruments. This means that the equipment can be made intrinsically safe rather than explosion-proof.

There are however some cases, in particular in large oil installations and mines, where long cables can cause an explosion if earthed in the safe area and again in the hazardous area, as shown in Fig. 1.

If a sufficiently high earth-potential exists between point A and B, sparking can occur even if the equipment is switched off. The conventional way to overcome it is by using an isolator which is inserted in the line, at the dangerous interface. This gives complete isolation between points A and B. An example of such a device is the Kent-Evershed ER 330 isolator. This ingenious device modulates the incoming signal,

passes it through a high-quality current transformer, and then demodulates the output from the secondary windings.

In the case of f.m. a simple isolating transformer achieves the same thing without any deterioration of the information, and without the use of mains to supply the modulator. Furthermore, pneumatic f.m. signals can be transmitted over much longer distances than the conventional 3–15 lb/in^2 (0·2–1·05 kg/cm^2) a.m. signals, thus improving safety in plants by eliminating electrical transmission all together.

Some fluidics f.m. transducers are described later, and an electropneumatic convertor is described in Reference 1.

(v) Ease of commutation

Frequency modulation eases commutation considerably, as it enables the simultaneous detection of eight channels in the frequency band between 400 Hz and 3000 Hz (telephone bandwidth). As isolation is achieved with transformers, simple solid-state devices can be used safely at high speeds, without the need to introduce mechanical switches. This overcomes relay chatter, interference from thermoelectric voltages and other problems associated with mechanical switches. When f.e.t.s. are used, the risk of damage due to high-voltage pick-up is removed by the transformers.

(vi) Ease of computation

Frequency modulation can be used in a similar way to a.m. to perform various computations by using binary circuits. In fact any computation that can be performed on an analogue computer can be performed digitally in f.m. by using the same 'block diagram'. The basic analogue computer elements are: integrators, multipliers (including potentiometers), non-linear elements and delay lines. With these elements it is possible to generate a wide variety of functions such as square roots, etc. The accuracy of the computation depends on the drift of amplifiers and components. In the case of f.m., the integrator is a simple counter, the multiplier, the potentiometer, the non-linear elements are the binary rate multipliers, and the delay line is the shift register.[2,3] With these 'bricks' the same equations can be set up as on the analogue computer, thus utilizing the same well-established mathematical approach (except that the digital computer approach is a numerical one). The only difference is that the accuracy does not depend on the drift of components, but only on the number of binaries used to perform each computation. There are quite a few commercially available electronic instruments which utilize these techniques to multiply and linearize the output of f.m. transducers.

(vii) Ease of tape recording

Recording of f.m. information on tape is done with great ease and accuracy, if an accurate 'clock' signal is recorded simultaneously. Tape speed fluctuations do not matter, as the relative periodic time between the clock and the information channel remains constant. Tape speed can be greatly reduced to save tape. All this is done without any manipulation of the original signal as received from the f.m. transducer.

2. Detailed Description of F.M. Transducers

2.1. *The Vibrating Spool Fluid Density Meter*

This instrument is typical of f.m. transducer approach. The principle of operation is shown in Fig. 2. Figure 3 shows the flanged version exploded, while Fig. 4 shows the flanged and by-pass versions. The sensing element is a tube thickened at the two ends (spool), which is set in the circumferential mode of oscillation (i.e. the spool rings like a bell). The spool is maintained in oscillation by the maintaining amplifier. The measured fluid is allowed to surround the spool and thus is set in oscillation as well. The frequency of oscillation depends on the tube stiffness and the total oscillating mass, i.e. the tube walls and the surrounding fluid. An increase in the density of the fluid lowers the frequency of oscillation. The output of the amplifier is monitored by a frequency meter whose display is calibrated in the desired units of density.

The meter measures true density very accurately (better than 1 in 10^4 of f.s.d.).

The spool is clamped to the body by one retaining ring. Unscrewing it releases the spool for cleaning. There are no obstacles in the pipe and the only materials in contact with the fluid are the spool and the stainless steel body.

2.1.1. Hysteresis and long-term stability

The sensing element (the vibrating spool) is suspended in the fluid and is not stressed at all. Increasing the fluid pressure from vacuum to 10 000 lb/in^2 (700 kg/cm^2) and bringing it back to vacuum does not effect the frequency of oscillation, as the spool is not stressed at this high pressure. The minute amplitude of oscillation is well below any fatigue level and therefore the instrument exhibits extremely good long-term stability.

2.1.2. External vibrations

Due to the high mechanical Q of the spool (a few hundreds), the instruments reject plant and other 'noise' sources.

2.1.3. Temperature effect

Temperature changes affect the linear dimension of the spool and its Young's modulus. By choosing the same alloy as used in tuning forks and heat-treating

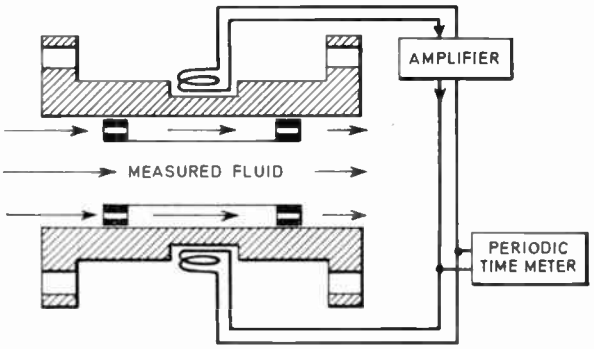

Fig. 2. Diagram of the fluid density meter illustrating the principle of operation.

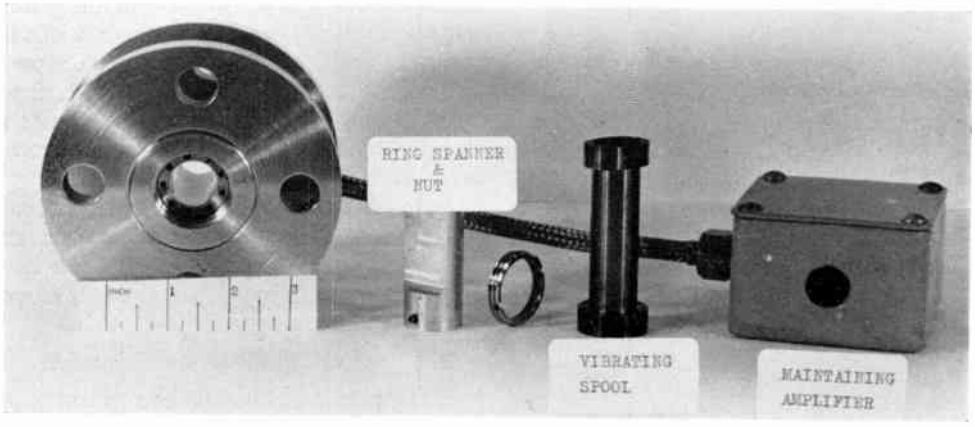

Fig. 3. Exploded view of the flanged fluid density meter (*Joram Agar & Co. Ltd.*)

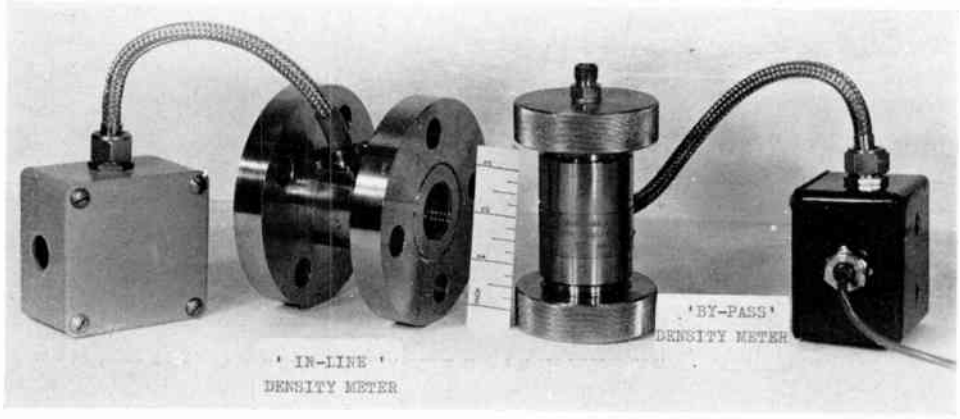

Fig. 4. Flanged and by-pass versions of fluid density meter (*Joram Agar & Co. Ltd.*).

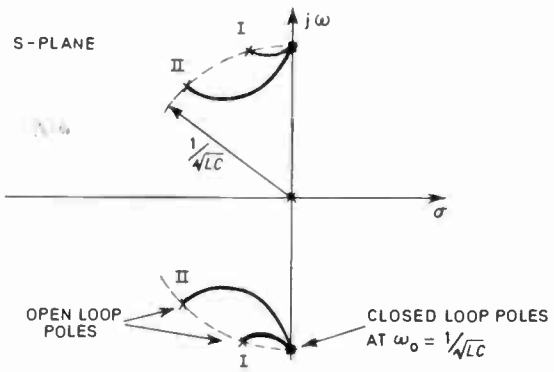

Fig. 5. Root-locus of a second-order oscillating system and an integrator.

it, a temperature coefficient of better than 50 parts in 10^6 per degC of full-scale deflection can be achieved.

2.1.4. Viscosity effects

Over a narrow band around the frequency of oscillation, the vibrating system can be looked upon as a lumped mass-spring system or an LCR circuit. It is well-known[4] that by closing the loop through a finite bandwidth amplifier, the system will oscillate at a frequency just below $\sqrt{(k/M)}$ or $1/\sqrt{(LC)}$ depending on damping and amplifier, i.e. the ratio of R/R_a in case of a triode Hartley or Colpitts oscillators (where R_a is the internal anode resistance). Lord Rayleigh[5] however, indicated that by closing the loop through a precise 90° phase shift (an integrator), the frequency of oscillation will be maintained at $\sqrt{(k/M)}$ or $1/\sqrt{(LC)}$ irrespective of the value of the damping. This can be verified at a glance from the pole-zero plot (Fig. 5) of the simplified second-order equation.

Note that the damping of the pole-pair II is much more severe than that of I, but that the root locus in either case crosses the jω axis at the same point, namely, at $\omega_0 = 1/\sqrt{(LC)}$. A typical calibration curve is given in Fig. 6.

Note also the wide range of change in the periodic time from air to trichloroethylene and the predetermined non-linearity:

$$\rho = \rho_0[(T/T_0)^2 - 1] \qquad \ldots\ldots (1)$$

where ρ = measured fluid density

ρ_0 = scale factor

T = measured periodic time of oscillation

T_0 = periodic time of oscillation in vacuum.

Figure 6 is drawn as periodic time/density, rather than frequency/density, as is more familiar from other f.m. applications, because the 'carrier' frequency is rather low, and pure frequency measurement would dictate a long measuring time, in order to get the required accuracy. If however the periodic time is measured, the information is registered within a few milliseconds. The importance of reducing the measuring time is very important in control, where this dead time can cause instability. In particular, it is of paramount importance for multi-loop control systems. The following example will demonstrate the difference between conventional frequency measuring technique, and periodic time measurement.

If the required density span is 100 mg/cm^3, say from kerosene to motor oil, the corresponding periodic time change is from 300 μs to 330 μs (Fig. 6). The corresponding frequency change is from 3333 Hz to about 3000 Hz. To measure this information to an accuracy of 0·1% in terms of frequency, a time of 3 seconds is required. If periodic time is used, however, this accuracy can be achieved at a fraction of this time. Accordingly, the signal is counted (averages) over say 10 cycles, which takes only 3·3 ms. During this period, a 1 MHz 'clock' will fill up the information storage register with 3300 pulses, which is 3 times more than the required 1000. The 'pulse dropping' technique of computation is performed with the binary rate multipliers, which operate on the 1 MHz pulses rather than the incoming information pulses, which are much slower. Thus by measuring the periodic time of the incoming f.m. signal, we can record the information and *linearize* it in less than 5 ms.[2,3] This 'dead time' is extremely small and allows for 200 channels to be scanned in 1 second, which is considered extremely fast.

2.2. *Vibrating Wire Pressure Transducer*

This instrument utilizes the 'violin string' principle, and offers a very cheap and reliable instrument suitable for pore-water pressure gauging and other applications. In a modified form, the vibrating wire can be used as the sensing element of a strain gauge. Figure 7 shows the principle of operation.

The wire can be maintained in continuous oscillation as in the previous instrument, or 'plucked' by sending

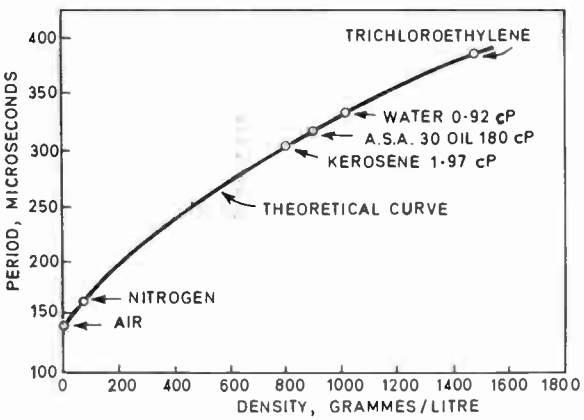

Fig. 6. Calibration curve of a fluid density meter.

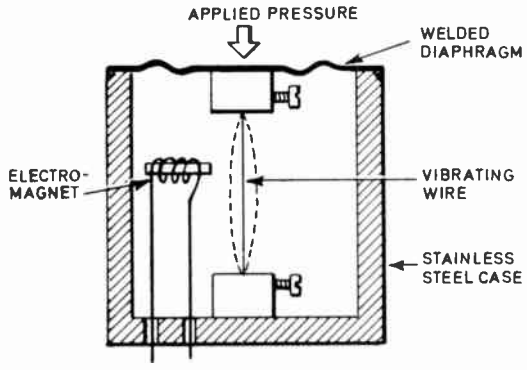

Fig. 7. Vibrating wire pressure transducer.

an electric current impulse, and then monitoring the frequency of the decaying oscillation. The frequency/pressure relationship takes the same form as eqn. (1), i.e.

$$P = P_0[(f/f_0)^2 - 1] \qquad \text{.....(2)}$$

where P = applied pressure

P_0 = scale factor

f_0 = frequency of oscillation at zero pressure

f = measured frequency at applied pressure.

These instruments can be made very cheaply for an accuracy of about 1%. To improve the accuracy further, the following points need modifying: the clamps should not bite the wire, the temperature expansion coefficient of the wire and the case must be matched; the initial high stress level in the wire must be reduced; the requirements of the diaphragm must be relaxed by making another member take up more of the reaction stress. These requirements can be met and are a subject of a new patent. With the appropriate modifications the instrument's accuracy is improved to better than 0·1% of f.s.d.

The same principles can be applied to strain gauges, load-cells, weighing machines etc., where the high reliability, quick response and ease of digitization make these type of f.m. transducers very attractive.

2.3. *Ultrasonic Flow Meter*

This instrument gives some of the advantages of f.m. transducers, such as clean unobstructed flow as in the case of the fluid density meter, f.m. output, and simplicity of the sensing element. On the other hand, the lack of a high mechanical-Q sensing element makes the instrument susceptible to external vibration, flow pattern, etc. The principle of operation is based on the sound velocity meter,[6] illustrated in Fig. 8.

A short sound pulse is transmitted from the piezo-electric device on the right and travels through the fluid at a velocity of $c \pm v$ to the receiving device on the left; c is the velocity of the sound in a static fluid,

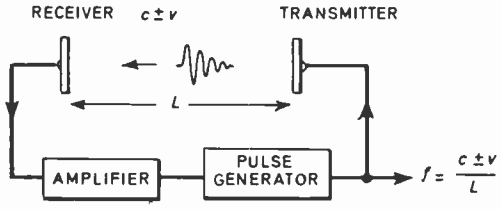

Fig. 8. Principle of a sound velocity meter.

and v is the average relative velocity of the fluid between the receiver and transmitter device. The pulse is then amplified and shaped and is re-transmitted again. The repetition rate (or frequency) is determined by

$$f = \frac{c \pm v}{L} \qquad \text{.....(3)}$$

In the flow meter, shown in Fig. 9, two such channels are used. The frequency of one channel is $f_1 = (c+v)/L$ while the other is $f_2 = (c-v)/L$.

The output frequency from the low-pass filter is proportional to the average linear velocity v in the pipe line, and multiplying it by the constant A, the pipe cross-section area, gives the volumetric flow. Since the velocity of sound in a fluid is inversely proportional to the square root of the density, the output of the high-pass filter can yield information about the density. Multiplying this by the volumetric flow gives mass-flow. As mentioned in the previous sections, all these calculations can be done by binary circuitry without introducing any significant error. This instrument is extremely attractive for high flow-rates, near the velocity of sound, but much less attractive at low velocities and under conditions where the flow pattern changes from laminar to turbulent.

Other flow meters which should be mentioned are the turbine flow meter and the f.m. differential pressure transducer used in combination with an orifice plate.

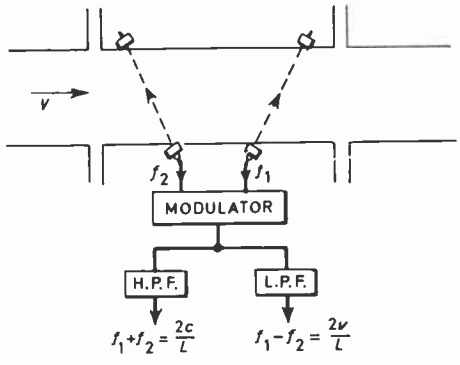

Fig. 9. Principle of operation of an ultrasonic flow meter.

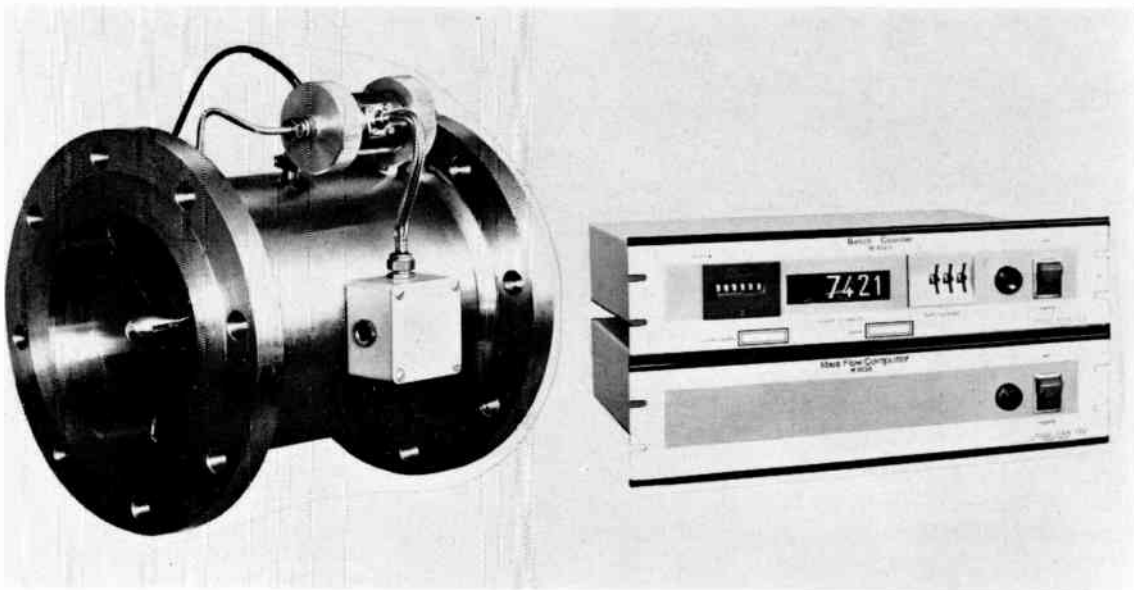

Fig. 10. Digital mass flow system (*Meter-Flow Ltd.*).

Both devices give an f.m. output. A commercially available mass-flow meter incorporating the vibrating spool density meter, a turbine flow meter and a binary rate computer is shown in Fig. 10.

2.4. *Temperature Measuring Devices*

The dependence of Young's modulus on temperature can be exploited for temperature measurement by two basic types of instrument:

(i) Delay-line technique.

(ii) Self-oscillatory technique.

The second method is the preferred one for the same reasons given in the case of the ultrasonic flow meter, namely that an oscillatory system with a high mechanical Q rejects plant noise, makes the device more robust, and simplifies the electronic design as it does not call for amplifiers with short propagation times. Figure 11 shows the delay-line type of thermometer.

The delay between the transmitted pulse to the received pulse depends on the ratio of the rod's length, and the velocity of sound. Since the latter depends on the square root of Young's modulus, the temperature can be derived from the calibrated thermoelastic coefficient of the material. High temperature ceramics are much favoured for many applications, as they usually also exhibit low sonic losses and high corrosion resistance. The measuring member need not be a solid rod, neither need the sound medium be solid. Gas at low pressure will do, as the velocity in gases is proportional to the square root of the absolute temperature. If the delay time is long enough, the receiving and transmitting mechanism can be fluidic devices.[7]

The Hewlett Packard thermometer utilizes the second principle. The sensing element is a high frequency (about 28 MHz) quartz crystal which is cut in a plane to yield maximum temperature sensitivity. The crystal is maintained in continuous oscillation, the frequency of which is measured and displayed digitally as linear temperature. The scale adjustment is done digitally as described earlier. The instrument was originally designed for oceanographic measurements, and gives a resolution of $\pm 0{\cdot}0001$ degC.

3. Conclusions

The advantages of frequency modulation in transmitting and manipulating information in process control have been discussed, and some pure f.m. transducers which measure density, pressure, flow and

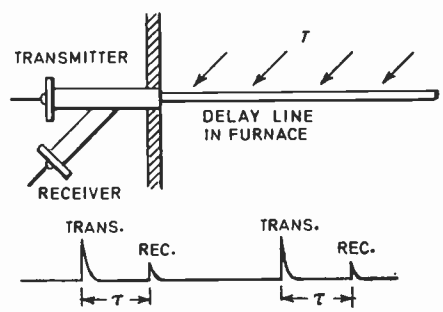

Fig. 11. Delay-line thermometer.

temperature described. There are many other transducers such as the molecular weight meter which have not been described, as their basic principle of operation adopts one of the described techniques. The description has also omitted conventional instruments with a capacitive or inductive pickup for frequency-modulating an LC oscillator, as they are more familiar in concept. The advantages of pure f.m. transducers are their simplicity, high accuracy and reliability; these points were stressed for each particular principle of operation.

It is hoped that the process control industry will follow the construction and oceanographic industries, and will adopt f.m. as the main source of measurement and transmission.

4. Acknowledgment

The author wishes to thank Professor V. S. Griffiths, Head of the Chemical-Physics Department, University of Surrey, in whose department some of the research was done and in particular for his continuous encouragement.

5. References

1. 'Electric-to-fluidic transducer uses frequency modulation', *Control Engineering*, **15**, No. 9, p. 65, September 1968.
2. Talbot, G. C. A. and Senior, R., 'Rescaling a pulse train', *Electronic Engineering*, **40**, No. 480, pp. 95–6, February 1968.
3. Winston, G. C., 'Curvilinear rate multiplier for precise interpolation', *Control Engineering*, **15**, No. 4, pp. 81–2, April 1968.
4. Pridham, G. J., 'Analyses of feedback oscillators', *Electronic Engineering*, **40**, No. 483, pp. 285–7, May 1968.
5. Rayleigh (Lord), 'The Theory of Sound' Vol. 1, Chap. 3, para. 64. (Macmillan, London, 1894).
6. Williamson, R. L., Hodges, G. and Eady, E., 'A new sound velocity meter', *The Radio and Electronic Engineer*, **33**, No. 6, pp. 387–93, June 1967.
7. Johnson, E. G., 'Fluidic jet engine controls: faster, cheaper, lighter', *Control Engineering*, **14**, No. 7, pp. 58–62, July 1967.
8. Hewlett Packard Publication, 2801A, May 1968.

Manuscript first received by the Institution on 30th December 1968 and in final form on 27th February 1969. (Paper No. 1273/IC9.)

DISCUSSION

Under the chairmanship of Mr. S. L. H. Clarke

Mr. L. C. Towle: The points I would like to make are primarily concerned with the introductory section of Mr. Agar's lecture and the published paper may well expand these points to clarify some of the basic ideas.

The fundamental points made by Mr. Agar were that a frequency modulated signal was better than an analogue signal for process instrumentation purposes for the following reasons:

(1) It was not subject to line resistance and leakage resistance effects.

(2) It was more easily multiplexed by process control computers.

(3) It was less prone to interference effects.

(4) It was much easier to make intrinsically safe.

It is difficult to consider these arguments without discussing them at some length but I believe that the degree of difficulty is not in practice significantly different. I would argue that the use of transmitter with a frequency output is complementary to those with an analogue output and that the normal criteria of suitability for the application, cost and availability will decide their relative usage: the factors referred to by Mr. Agar will not play a major part.

To consider the points briefly and stating the case without repeating the points in favour of frequency modulation.

It seems reasonable to compare a high-level analogue signal with the high-level output from a frequency transducer. The output impedance of the majority of current transmitters is about 1 MΩ and hence line resistances as experienced within a plant of less than, say, 100 Ω do not cause any problem. A typical process loop uses load resistance of approximately 500 Ω and with modern materials insulation resistance of 500 kΩ are easily maintained even in very adverse conditions. In practice the malfunction of analogue equipment due to cable and installation series and shunt resistance simply does not occur except when the cables are severely mechanically damaged and under these circumstances *any* type of signal would not be reliable.

The hardware for multiplexing high-level signals exists in computer installations. The increased cost for good electronic switches is not great and in common with most other hardware costs is rapidly becoming insignificant compared with the software cost. If one chooses a low-frequency signal, say 200 Hz, then the time taken to 'read' this signal is long compared to an analogue signal. The general question of multiplexing cannot be discussed in a simplified generalization of the type used in this lecture. The basic point remains that a process control computer can deal with most types of information rapidly at a relatively low hardware cost and consequently the choice of signal is very wide.

Interference in a modern industrial plant was assumed by Mr. Agar to be predominantly at 50 Hz. The advent of thyristor control, ultrasonic cleaning, r.f. heating and other techniques has meant that interference at higher frequencies has increased. In practice most analogue instrumentation can deal with this problem by RC filtering and unless there is some rectification within the system before the filtering no errors are caused. Where a frequency modulated signal is concerned the interference and the information could have exactly the same form but are usually satisfactorily dealt with by trigger level adjustment or digital filtering. Again the problem has to be considered and dealt with and the degree of difficulty is not appreciably different in the two cases.

The point on intrinsic safety was based on the assumption that transformer isolation provides safeguards against the hazard which can be created by two earth faults on an intrinsically safe system. The subject of earth faults on these systems has been the subject of a long debate for at least the last three years and is worthy of several papers on itself. The primary problem is however that a multiple earth fault is an ill-defined situation; no one has any real idea how large the difference in earth potentials are, or of the magnitude of the earth currents, or even what the impedance of the earth path is. It seems improbable, however, that any real hazard exists or the numerous pipes, air-supply lines, hand-rails, bonded conduit and other continuous low-resistance paths which occur in the majority of process plants would have caused numerous accidents by now. The multiple-earth problem is basically that the ill-defined situation makes certification difficult. If however a practical view that an 'intrinsically safe circuit is one which does not materially change the degree of hazard' is accepted, then the multiple-earth problem disappears.

Because of the ill-defined and probably transitory pattern of the earth potentials problem, the transformer coupling proposed by Mr. Agar is not a complete solution since if multiple-earth faults can occur, they might occur on one side of the proposed transformer, creating the hazard. There is in fact no well-defined point to position this isolating transformer.

A more significant point is that in considering the safety of an a.c. circuit, it is the peak open circuit voltage and short circuit current that has to be considered. If a sinusoidal 50 Hz signal is used as proposed, the peak levels will be $\sqrt{2}$ times that of the d.c. system delivering the same power. This may still be safe in the particular case of the density meter discussed but as a fundamental point is a strong argument in favour of d.c. power in intrinsically safe systems. This point of view will, I believe, receive strong support when the revised standards for bell signalling transformers are available.

As a practical point, Zener barriers suitable for d.c. power exist as a certified and available unit, and I am not aware of a comparable a.c. general-purpose coupler.

To summarize, I would argue that for process control purposes on these particular points there is little to choose between the two systems. There are other systems such as pulse-width modulation and the transmission of coded signals which are attractive in particular circumstances. My principal point is that Mr. Agar weakens the case for frequency-modulated measurements by obscuring their very real merits in generalizations which cannot be defended.

The ease with which relatively low-level signals can be manipulated from one form to another quite economically was shown in the supporting demonstrations. The basic point remains that the first consideration of an electrical transmitter must be the accuracy, stability and economy of the initial measurement and its conversion to a high-level electrical signal. The manipulation of the available signal whatever its form is now so easy that it should not be a prime consideration in determining the form of the initial measurement.

Mr. J. Agar (*in reply*): Mr. Towle's comments relate mainly to the introduction and I have covered most of his points at greater length in the text. I must leave some points as being matters of opinion.

Mr. C. J. Mills: I am interested in the possible application of the density gauge for measuring sudden density changes in water due to the presence of steam, could you please tell me the maximum frequency response of your gauge?

With reference to the vibrating-wire strain gauge, do you think it is possible to design a much smaller f.m. gauge for measuring internal strain in concrete?

Mr. Agar (*in reply*): The response of the water density meter is 4 ms. With regard to the small size of a f.m. strain-gauge, it is possible in my opinion to manufacture it as small as 1 cm, but I do not know of any which are commercially available.

Mr. J. Willis: One would expect most of the transducers described to give a basically non-linear relationship between the input variable and the output frequency. Is this not a considerable disadvantage of the system described? Either the non-linearity must be corrected in the read-out system, with a resulting increase in complexity and cost, or conversion tables must be used, at some inconvenience. It is true that if the transducer output is being processed in a digital computer then correction for non-linearity is easily applied, but this sort of facility is not always available.

Mr. Agar (*in reply*): Most f.m. transducers give a non-linear relationship. The amount of non-linearity is small and in cases of small spans can be ignored. Linearization can be achieved at a slight increase in cost in the read-outs, or by push-pull arrangement in the transducer itself. Resistance and thermocouple thermometers are also non-linear, but this did not stop their wide acceptance in industry.

Mr. G. B. Jackson: What is the reproducibility of the calibration from one f.m. transducer and the next? How does this compare for accuracy and price with a standard transducer and a voltage- or current-to-frequency converter using a simple transistor circuit?

Mr. Agar (*in reply*): The reproducibility of f.m. transducers depends on dimensions and Young's modulus. The same applies to Bourdon tubes, diaphragms and other

'standard transducers', which have to be calibrated individually, and the zero and span adjusted accordingly in the electronic equipment. I would say that there is not much to choose between the two systems.

Mr. B. W. Balls: I would like to know to what extent the applications of transmitters using the frequency principle which Mr. Agar showed are truly commercial applications or whether they are essentially development projects. Also, can he comment as to whether the applications described are strictly valid in an industrial-process control context.

Mention has been made of the use of ultrasonics for flow measurement. It is my opinion that this principle has been well explored experimentally but that no system has been commercially successful. Work carried out at the British Scientific Instrument Research Association more than ten years ago has been described in a paper by R. E. Fischbacher†.

Can Mr. Agar give the approximate cost per channel of the transmission system which he has described.

Mr. Agar (*in reply*): The paper gives details of a number of commercially available f.m. transducers, which are available from Hewlett Packard, Meter-Flow, Joram Agar & Co. and others.

The ultrasonic flow meter was brought in to show that f.m. thinking existed some time ago, although it did not bring as neat an overall solution to flow measurements, as the turbine flow meter. The latter is a much better example of a successful f.m. transducer.

With regard to the cost per channel, it varies from £25 to £500, depending on complexity and the measured variable.

† 'The ultrasonic flowmeter', *Trans. Soc. Instrum. Technol.*, **11**, No. 2, pp. 114–9, June 1959.

Mr. C. F. Barnett: Although you have shown an ultrasonic method for measuring temperatures directly in a digital way (and it is not too difficult to think of other semi-digital ways), surely very high temperatures are still a problem?

What is the repeatability of output temperature with one of these transducers in various typical installations? What is their stability over 6 months—in use of course?

Are they commercially available now and what is their cost to a buyer?

Mr. Agar (*in reply*): The 'delay-line' method of measuring temperature is used mainly for extremely high temperature and nuclear radiation environment. Ceramic materials are very popular not only because of their high radiation and temperature resistance, but also their high acoustical Q.

The repeatability under this severe environment is very good, and cannot be matched by other means of measurements, while over 6 months the repeatability is within the accuracy of measurement.

I know of two U.S.A. manufacturers[8] and one in the U.K., who cover different ranges and applications.

Mr. R. H. Sunderland: Ultrasonic flowmeters suffer badly from effects due to bubbles in fluids. This fact among the other objections already mentioned probably accounts for their low acceptance in the process control industries.

Intrinsic safety problems as discussed by Mr. Agar cannot be solved as he suggests in practice, since the location of the transformer is critical.

Mr. Agar (*in reply*): The problem of locating the transformer in the exact place does not arise in f.m., since more than one transformer can be inserted without any deterioration in accuracy. This example certainly emphasizes the advantage of f.m. in improving the intrinsic safety of plants.

Satellite Communications Station in Middle East

A new satellite communications station was formally opened in Bahrain on July 14th by the Ruler, His Highness Sheikh Isa bin Sulman Al Khalifa, K.C.M.G. Cable and Wireless will operate the terminal, situated at Ras Abu Jarjut, 20 miles from the capital, Manama, and built by the Marconi Company, as part of a global scheme which will provide telephone and data links, using principally *Intelsat II* and *Intelsat III* synchronous satellites. In association with tropospheric scatter systems already installed by Marconi elsewhere in the Gulf, the Bahrain station is a major part of a plan to provide the Gulf States with an ultra-modern communications system linking them with every part of the world.

The station has a 27·4 m (90 ft) diameter, fully-steerable dish, mounted on a 18·3 m (60 ft) concrete tower. New electronic techniques have been incorporated to achieve complete reliability and the highest standard of performance for the terminal, to meet the stringent requirements laid down by the Interim Communication Satellite Committee (ICSC). Major equipment throughout the system is duplicated and coupled to a versatile monitoring system to give a theoretical mean time between failures of about 2000 hours. Effectively this means that the station will be operational 99·9% of the time.

The main equipment building which houses the control console and its associated supervisory equipment together with communications intermediate frequency and base-band equipment is situated about 90 m (300 ft) from the tower. This building also contains the power generation equipment and the domestic accommodation.

Antenna. The antenna employs a 27·4 m diameter computer-profiled quasi-parabolic dish incorporating a Cassegrain sub-reflector assembly for the r.f. illumination of the system. At the centre of the main reflector and protruding both in front and behind is the r.f. feed horn and behind the main reflector and incorporated into the central cone assembly of the antenna are the two low-noise wide-band cooled parametric amplifiers.

An elevation-over-azimuth arrangement is used. The elevation movement of the main reflector over the range $-2°$ to $+92°$ is actuated from twin re-circulating ball screw jacks which are driven from servo equipment, duplicated for maximum operational availability. Azimuth movement of the antenna is carried via a kingpost mount supported on upper and lower bearings. The azimuth drive is provided by servo systems which incorporate two 10 hp d.c. motors, actuated from thyristor power drives, fully duplicated to provide maximum availability. Fast slewing movement is by two 40 hp motors.

Tracking system. Satellites are tracked using a beacon signal transmitted from the satellite. The signal from this beacon is separated from the communication carrier signals after the low-noise amplifier stage, and fed to a tracking receiver.

The tracking signal itself is derived from the rotation of a section of the feed horn at the vertex of the dish, to produce conical rotation of the beam, at the beacon frequencies only. This technique, called 'mode conversion scan', produces a modulation of the received beacon signal from the satellite, which reduces to a zero when the beam is pointing directly at the satellite. The depth of modulation will be directly proportional to the antenna pointing error, and is used to control the servo system which drives the antenna into the correct position. The direction of this error will be determined by the phase of the error signal, and two voltages, produced by comparison of the received signal with reference signals derived from the rotating horn section, will give error voltages initiating corrections in the two axes of rotation of the antenna.

The transmitter system. Two high power amplifiers are installed, one operational and one standby; these use a travelling-wave tube which has a peak saturated r.f. power output of 12 kW and a bandwidth of 500 MHz. The amplifiers can therefore cover the entire civil satellite communication transmission band of 5925 MHz to 6425 MHz.

Simple, but effective, auto level control units are employed by which each radiated carrier is maintained within 0·25 dB. This is achieved using variable ferrite attenuators in the individual waveguide feeds.

Modulation and drive equipment. The communications traffic is frequency modulated on a 70 MHz intermediate frequency carrier by equipment installed in the main building. This i.f. signal, at a level of about 0·5 V r.m.s. is fed via the i.f. inter-facility connection to the transmit drive equipment housed in the antenna building. The signal is fed to a varactor diode up-converter which changes the 70 MHz signal to the r.f. transmission frequency in the 6000 MHz band. It is then fed to the main power amplifier at a level of approximately 10 mW. Provision for combining additional outgoing telephony and television carriers is made at this point in the transmit system.

The receiving system. Signals received at the Earth station are within the civil satellite communication band extending from 3700 MHz to 4200 MHz. They are fed via the Cassegrain feed system to a parametric amplifier which has a bandwidth of 500 MHz and is mounted close to the feed.

The amplifier consists of three identical gallium arsenide varactor diode stages, connected in cascade. These three stages are mounted together with their associated circuitry, inside a low-temperature enclosure. Cooling is provided by a closed-cycle cryogenic system which uses gaseous helium, operating at approximately $-257°C$, close to liquid helium temperature. This system has the advantage that it will operate for long periods without any need for topping up. Each of the three stages is fed from a klystron pump source through a 3-way passive splitter.

After amplification, using a low-noise t.w.t. at the receive frequency, the signal is passed via a waveguide connection to the main building and into a passive splitting network with 16 outlets, thereby separating the individual r.f. carriers. The outlets are connected to separate frequency down-converters using a balanced diode mixer with a crystal-controlled local oscillator, followed by i.f. amplification, channel capacity band-pass filtering and group delay equalization.

For telephony traffic, the capacity is 132 channels of 4 kHz bandwidth.

U.D.C. 621.391.812.621 (540)

Some Aspects of Tropospheric Radio-refractivity over India

By

S. C. MAJUMDAR,
M.Sc.(Tech.)†

Summary: Some features of radio-refractivity which are important from engineering point of view are described with reference to published data on radio-refractivity up to a height of 3 km from the surface of the Earth and radiosonde data on pressure, temperature and humidity up to 4·5 km covering a period of five years. Three broad radio-climatic areas having distinct meteorological and refractivity characteristics are delineated. Correlation between surface refractivity N_s and the difference of refractivity over height-intervals of 1 km and 2 km from the surface, designated as ΔN_1 and ΔN_2 respectively, is examined. For coastal areas and islands, correlation with either ΔN_1 or ΔN_2 is found to be poor, while for land-based stations, it is observed to be good. An approximately exponential relationship relates the variation of N_s and ΔN_1. Several models for height variation of refractivity are examined and compared with observed structures. A bi-exponential model for inland region and a two-part model consisting of a linear variation up to 1 km or 1·5 km followed by an exponential variation for coastal areas appear to be satisfactory. The long-term transmission loss predicted on the basis of this model and corresponding observed values in case of one trans-horizon radio circuit are found to be in fair agreement.

1. Introduction

This paper is concerned with radio-climatic features of India based on characteristics of surface radio-refractivity and vertical structure of refractivity. The distribution of refractive index, both surface and upper air, has been studied extensively in a number of countries.[1–5] These studies have proved extremely useful for computing ray-bending, estimation of long-term transmission loss for trans-horizon radio circuits and also long-term variation of this loss. For the sake of simplicity, the vertical variation of refractivity has often been taken into account by an assumed linear gradient, or what amounts to the same thing, by means of an effective radius of Earth equal to $\frac{4}{3}$ times its actual value.[6] However, the actual distribution of refractive index in a number of countries has been found to be substantially different from this assumed distribution.[7]

While investigating characteristics of transmission loss on trans-horizon tropospheric communication circuits, the author observed that the average level of signal was consistently higher than that predicted by '$\frac{4}{3}$-rds effective Earth's radius' model.[8,9] It was also observed that the change of radio-refractivity with height on a number of occasions was substantially different from the expected monotonic decay under ideal conditions. This departure of refractivity variation from uniform lapse-rate appeared to have considerable effect on path-loss. In view of this, the necessity for detailed investigation of the structure of refractive index over this country has been strongly felt. With the publication of a series of papers on 'Radio climatology of India' recently,[4] this requirement has been partially met. However, in order that such data are brought to a form readily usable by communications engineers, it is necessary to examine the refractive index distribution in the background of analytical models and work out simple methods for estimating the long-term characteristics of signal over trans-horizon paths. The aim of the present paper is directed to this end.

2. Source of Meteorological Data

The present investigation covers a period of five years from 1959 through 1963. The surface meteorological data for this study have been collected largely from Reference 4. Upper-air data based on radiosonde ascents were obtained partly from the above Reference and partly from routine publications of the India Meteorological Department. The locations of the radiosonde stations are shown in Fig. 1, using standard abbreviations for the names of the places. The actual names are given in Table 1 along with these abbreviations.

The radiosonde data are usually available up to a height of about 4·5 km. In this paper, values of refractivity up to a height of 3 km for the period 1959–60 given in Reference 4 have been used. The rest of the upper-air data are calculated values derived from radiosonde results. The scaled-up radio refractivity, also called co-index of refraction, is given by

† Radio Development Unit, Civil Aviation Department, New Delhi-23.

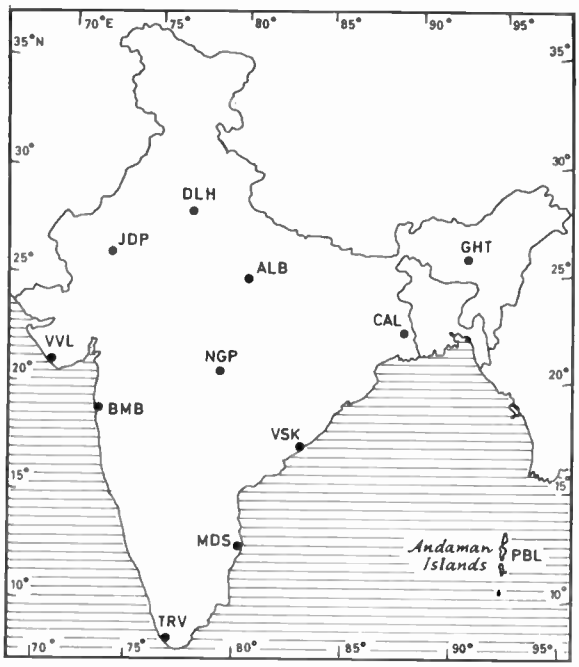

Fig. 1. Radiosonde station location map.

the Smith-Wientraub relationship:[10]

$$N = (n-1)\times 10^6 = \frac{77{\cdot}6}{T}\left(P + \frac{4810}{T}\,e\right), \qquad \text{.....(1)}$$

where N is the radio-refractivity in N-units, n is the radio refractive index, P is the atmospheric pressure in millibars, e is the water vapour pressure in millibars, and T is the temperature in degrees Kelvin.

3. Broad Radio-climatic Divisions in the Country

The broad picture of the climate of a region is determined by its geographical situation and physiographical features. In a published report[11] on weather and climate of India, the country has been divided into five regions with more or less similar patterns of climate and weather. These regions are:

(i) north-west India,
(ii) central India,
(iii) north-east India,
(iv) the plateau region comprising part of Madhya Pradesh and Deccan plateau and
(v) the peninsula consisting of coastal lands and plains.

This division is based on wind circulation, temperature, humidity and rainfall during four well-defined seasons, namely, winter, summer, rains and autumn. During winter, broad pressure distribution can be represented by four major isolines, one along west and south coast, a second across the south-central plateau and eastern coast, a third covering north and north eastern region and a fourth over the north western part. A similar situation approximately holds during summer. The distribution of isothermals in typical winter and summer months shows more or less similar characteristics over the coastal region and southern tip, over the Deccan plateau and eastern coast and over north, central and north-eastern region. Humidity distribution is determined by the distance from the sea and the character of prevailing winds. Humidity is generally lowest in notth-west India and increases towards the sea in all directions. During warm season, relative humidity decreases rapidly from coast to interior and is very low in central and upper India. There is a high degree of turbulent motion in the first kilometre or so in this region. During the winter months, the main features of wind circulation are a slow drain of cold air from north-west in North India, the curving of this air around high-pressure area extending from Gujrat to Orissa and an easterly to north-easterly current in the south of the Bay of Bengal and south of the peninsula. During summer, the major air flow over north and north-eastern part is from north-west and partly from south-west. Over central India and eastern coast, wind-flow is from west and south west, while over the west coast and peninsula, wind direction is towards east and north-east. From the above meteorological features it is fairly clear that the climatic characteristics over the coastal region and adjoining areas are markedly different from those over the inland regions.

In relation to characteristics of tropospheric propagation, radio-climatic features based on refractive-index distribution are more important than meteorological climate. Although radio-climatic condition depends upon meteorological factors, they may not always exhibit identical regional bias since the refractivity is a function of three climatic parameters, namely, pressure, temperature and humidity. A radio-climatic division useful to estimate the gross long-term variability of transmission loss in tropospheric propagation has been attempted here. The characteristics that have been taken into account for this division are: (i) general climatological features such as pressure, temperature, humidity, wind circulation and (ii) the pattern of distribution of annual mean surface refractivity, N_s, and its annual range of variation. The nomenclatures for different radio-climatic areas employed here are the same as used by ESSA.[12]

Figure 2(a) shows the distribution of mean values of N_s over the country in the form of isopleths and Fig. 2(b) presents the mean annual range of N_s. It is interesting to note that the mean as well as the range of N_s are markedly dependent on proximity to sea as is more or less the case with pressure, temperature and humidity. Three types of radio-climates can be distinguished over this country. The coastal areas

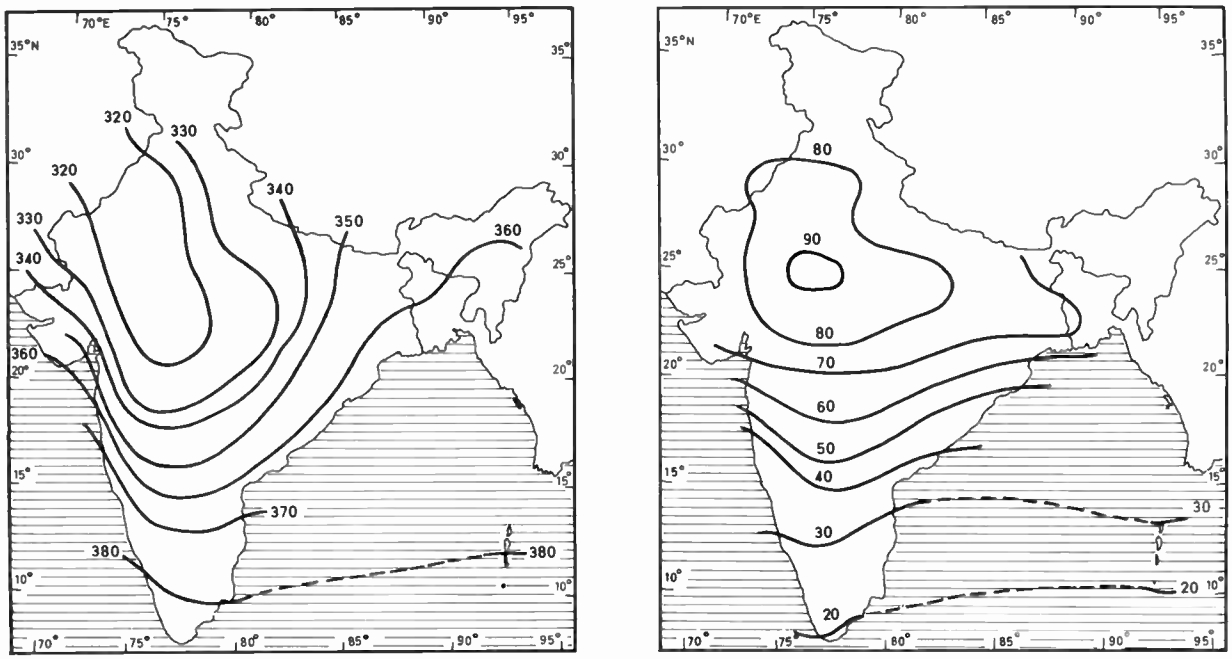

(a) Annual mean values of N_s (N-units).

(b) Annual range of variation in N_s (N-units).

Fig. 2.

south of 20° N latitude and also the ocean islands are characterized by a high annual mean N_s around 380 N-units and an annual range of 10 to 50 N-units. High humidity and low range of temperature-variation are important meteorological features here. Because of the influence of sea-breeze, this radio-climate will be described as maritime sub-tropical oversea climate. Although no clear line of demarcation can be drawn, this climate appears to prevail over the immediate coastal area. The second group comprises inland region not very far from the coast where the annual mean value of N_s is about 350 N-units, while its annual range is 40 to 70 N-units. This area is less humid and variation of temperature is somewhat higher. Winter season is more or less anticyclonic but the pressure comes down during summer. This may be described as maritime sub-tropical overland climate. The third area comprises inland stations in the north and central parts of the country having well-defined winter and summer seasons. The annual variation of humidity is very high in this region. The mean value of N_s here is about 320 N-units and the range is 50 to 90 N-units. This will be described as continental sub-tropical overland climate.

The long-term variability of transmission loss in tropospheric communication circuits has been found by a large number of investigators to be a function of the radio-climate and empirical curves relating this variability for some climates have been published.[12] These curves may be employed to determine the gross variability in this country on the basis of the above radio-climatic divisions. This method may not lead to very accurate results but until actual radio studies are carried out extensively in this country, this method may serve as a basis for planning of radio circuits.

4. Correlation between N_s and ΔN_1 or ΔN_2

As a result of investigations by a large number of workers,[13,14] it has been found that the long-term characteristics of radio wave propagation over trans-horizon tropospheric circuits are correlated well with simple meteorological parameters such as N_s and ΔN_1 (difference of refractivity over 1 km height-interval from the surface). It has also been found that good correlation between signal and N_s is observed in those areas where N_s is correlated with ΔN_1. In addition, studies on correlation of ΔN_1 or ΔN_2 (difference between refractivity at the surface and at 2 km above surface) with N_s give insight into the vertical structure of refractivity. Thus, if the correlation between mean N_s and mean ΔN_1 or ΔN_2 is good, it indicates that the lapse-rate of refractivity with height is uniform and it is possible to derive empirical relationships for predicting ΔN_1 or ΔN_2 from N_s. In fact, this is the starting point for development of a model refractivity atmosphere. To investigate this aspect, correlation coefficients over 12 available radiosonde stations (Fig. 1) in India have been determined. For the purpose of calculation, ΔN_1 and

ΔN_2 have been considered positive, i.e., only the magnitudes have been taken into account, although ΔN_1 and ΔN_2 are decrements and are therefore negative quantities. With this convention, a positive correlation is expected in the ideal case of uniform decrease of N with altitude.

Table 1 gives the correlation coefficients relating monthly average N_s and $\Delta N_1/\Delta N_2$. Sixty monthly mean values over five years for each place were employed to calculate the correlation coefficients. The 95% confidence limits for true correlation coefficient are also given in this Table.

Table 1

Coefficient of correlation between monthly mean N_s and $\Delta N_1/\Delta N_2$

Stations	Coefficient of correlation relating $\bar{N}_s$ with			
	$\Delta\bar{N}_1$		$\Delta\bar{N}_2$	
	Sample correlation	95% confidence limits	Sample correlation	95% confidence limits
Allahabad (ALB)	0·66	0·50/0·79	0·92	0·88/0·95
Bombay (BMB)	−0·53	−0·30/−0·70	0·61	0·44/0·76
Calcutta (CAL)	0·40	0·17/0·60	0·83	0·73/0·89
Delhi (DLH)	0·36	0·12/0·57	0·86	0·78/0·91
Gauhati (GHT)	0·57	0·38/0·73	0·55	0·34/0·70
Jodhpur (JDP)	0·78	0·67/0·87	0·87	0·81/0·92
Madras (MDS)	−0·07	−0·31/0·19	0·34	0·38/0·54
Nagpur (NGP)	0·76	0·64/0·85	0·69	0·54/0·80
Port Blair (PBL)	0·73	0·60/0·83	−0·07	−0·31/0·19
Trivandrum (TRV)	0·70	0·56/0·81	−0·45	−0·22/−0·63
Veraval (VVL)	0·78	0·67/0·87	0·62	0·46/0·77
Visakhapatnam (VSK)	0·11	−0·16/0·35	0·23	00/0·46

Broadly, two distinct areas can be identified from analysis of these results. The first one comprises coastal region and islands, where correlation of N_s with either ΔN_1 or ΔN_2 is poor. An exception in this group is probably Veraval, where correlation appears to be good. In case of Bombay and Madras, correlation with ΔN_1 is actually negative, and in case of Port Blair and Trivandrum, correlation with ΔN_2 is negative. In addition, correlation with neither ΔN_1 nor ΔN_2 is good over Madras and Visakhapatnam. This result leads to the conclusion that the variation of refractivity over the coastal areas and islands does not conform to monotonic decrease with height. This provides indirect evidence about occurrence of super-refractive layers in this region. It is fairly easy to visualize that below the base height of a super-refractive layer, correlation of ΔN up to that height with N_s will be poor. The origin of such layers over coastal areas might be wind-shear or subsidence. Some radio studies made during the past years have established the existence of super-refracting conditions on the western coast.[15] It appears that a similar situation exists over the entire coastal region.

Observations over the inland region are however seen to be different. Here good correlation is observed between N_s and $\Delta N_1/\Delta N_2$. A minor exception in this case is Delhi where correlation with ΔN_1 is somewhat poor. The situation over Calcutta is similar to that over Delhi, but this place might represent the features of both these groups, because of its location near the coast.

It is therefore observed that over the inland region in India, good correlation between N_s and refractivity gradient exists. Under these circumstances, it is possible to derive empirical relationships between N_s and these gradients. These relationships which enable the vertical structure of refractivity to be determined from simple surface data, would be very useful for places where radiosonde data are not available. With this idea, the refractivity data have been examined to determine if they fit in with some theoretical model of variation.

5. Examination of the Vertical Structure of Refractivity against Model Atmospheres

5.1. *The Single Exponential Model*

It has been suggested[16] that the variation of mean refractivity of atmosphere may be approximated by the following exponential relation:

$$N(h) = N_s \exp(-bh) \qquad \ldots\ldots(2)$$

where h is the height above the surface in kilometres and the constant b is determined by the relation:

$$\exp(-b) = 1 + \frac{\Delta N_1}{N_s}, \qquad \ldots\ldots(3)$$

ΔN_1 being considered negative.

On the basis of the exponential decay of refractive index as suggested by eqn. (2), the C.C.I.R. has recommended that the basic reference atmosphere may be defined by the relationship:

$$N(h) = 289 \exp(-0{\cdot}136h) \qquad \ldots\ldots(4)$$

where h is the height in kilometres above mean sea-level.

5.2. *Three-part Model Atmosphere*

Bean and Thayer[1] have worked out a three-part model atmosphere in which the refractivity decreases linearly from surface up to a height of 1 km. The decrease over 1 km, ΔN_1, can be derived from an empirical relationship between N_s and ΔN_1. From 1 km up to a height of 9 km, the refractivity is supposed to vary exponentially in accordance with the following expression:

$$N(h) = N_1 \exp -C[h-(h_s+1)] \qquad \ldots\ldots(5)$$

where $(h_s+1) \leqslant h \leqslant 9$ km, h is height above mean sea level, and h_s is the station elevation above mean sea level in km. The exponent C is given by:

$$C = \frac{1}{8-h_s} \ln \frac{N_1}{105} \qquad \ldots\ldots(6)$$

where N_1 is refractivity at 1 km height above the surface and 105 is the value of refractivity at 9 km above mean sea level, which has been found to be essentially constant. Above 9 km, the decrease of refractivity is exponential again, but the exponent is different from that given by eqn. (6). This portion of the model, however, is not considered here since no observed data above 4·5 km are available.

5.3. *Analysis of Results*

As a starting point, the relationship between monthly mean N_s averaged over a five-year period and corresponding values of ΔN_1 for all the twelve radiosonde stations has been examined. Figure 3 shows a plot of data where ΔN_1 has been given in a logarithmic scale, the bars indicating that mean values have been taken. The relation between $\log_e \overline{\Delta N_1}$ and $\overline{N}_s$ appears to be somewhat diffuse at higher values of N_s. This is a feature for the coastal area. An approximately linear relation, however, exists and permits the following expression for the regression line to be derived.

$$\Delta \overline{N}_1 = 5{\cdot}56 \exp (0{\cdot}0061 \overline{N}_s) \qquad \ldots\ldots(7)$$

Expression (7) would give a very rough estimate of $\Delta \overline{N}_1$ from $\overline{N}_s$ for any particular area because as mentioned in Section 4, the refractivity structure over the coastal area is quite different from that over the mainland. In view of this, it has been considered more realistic to derive different expressions for different areas having distinctive $N_s/\Delta N_1$ relationships. For this purpose, it has been found necessary to divide the country into four areas as follows. The first one comprises the inland stations far away from the influence of the coastal climate. This includes a very large area of the country covering the whole of north and central India. The second group consists of islands (Andamans and the rest) and south coast of peninsula including Trivandrum. The third region covers the coastal areas of Bengal and Orissa and the fourth division consists of south-eastern coast including Visakhapatnam and Madras and the western coast including Bombay. The following relations based on least square fits have been derived for these different regions.

(a) For inland stations:

$$\Delta \overline{N}_1 = 3{\cdot}49 \exp (0{\cdot}0074 \overline{N}_s) \qquad \ldots\ldots(8)$$

(b) For islands and south coast:

$$\Delta \overline{N}_1 = 7{\cdot}12 \exp (0{\cdot}0054 \overline{N}_s) \qquad \ldots\ldots(9)$$

(c) For eastern coast:

$$\Delta \overline{N}_1 = 11{\cdot}53 \exp (0{\cdot}0039 \overline{N}_s) \qquad \ldots\ldots(10)$$

For the western and south-eastern coast, the approximate relationship given by eqn. (7) may be accepted as a very gross estimate, and in view of poor correlation, a more accurate expression for $\Delta \overline{N}_1$ cannot be derived. For greater accuracy, it will be necessary to employ the observed average values of ΔN_1 based on radiosonde data.

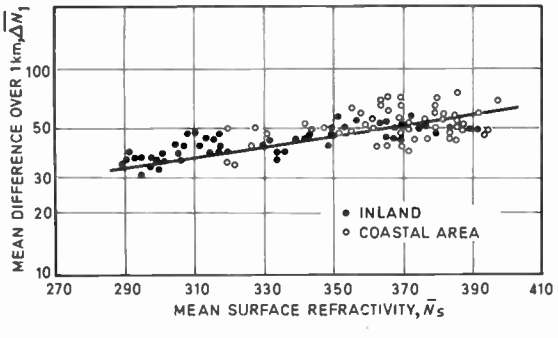

Fig. 3. Regression line of ln $\overline{\Delta N_1}$ vs. N_s.

As the single exponential model is simple and is a continuous function of height, the validity of this model in relation to observed structure has been determined first. Equations (2), (3) and one of the expressions out of (8), (9) and (10) depending upon the area considered describe the structure predicted by this model. The values of refractivity at 1·5 km and 3 km above the surface given by the model have been compared with observed five-year average monthly mean values. Figures 4(a) and 4(b) give the results for the inland region north of 20°N latitude. Unfortunately, no radiosonde station far from the coast south of 20°N latitude is available and therefore no upper-air data for this region could be obtained. Figure 4(a) depicts the results at 1·5 km. It is seen that the agreement between the predicted and observed values is fairly close. For observed co-index of up to 270 N-units, the predicted values are slightly higher and above 270 N-units, predicted values are somewhat lower. The root-sum-square of deviations of predicted from observed values is 5·5 N-units. For N (3 km), a

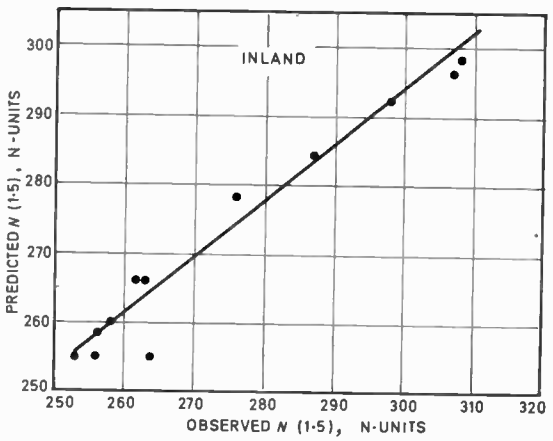

(a) Predicted vs. observed mean refractivity at a height of 1·5 km (inland region).

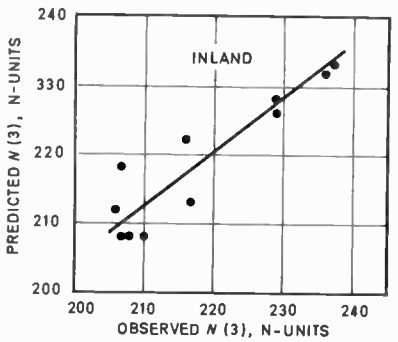

(b) Predicted vs. observed mean refractivity at a height of 3 km (inland region).

Fig. 4.

similar trend as for N (1·5 km) is observed around 220 N-units. The single exponential model given by eqns. (2), (3) and (8) is, therefore, applicable up to 3 km for this region. Above 3 km, observed data are available at a height of about 4·5 km and it has been found that at this height, the agreement is not very satisfactory. As a further check as to the validity of the single exponential model at higher altitudes, the value of N at 9 km above mean sea level has been worked out and found to be 80 N-units. However, it is known from both theoretical considerations and actual observations[1] that at an altitude of 9 km the co-index of refraction assumes almost a constant value of 105 N-units. This applies irrespective of climatic condition and geographical location. Therefore, above 3 km, the single exponential model cannot give satisfactory results.

Results for other areas are given in Table 2. Here, the monthly mean observed values at 1·5 km and 3 km have been compared with predicted values given by the respective models. In case of south east/west coast, since there is no specific $\Delta N_1/N_s$ relationship, expression (7) has been employed for the model ΔN_1.

Table 2

Validity of single exponential model for coastal areas and islands

Region	R.m.s. deviation of observed monthly mean value of N from predicted N, (N-units) at	
	1·5 km	3 km
South coast and islands	5	12·6
East coast	10	18·2
South-east/west coast	17	14·6

From this Table it is seen that for the south coast and islands, the agreement between predicted and observed values at 1·5 km is fairly close but at 3 km there is considerable amount of divergence. For the other coastal areas, it is observed that deviation at both 1·5 km and 3 km is quite considerable. It is concluded, therefore, that the single exponential model for the decay of radio-refractivity is applicable to the inland region up to an altitude of 3 km and to the south coast and islands up to 1·5 km.

Next, the applicability of a two-part model atmosphere of a type similar to that discussed in Section 5.2 has been examined. As has been already mentioned, a single exponential variation up to 3 km is adequate for the inland region. A second segment of exponential decay in accordance with eqn. (5) has been found satisfactory above 3 km. Table 3 gives the root mean square deviations of the monthly average values from predicted values based on the bi-exponential model. The deviations at standard heights of 1·5 km, 2 km, 3 km and 4·5 km are shown here. The predicted structure is seen to be in close agreement with the observed structure. Unfortunately however, no observed data above 4·5 km were usually available and consequently, this analysis has been limited up to a height of 4·5 km.

For the south coast and islands, since the exponential variation has been found satisfactory only up to a height of 1·5 km, a two-part model with linear variation from N_s to N_1 as predicted by eqn. (9) followed by exponential variation given by eqn. (5) has been employed. The departure of the observed structure of refractivity from the values given by the model are shown in Table 3. Results show that the model is satisfactory.

In case of the eastern coast and the south-east/west coast, it is seen from Table 2 that the exponential model based on eqns. (2), (3), (7) and (10) do not give very satisfactory results right from an altitude of 1·5 km onwards. To get better results, it has been found necessary to use the observed values of co-index up to a height of 1·5 km, for it is up to this height that super-refractive layers appear to exist more frequently thereby affecting the correlation between N_s and ΔN up to this height. The model of gross variation in this case consists of a linear segment from N_s up to observed $N_{1\cdot5}$ and thereafter an exponential variation given by:

$$N(h) = N_{1\cdot5} \exp -p[h-(h_s+1\cdot5)] \quad \ldots\ldots(11)$$
$$(h_s+1\cdot5) \leqslant h \leqslant 9 \text{ km},$$

where p is given by:

$$p = \frac{1}{7\cdot5-h_s} \times \ln \frac{N_{1\cdot5}}{105} \quad \ldots\ldots(12)$$

Table 3 shows the departure of observed refractivity from predicted values given by this model at 3 km and 4·5 km for these areas. The model appears to be satisfactory at these altitudes.

Table 3
Observed refractivity structure against predicted structure by models

Region	Type of model	R.m.s. departure in N-units at			
		1·5 km	2 km	3 km	4·5 km
Inland	Bi-exponential with one segment up to 3 km and another above 3 km	5·5	4·5	5·0	4·0
South coast and islands	Linear variation up to 1 km and exponential above 1 km	3·0	4·0	6·0	5·5
East coast	Linear variation up to 1·5 km and exponential above 1·5 km		4·0	5·0	4·5
South-east/ west coast	Same as that for East coast		5·0	6·0	5·5

It is concluded from these results that except for the lower troposphere in some coastal areas, a two-part model can be adjusted to fit in with the observed structure of co-index of refraction up to at least 4·5 km all over the country. For the major part covering stations away from coast, a bi-exponential model works out well. For coastal areas, the model allows linear variation for the gross structure up to 1 km or 1·5 km and exponential variation thereafter.

It would be interesting to compare the values of refractivity given by the C.C.I.R. basic reference atmosphere (eqn. (4)) with the observed values. According to expression (4), the sea-level refractivity is 289 N-units and is lower than the long-term average surface value observed almost everywhere in the country. Only in the arid zones where refractivity is lowest, long-term average N_s has been found to be near this value. The sea-level refractivity N_o corresponding to surface refractivity N_s is given by[17].

$$N_o = N_s \exp(0\cdot1057h_s), \quad \ldots\ldots(13)$$

where h_s is the station elevation above mean sea level in km. The calculated long-term average value of N_o from eqn. (13) has been found to be higher than 289 N-units in all parts of the country.

6. Test for Validity of the Proposed Models

As a critical test for validity of these models, actual radio experiments have been carried out over an air/ground radio circuit extending up to a distance of nearly 700 km. This circuit is situated in the inland region over Delhi/Calcutta airway with Delhi as the fixed terminal. The long-term transmission loss observed over this path has been compared with values predicted by means of empirical formulas which could be adjusted for observed values of N_s and ΔN_1 given by the model. The prediction procedure was first established by examining an empirical formula based on N_s and then the degree of success achieved with a prediction technique based on model ΔN_1 showed to what extent the proposed model was valid.

The ground-based radio facilities at Delhi consisted of a v.h.f. (120 MHz) transmitter with a nominal carrier output of 1 kW, a receiver having a noise-limited sensitivity of 0·5 μV with a 10 dB signal/noise ratio, and an antenna system for transmission/reception with a gain of 20 dB over an isotropic radiator. The 3-dB azimuthal beamwidth of the antenna was 48° and vertical beamwidth was 7·5°, the beam-maximum being directed towards the horizon with an orientation 117° relative to north from Delhi. Transmissions sent from aircraft at trans-horizon distances were received at Delhi and transmission loss was worked out in each case. The parameters of path geometry such as horizon distances, angular distance etc. were determined for each position of the aircraft. Observations have been made for a period of three years from June 1964 through May 1967. The long-term monthly median basic transmission loss from these data have been compared with the predicted loss on the basis of five-year mean radio-refractivity structure as discussed in the foregoing paragraphs.

At great distances beyond the radio horizon, the reference value of long-term transmission loss is given

as a function of N_s by[12]:

$$L_{bsr} = 30 \log f - 20 \log d + F(\theta.d) - F_o + H_o \text{ dB} \quad \ldots\ldots(14)$$

where L_{bsr} is the reference value of long-term median basic transmission loss, f is frequency in MHz and d is the path length in km. The function $F(\theta.d)$ is a function of the product of angular distance in the great circle plane in radians and path length d in km—the value of this expression being adjustable for observed value of surface refractivity N_s. The last two terms in eqn. (14), namely F_o and H_o, are respectively the scattering efficiency correction term and frequency gain function. The predicted median long-term basic transmission loss, $L_n(50)$ is given by:

$$L_n(50) = L_{bsr} - V_n(50 d_e), \quad \ldots\ldots(15)$$

where the correction term $V_n(50 d_e)$ is a function of effective distance d_e and depends upon the radio-climate of the area. The value of the correction term was experimentally determined in this case. This was done by subtracting from the value of path loss realized under well-mixed condition of the medium (afternoon hours) the transmission loss not exceeded by 50% of observations during all hours. The predicted $L_n(50)$ was then compared with observed long-term median basic transmission loss.

The long-term reference median basic transmission loss as a function of ΔN_1 is given by:

$$L_{bsr} = 131{\cdot}4 + 30 \log f + 35 \log \theta + 15 \log d + 0{\cdot}27(\theta.d) - b[(N_1) - 39{\cdot}23] \text{ dB} \quad \ldots\ldots(16)$$

where the symbols have the same meaning as in eqn. (14) and b is the change of transmission loss in dB per unit change of ΔN_1, and has been found to be nearly 0·5 dB per N-unit during this and some earlier investigations.[18] To calculate $L_n(50)$, the same correction as given in eqn. (15) was applied.

It is not possible to go into the details of the prediction procedure here. The essential features are, however, as follows. The prediction process depends upon correlation between transmission loss and meteorological parameters concerned namely, N_s and ΔN_1. It was observed that correlation coefficient of monthly median transmission loss with monthly average N_s at Delhi was about 0·60 and that with observed ΔN_1 was about 0·85. The corresponding 95% confidence limits were 0·38 and 0·75 for N_s and 0·77 and 0·90 for ΔN_1. It was in fact observed that the annual cycle of variation of monthly medians could not be predicted well by N_s but very good correlation was observed between N_s and the maximum and minimum monthly medians. Thus, the best and worst months could be identified by the highest and lowest monthly mean values of N_s. In course of three years' radio studies, it was found that the maximum signal occurred in August which coincided with maximum monthly mean N_s and the minimum signal occurred either in April or May during which a trough occurred in N_s-pattern. The monthly median radio data are given in the Appendix.

As regards ΔN_1, it was found possible to work out the annual cycle of monthly median signal with its observed value. In this paper, the signal level during the best and worst months predicted by means of eqns. (14) and (16) are presented. Figure 5 depicts the predicted and observed long-term monthly median basic transmission loss as a function of angular

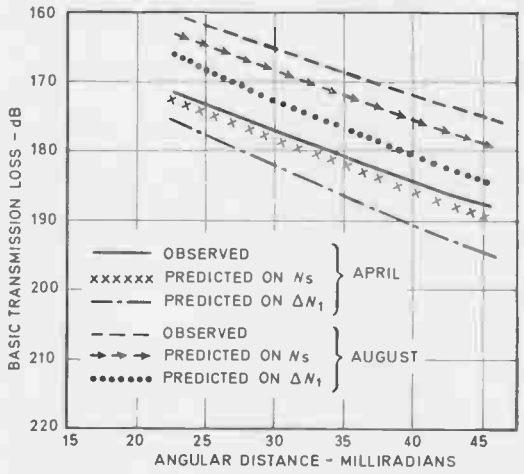

Fig. 5. Observed and predicted monthly median basic transmission loss on the basis of observed mean N_s and model ΔN_1.

distance for the months of August and April. It is seen from this figure that the predicted long-term monthly median on the basis of observed average N_s agrees very well with the observed loss levels during the best and worst months. The predicted curves based on model ΔN_1 given by relation (8) show that although these do not agree with observed loss level as closely as those on the basis of N_s, they are at least within 10 dB of each other at all angular distances. The results of the radio experiment consequently provide additional evidence for the validity of the model for the inland region.

7. Conclusions

It is concluded that from radio-meteorological point of view, India can be broadly divided into the following three regions having the following climates: (i) maritime sub-tropical oversea, (ii) maritime sub-tropical overland and (iii) continental sub-tropical overland. This division is useful for planning of radio circuits since the long-term variability of transmission loss in a tropospheric circuit is primarily dependent

upon radio climate. It has been observed that the variation of radio-refractivity with height is fairly uniform overland but at and near the coastal regions, the lapse-rate is substantially different in nature. Models for height-variation of refractivity have been developed for different areas. A two-part exponential model with one segment from surface to 3 km and another above 3 km has been found to agree with observed decay of refractivity. The predicted long-term radio transmission loss on the basis of this model conforms to observed values over a trans-horizon tropospheric circuit fairly well. For the coastal regions and islands, a two-part model consisting of a linear initial decay of N followed by an exponential decrease is found to be satisfactory.

8. Acknowledgment

The author is grateful to Dr. Saroj Dutta, Director of Communications, Civil Aviation Department, for his valuable guidance in this work.

9. References

1. Bean, B. R. and Thayer, G. D., 'Models of the atmospheric radio refractive index', *Proc. Inst. Radio Engrs*, **47**, pp. 740–55, May 1959.
2. Bean, B. R., 'The radio refractive index of air', *Proc. I.R.E.*, **50**, pp. 260–73, March 1962.
3. Lane, J. A., 'The radio refractive index gradient over the British Isles', *J. Atmos. Terrestr. Phys.*, **21**, p. 157, June 1961.
4. Kulsrestha, S. M. and Chatterjee, K., 'Radio climatology of India', *Indian J. Met. Geophys.*, Part 1, **17**, No. 2, 1966; Part II, **17**, No. 4, 1966; Part III, **18**, No. 2 1967; Part IV, **18**, No. 3, 1967.
5. Bean, B. R., 'The geographical and height distribution of the gradient of refractive index', *Proc. I.R.E.*, **41**, pp. 549–50, April 1953. (Letters).
6. Schelleng, J. C., Burrows, C. R. and Ferrel, E. B., 'Ultra-short wave propagation', *Proc. I.R.E.*, **21**, pp. 427–32, March 1933.
7. Misme, P., 'Influence of the equivalent gradient and of the atmospheric stability on transhorizon links in the Sahara and the Congo', *Ann. Telecomm.*, **16**, pp. 110–16, May–June 1961 (in French).
8. Majumdar, S. C., 'Investigation of extended range vhf propagation through troposphere', *J. Instn Telecom. Engrs (India)*, **12**, pp. 376–90, July 1966.
9. Majumdar, S. C., 'Transhorizon vhf propagation over ground/air paths, *J. Instn Telecom. Engrs (India)*, **13**, pp. 229–39, June 1967.
10. Smith, E. K., Jr. and Wientraub, S., 'The constants in the equation for atmospheric refractive index at radio frequencies', *Proc. I.R.E.*, **41**, pp. 1035–7, August 1953.
11. Basu, S., 'Gazetteer of India', Chapter II, pp. 1–45, 1966.
12. Rice, P. L., Longley, A. G., Norton, K. A. and Barsis, A. P., NBS Technical Note 101, Vols. 1 and 2, 1967.
13. Bean, B. R. and Meaney, F. M., 'Some applications of the monthly median refractivity gradient in tropospheric propagation', *Proc. I.R.E.*, **43**, pp. 1419–31, October 1955.
14. Bean, B. R. and Cahoon, B. A., 'Correlation of monthly median transmission loss and refractive index profile characteristics', *J. Res. Nat. Bur. Standards*, **65-D** (Radio Propagation), No. 1, pp. 67–74, January 1961.
15. Booker, H. G., 'Outline of Radio Climatology in India and Vicinity', T.R.E. Report No. T 1727, 1944.
16. 'Reference Atmospheres', Report No. 231, C.C.I.R. documents of the Xth plenary assembly, Geneva, 1963. Volume II, Propagation, pp. 74–5.
17. 'Influence of the Atmosphere on Wave Propagation', Report No. 233, C.C.I.R. documents of the Xth plenary assembly, Geneva, 1963. Volume II, Propagation, pp. 76–120.
18. Majumdar, S. C., 'Characteristics of vhf propagation at 50 km beyond radio horizon', *J. Instn Telecom. Engrs (India)*, **14**, pp. 451–7, October 1968.

10. Appendix

Monthly Median Transmission Loss at 45 mrad and Monthly Average Refractivity Data

1964 Months	Basic transmission loss L_b, dB	N_s (Delhi) N-Units	Observed ΔN_1 (Delhi) N-units
June	181	322	37·0
July	179	370	44·5
August	173	378	46·5
September	180	363	44·0
October	182	332	37·0
November	179	316	42·5
December	178	313	41·5
1965			
January	177	314	41·0
February	182	311	38·5
March	184	298	29·0
April	186	300	29·0
May	187	306	30·0
June	182	320	36·0
July	179	368	45·0
August	176	375	47·0
September	180	364	43·0
October	181	336	37·5
November	178	318	43·0
December	177	314	40·0

1966 Months	Basic transmission loss L_b, dB	N_s (Delhi) N-Units	Observed N_1 (Delhi) N-Units
January	176	316	39·0
February	181	310	37·5
March	184	295	30·0
April	188	302	30·5
May	183	305	31·5
June	180	318	35·0
July	175	365	44·0
August	176	374	46·0
September	179	365	44·0
October	182	337	39·0
November	179	320	44·0
December	177	315	41·0

1967 Months	Basic transmission loss L_b, dB	N_s (Delhi) N-Units	Observed N_1 (Delhi) N-Units
January	177	312	41·5
February	183	310	40·0
March	185	300	29·0
April	189	297	2·80
May	183	308	29·0

Manuscript first received by the Institution on 20th January 1969 and in final form on 1st April 1969. (Paper 1274/Com. 20.

Acoustics the Key to Further Miniaturization?

The wavelength of sound waves in solids is about one hundred thousand times smaller than the wavelength of electromagnetic waves at the same frequency. This fact implies that true microminiaturization has not yet reached industry, and is only waiting for the appropriate acoustic-wave circuits to be devised.

An outline of the present effort in a microwave approach to guided acoustic waves is to be given in a survey lecture at the European Microwave Conference to be held at the Institution of Electrical Engineers, Savoy Place, London, W.C.2, from the 8th to 12th September.

The lecture will be given by Dr. A. A. Oliner of the Polytechnic Institute of Brooklyn, New York, U.S.A. as part of a complete session devoted to microwave acoustics. This is believed to be the first occasion at which this increasingly important aspect of microwave technology will be discussed in depth at a European conference on microwaves.

The conference is the first of a proposed biennial series on microwaves which will alternate with the now well-established microwave and optical generation and amplification conference (MOGA) first held in 1956. It is expected that over 600 delegates will be attending the conference.

In addition to the session on microwave acoustics there will be others (some held in parallel) on:

microwave networks and integrated circuits
ferrite devices
microwave antennas
microwave measurements
computer techniques
scanning and active antennas
low-noise receiving and amplifying devices
filters and directional couplers
control and switching devices
transferred electron devices
microwave and optical waveguide components
avalanche diode generation.

Organized by the I.E.E. the conference is being held in association with the Institution of Electronic & Radio Engineers and the Institute of Electrical & Electronics Engineers. Further details and registration forms are now available from the Conference Department, I.E.E., Savoy Place, London, W.C.2.

U.D.C. 621.37/8:681.26

Weighing Vehicles in Motion

By

A. C. FERGUSON†
B.Sc., C.Eng., M.I.E.E.

Reprinted from the Proceedings of the Conference on 'Electronic Weighing' held in London on 30th-31st October 1968.

Summary: Weighing objects in motion poses problems which are quite distinct from those encountered in static weighing. Until recently no serious attempt had been made to tackle these problems.

The paper discusses the weighing errors caused by the motion of the object being weighed. Methods of reducing these errors are described and an assessment is made of the effectiveness of these methods.

A novel approach to this problem is outlined with graphs of performance. Results obtained by this approach are compared with those obtained by current methods.

1. Introduction

Accurate weighing is essential in many continuous processes and the process efficiency is reduced considerably due to speed limitations imposed by the weighing operation, in many cases requiring complete stoppage of the process. A long weighing period is necessary because of vibrations associated with the motion of the object being weighed. These vibrations are superimposed on the true weight of the object and a considerable 'smoothing' period is required to obtain an accurate estimate of weight.

Using bonded or unbonded strain-gauge load cell transducers, a weight indication can be obtained in a few milliseconds, and this indication can represent accurately the instantaneous force on the transducers. Hence it would appear that articles can easily be weighed in motion, to a high accuracy in a short period of time. The flaw in this assumption lies in the vibration associated with the motion of the article. The instantaneous force on the transducers comprises a force equivalent to the true static weight together with a vibrating component. The amplitude of the latter will determine the accuracy of weighing which can be guaranteed. Obviously the indication obtained can differ from the true static weight by the peak amplitude of the vibration. To obtain an accurate indication of weight therefore, some means of attenuating this vibration is necessary.

2. Methods of Dynamic Weighing

The vibrations associated with an article in motion can be divided into two categories, those originating within the weighing equipment and those originating within the article being weighed. The former are caused by the impact of the article on the weighing machine platform and the vibration frequencies are a function of the stiffness of the weighing machine. By designing the weighing machine to have a high stiffness and therefore a high natural frequency, these impact vibrations can be attenuated quite simply by conventional means. A short delay would normally be introduced after impact before the commencement of weighing. In this way the initial peak value of the transient impact vibration would be avoided. Then with careful design of the means of transfer of the article on and off the weighing machine platform, virtual elimination of the impact vibration effects can be obtained.

2.1. *Errors in Dynamic Weighing*

Significant reduction of the errors due to continuous vibrations inherent in the vehicle being weighed may not be so easily accomplished. Where the period of the vibration is very short relative to the available weighing time, conventional filtering techniques should prove effective but where the vibration period is comparable with the weighing period, known techniques are inadequate.

Investigations into rail vehicle dynamic characteristics have shown that at speeds of 8 km/h (5 mile/h) vibrations with frequencies as low as 2·5 Hz can be obtained with amplitudes approaching 10% of the vehicle weight.

Obviously, weighing accuracy must be guaranteed to much better than 10% if the weight measurement is to be at all worthwhile. If we consider 0·25% to be a reasonable guaranteed figure for accuracy in dynamic weighing, then 0·1% should be attainable without too much difficulty. There will be sources of error in addition to those due to vibration and so an attenuation of at least 200 : 1 would be desirable.

In Fig. 1 is shown the weight signal generated by a load cell contained within a weighing structure having a high natural frequency of resonance. This shows that on arrival of the first axle of the vehicle on the weighing machine platform there is an initial transient period. Following this transient period, there is the weighing

† Development Unit, W. & T. Avery Ltd., Tame Bridge, Walsall, Staffordshire.

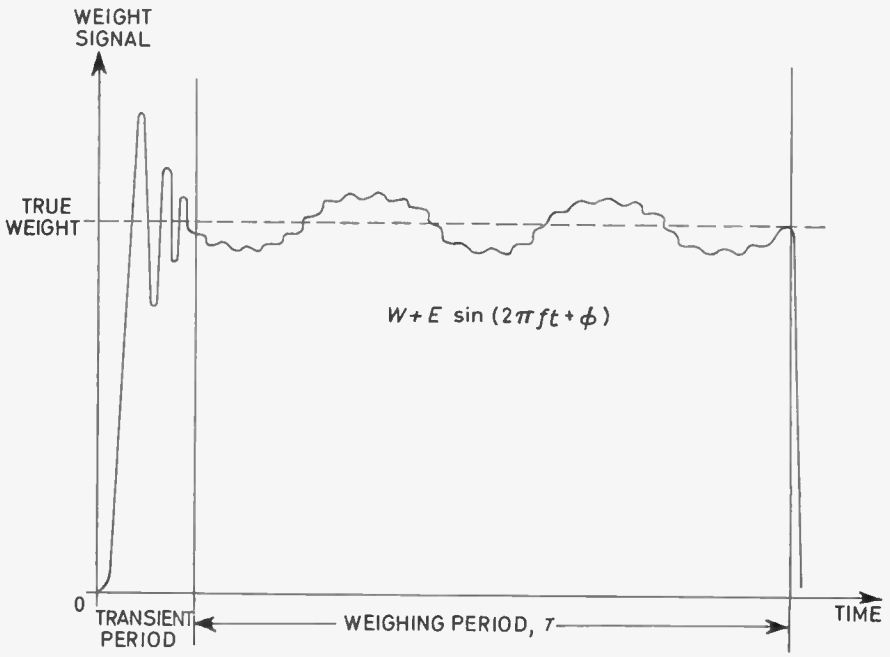

Fig. 1. Weight signal generated by transducers.

period T during which the signal comprises a steady value representative of the true static weight of the axle plus a fluctuating component. In practice, the fluctuating vibration will contain several components of different frequencies. However, the principle of superposition will hold on all methods of vibration attenuation to be considered and so the various components can be treated independently. Assuming therefore, that the vibration comprises a simple sinusoid of frequency f Hz of peak amplitude E, it can be expressed mathematically as $E \sin(2\pi ft+\theta)$ where θ is the phase angle at time $t = 0$.

In order to introduce some practical meaning into the evaluations, weighing period T will be made 1 second, the ratio of the vibration amplitude to the true static weight signal, E/W, will be assumed 1/10, the vibration frequency will be taken as $2\frac{1}{2}$ Hz, and a required weighing accuracy of 0·1 % will be assumed.

2.2. *Performance of Basic Filter*

To illustrate the problems associated with obtaining adequate attenuation of such low frequency vibrations, the capability of a conventional R-C filter will be considered. The weight signal is assumed to be presented to the network at the beginning of the weighing period T and the charge on capacitor C is assumed to be initially at zero. Choosing the time-constant or CR value for the filter which will give the minimum deviation from true static weight merely comprises obtaining the optimum compromise between rise-time and attenuation. In Fig. 2, V is a plot of the deviation from unity of the output level, 1 second after the application of a unit step function for different CR values. The minimum value is 0·2s giving a maximum attenuation of $2\frac{1}{2}$. Thus if the vibration amplitudes were 10% of the true static weight, an error of about 4% could be obtained, about 40 times the acceptable level of error.

2.3. *Active Filters*

With a simple R-C network a poor result may be expected and greater attenuation can be obtained by using more sophisticated filters. A disadvantage of conventional filters when dealing with such low frequencies lies in the values of lumped constants required. This disadvantage can be overcome by using active filters.

The conflicting requirements of fast response and high attenuation at low frequencies still apply. Because of these requirements, increasing the order of the filter improves performance up to a point but from then on the performance will deteriorate as the order of the filter is increased.

The optimum design of a particular type of filter depends on the specified operating conditions such as the frequency and magnitude of the ripple components and the maximum acceptable time delay. For the conditions specified in dynamic weighing, a reasonable design would comprise a maximally flat Butterworth filter of fourth-order. With such a filter, an attenuation of about 7 could be obtained which is still far short of dynamic weighing requirements.

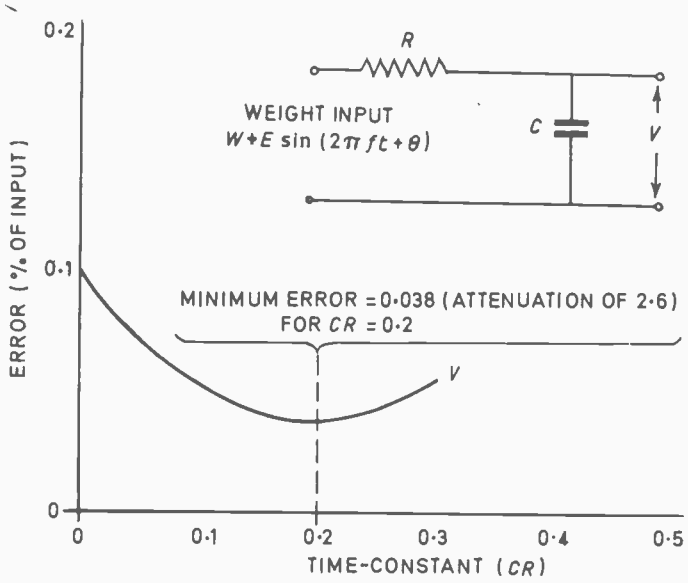

Fig. 2. Simple R-C filter.

Higher attenuation can be obtained by allowing some overshoot in the filter response. In such a filter, the ripple contained by the input signal is heavily attenuated, but the amplitude of the overshoot introduces an additional error. This error must be included in calculating the effective attenuation so that a meaningful performance comparison can be drawn with other techniques.

The overshoot error can be removed by sampling the filter output as it passes through a zero overshoot point. The error will then depend solely on the phase and amplitude of the attenuated ripple. In such a filter the parameters must be closely controlled as also must be the time delay between applying the weight signal to the filter and sampling the filter output. If, for example, a second-order filter were designed with a damping factor of 0·5 and a time-constant of 3·3 seconds, the first zero overshoot point would occur 1 second after application of the input signal. Under such conditions an effective attenuation of 50 would be obtained but an error in time delay of only 1 % would reduce this attenuation to 2½. To ensure an attenuation of 25 would require the time delay and the gain and time-constant of the filter to be controlled to within 1 part in 2000.

Significant effective attenuation, namely, of the order of 200 does not seem practicable with this approach.

2.4. *Straight Integration*

A method widely adopted to reduce errors due to vibration is to integrate the weight signal over the weighing period. This is done by analogue integration or by digital averaging. In principle the effect of both can be deduced mathematically by integrating with respect to time over the weighing period T and dividing by time T.

A convenient term specifying the efficiency of a system in terms of reduction of vibration is vibration attenuation defined as the ratio of the peak of the vibration (E) to the error resulting from the vibration.

In this case vibration attenuation, with worst phase conditions, is given by:

$$A = \frac{\pi N}{\sin \pi N} \qquad \ldots\ldots(1)$$

where N represents the number of cycles of vibration within the weighing period.

The curve of the single sample in Fig. 3 shows the reciprocal of the attenuation of vibration obtained with straight sampling or integration. This characteristic shows the general increase in attenuation with N and points of infinite attenuation when whole numbers of cycles of the fundamental vibration are contained within the weighing period. In the practical case, the attenuation obtained would be modified by the presence of vibration frequencies other than the simple sinusoid whose effect has been plotted. The effect of these higher frequencies would have to be taken into account and would prevent attenuation from approaching infinity.

The range of frequencies encountered in dynamic weighing applications extends down to 2½ Hz. A realistic comparison can be drawn between the effectiveness of various weighing systems by comparing their attenuation of the most significant fundamental frequency present in this range.

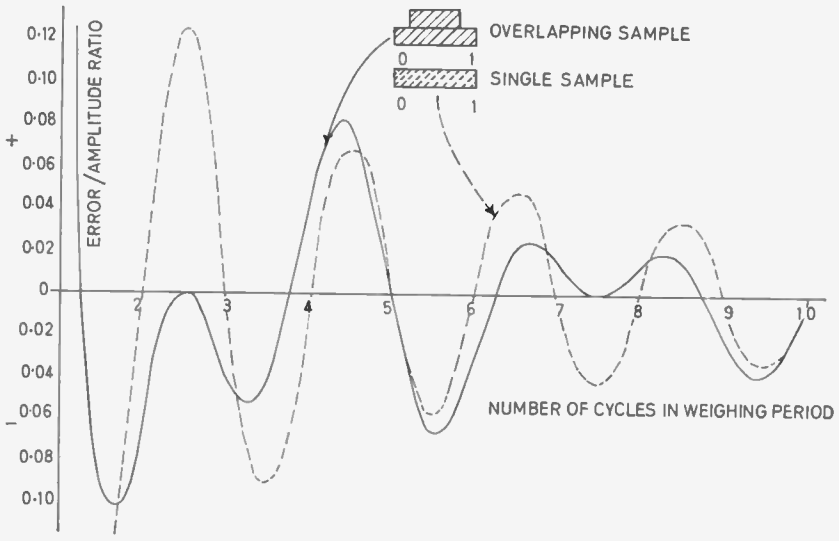

Fig. 3.
Attenuation characteristic—overlapping samples.

The lowest attenuation would in fact be obtained with a sinusoid of frequency 2½ Hz within a weighing period of one second.

Substituting these values in equation (1)

$$A = \frac{\pi 2{\cdot}5}{\sin \pi 2{\cdot}5} = 7{\cdot}86$$

If the amplitude of the vibration in this case were ±10% of the true static weight, the resulting error would be ±1·27% of the true weight.

For any simple sine-wave, a weighing period can be chosen to yield infinite attenuation[4] but comparison between systems is by means of the most significant frequency component in the range, not merely the lowest frequency component.

In the above case for example, integration over 0·4 s would eliminate the effect of the 2½ Hz component. The most significant frequency would then no longer be 2½ Hz and in fact, a lowest attenuation figure of less than 7·86 would be obtained.

Such errors are incompatible with the desired accuracy of dynamic weighing systems and so an investigation was initiated into ways and means of evolving a really effective method of vibration attenuation.

The limitations of conventional low-pass filtering and straight integration or averaging can now be seen. Obviously, a more elaborate approach is required if acceptable dynamic weighing performance is to be attained.

2.5. *Filter-Integrator Combination*

Most of the dynamic weighing systems known to be in use[1–9] combine low-pass filters and integrators. This combination has inherent advantages bearing in mind that a wide range of vibration frequencies may be present. Although the main problem is to attenuate the low frequencies, the higher frequencies cannot be neglected. Having a low-pass filter, whose attenuation increases with rise in frequency, deals effectively with the higher frequencies.

Quite reasonable results have been obtained with filter-integrator combinations. In one application of such a network,[2] an attenuation of over 130 : 1 is obtained, assuming the lowest vibration frequency to be slightly in excess of 3 Hz. To obtain this attenuation, a weighing period of 3 seconds is required. The signal is fed into a filter network which carries out an 'imperfect integration'. After 2 s, the vibration has been attenuated by about 13 : 1. This output is then integrated for 1 s, giving an overall attenuation of 133 : 1. With a weighing period 3 s only very low speeds would be possible or in the case of uncoupled vehicles, a very long weighing machine platform would be required. If this system were applied over a weighing period of only 1 s with vibration extending down to 2½ Hz, the performance would hardly be satisfactory. Some indication of the possible degradation in performance can be obtained by considering the effect of a reduction in integrating period. This period is normally 1 s, which with an assumed minimum vibration frequency of 3·2 Hz, gives an attenuation of about 10. Reducing the integration period to 0·33 s and extending the vibration range down to 2½ Hz would produce an attenuation of 2·6. The attenuation introduced by the integrator has thus been reduced by 10/2·6, almost 4 to 1. If the filter attenuation is reduced in the same proportion, the overall attenuation would then be less than 10.

Hence, if a filter-integrator combination is to be used, one or both components must be improved beyond what has been obtained in this case.

2.6. *Pre-set Filter*

Earlier, the limitations of the simple R-C filter were discussed. The major shortcoming in this unit is the difficulty of obtaining an acceptable response together with adequate attenuation. A significant improvement in performance could be obtained by using the initial weight signal transient to pre-charge the filter output capacitor through a low impedance.

An approximate value for the true static weight level is estimated from the peak value of the initial transient signal. The capacitive element of the filter is then charged to this estimated value during a short period immediately following the transient peak. The capacitor is charged from a low impedance source and hence reaches the pre-set level in a short period of time. The filter response can now be modified due to the much lower rate of response required. The overall system is illustrated in Fig. 4.

The electrical output from the load cells (4) is fed into a filter comprising impedance Z1, and capacitor C. The input is also fed to a peak detecting and storage circuit and a pre-set attenuator.

A switch S1 is actuated by passage of the vehicle axle on to the weighing platform. The switch is connected to a single pulse generator which closes switch S2 for a pre-set period of time. While the switch is closed, the capacitor C_2 is charged, via a relatively short time-constant circuit, to a voltage approximating to that representing the correct weight on the axle. Shortly before the axle reaches the end of the section 3, the voltage on the capacitor will have changed to a value much closer to the true weight, due to the integrating action of the filter on the load cell output voltage.

The pre-set filter is really a two-step variable filter tailored to suit a particular application, and capable of quite high attenuations. Filters with time-constants varying continuously from a low to a high value can also produce good attenuation figures. Precise prediction of the performance of such filters is extremely difficult and estimation by experimental methods is very time-consuming.

2.7. *Stepped Weighting Function*

Applying straight integration over a weighing period of 1 s, with a range of vibration frequencies extending down to 2½ Hz, the fundamental sinusoid producing the lowest attenuation would be of frequency 2½ Hz. Earlier, it was shown how the effect of this component could be eliminated by suitable choice of weighing or integrating period. With this method, lowest attenuation occurred at another frequency and the attenuation obtained was no better than that obtained by integrating over the full weighing period.

A significant improvement in attenuation can be obtained by integrating over two periods. As shown in Fig. 5(a), the periods T_1 and T_2 are each of length 0·8 s overlapping each other by 0·6 s.

If digital sampling were employed over a period of 1 s, a similar effect could be obtained by doubling the sampling rate from $t = 0{\cdot}2$ s to $t = 0{\cdot}8$ s as shown in Fig. 5(b).

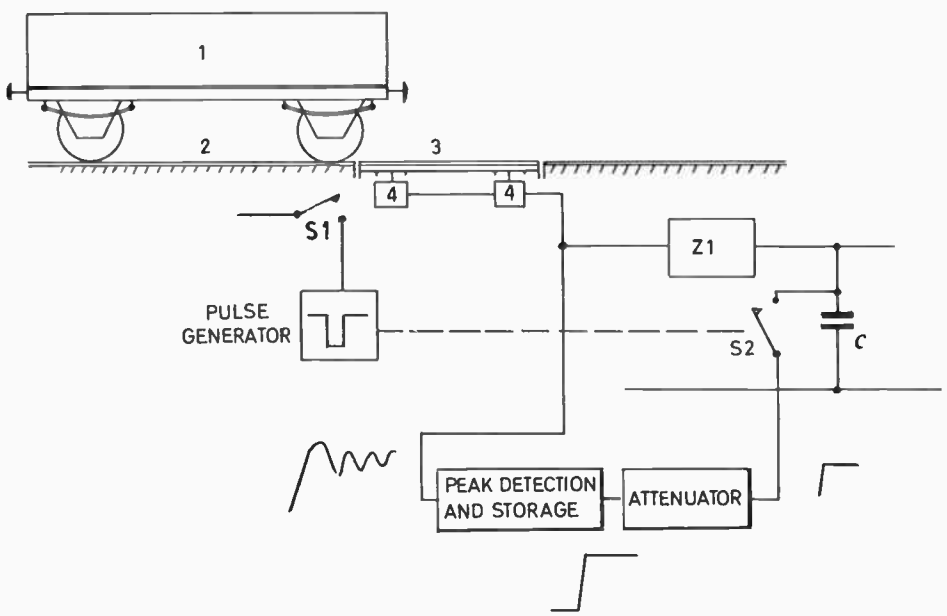

Fig. 4. Pre-set filter.

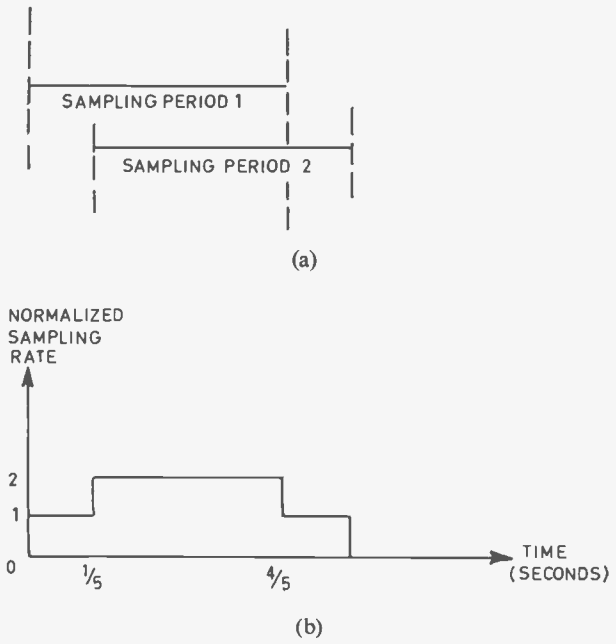

Fig. 5. Overlapping samples.

From the attenuation characteristic plotted in Fig. 3 it can be seen that the most significant frequency is now about 4½ Hz. The attenuation obtained is about 50% higher than that obtained from straight integration over the complete weighing period.

A method of improving attenuation without extending the weighing period has therefore been derived. Further improvement can be obtained by introducing additional steps. Basically a combination of steps has been selected which would eliminate the effect of the most significant component in the frequency range of the vibration present, in this case 2½ Hz. If the lowest frequency in the range had been different, a different combination of steps would have been chosen.

Combinations of steps could be selected from Pascal's Triangle, shown in Fig. 6. The greatest errors due to vibration occur where an odd number of half cycles of the vibration is contained within the weighing period. By 'weighting' the peaks of the vibration according to an appropriate set of binomial coefficients, alternate half-wave peaks are cancelled out. Consider for example, the case where, contained within the weighing period, are five half-cycles, of amplitude zero, at time zero, and assuming the first half-cycle to be positive-going. Select the coefficient set 1, 4, 6, 4, 1 and multiply the vibration by this step combination. The first peak, positive-going, is multiplied by unity giving +1, the second peak, negative-going, is multiplied by 4 giving −4, the third peak, positive-going, is multiplied by 6 giving +6, and so on. The final sum will be +1 −4 +6 −4 +1 equal to zero. The set of coefficients chosen will depend on the lowest significant frequency of vibration, for example, the coefficient set 1, 6, 15, 20, 15, 6, 1 would be chosen for seven half-cycles contained within the weighing period.

2.8. *Weighted Averaging*

Basically, the technique of weighted averaging involves multiplication of the weight signal by a 'weighting function' $F(t)$, integration of the product over the weighing period, and finally division of the integral by the integral of $F(t)$ over the same period.

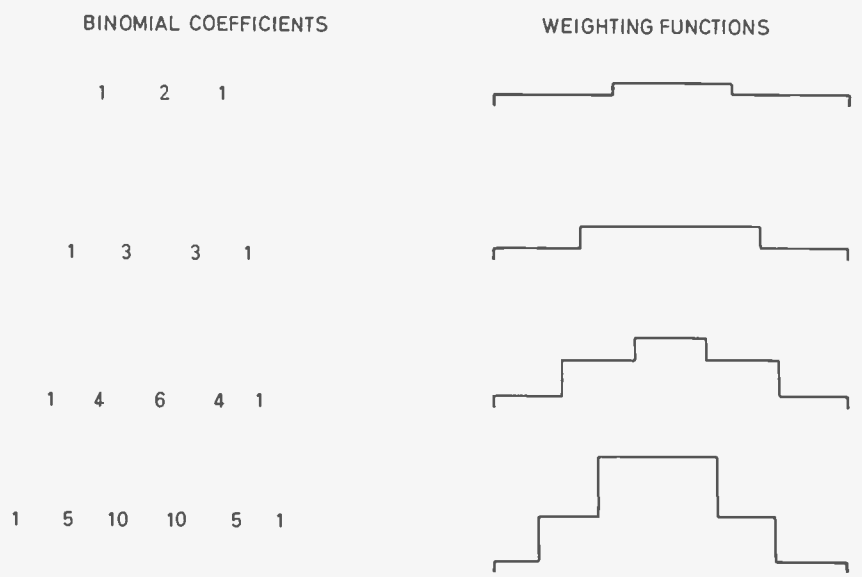

Fig. 6.
Stepped weighting function.

This can be expressed by:

$$\frac{\int_{-T/2}^{+T/2} W + E\sin(2\pi ft+\theta)F(t)\,dt}{\int_{-T/2}^{+T/2} F(t)\,dt} \quad \ldots\ldots(2)$$

Producing a value of vibration attenuation

$$\frac{\int_{-T/2}^{+T/2} F(t)\,dt}{\int_{-T/2}^{+T/2} \sin(2\pi ft+\theta)F(t)\,dt} \quad \ldots\ldots(3)$$

The actual weighting function chosen for a particular application will depend upon accuracy requirements and acceptable cost. Generally the magnitude of the attenuation obtained is related to the complexity and hence the cost of producing the associated weighting function.

The response characteristic contains a fluctuating term giving infinite attenuation when N is an integral number of cycles, as with straight integration. This factor is multiplied by a more complicated function, referred to as the 'decay function' $D(N, a)$ where a is a constant whose value can be selected as required and N is the number of cycles of vibration in the weighing period. In Fig. 7 the reciprocal of the decay function is plotted against N for two particular weighting functions $D(N, a)$ and $D(N, a, b)$. As the inclusion of the fluctuating term could only increase the attenuation it is omitted. On this diagram, the attenuation characteristic for straight integration is also plotted to enable a visual comparison of performance to be drawn.

The attenuation obtained by application of weighting function $D(N, a, b)$ is clearly superior to that obtained by application of $D(N, a)$. Nevertheless ($D(N, a, b)$ would only be applied where such a level of attenuation was really necessary as creation of this function requires a considerable increase in circuit complexity. By suitable choice of weighting function, attenuation curves can be obtained which will give minimum attenuations in excess of 500 for a range of vibration frequencies down to $2\frac{1}{2}$ cycles/weighing period.

Hence with a vibration of amplitude $\pm 10\%$ of true static weight, a maximum dynamic error due to vibration of less than 0·02% would be obtained. This result is markedly superior to the 1·27% error obtained from straight averaging. A-60 times improvement as has been obtained brings dynamic weighing accuracies within the range of accuracies obtained in static weighing.

Mathematical manipulation of the actual weighting function is rather involved but a convincing demonstration of the power of the technique can be given using a simple cosine weighting function.

The weighting function shown in Fig. 8 represents the expression

$$1+a-a\cos 2\pi\frac{t}{T} \quad \ldots\ldots(4)$$

where T represents the weighing period and a is a preselected constant.

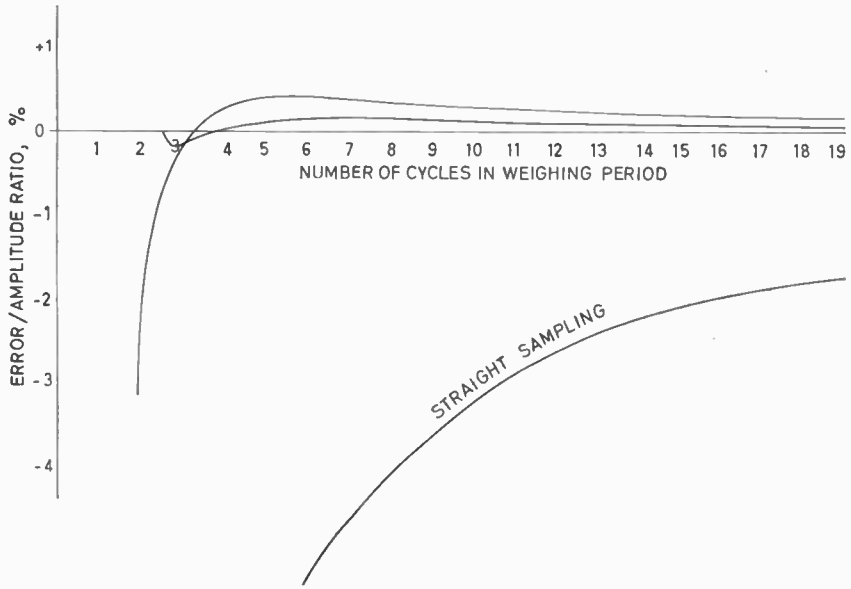

Fig. 7. Decay function $D(N, a)$.

If the low frequency be represented by $E \sin (2ft+\theta)$ then the error can be expressed as

$$\frac{\int_0^T E \sin(2\pi ft+\theta)\left(1+a-a\cos 2\pi \frac{t}{T}\right)dt}{\int_0^T \left(1+a-a\cos 2\pi \frac{t}{T}\right)dt} \quad \ldots\ldots(5)$$

In weighing, a guaranteed figure of accuracy is normally given and so only the maximum error is of interest. With an integration period of 1 s, eqn. (5) reaches a maximum of

$$\frac{E(1+a-f^2)}{(1+a)\pi f(f^2-1)} \quad \ldots\ldots(6)$$

Choosing $a = 7$ and with the most significant frequency equal to $2\frac{1}{2}$ Hz, the maximum error is $E/188$ which represents an attenuation of 188. This example merely demonstrates the effectiveness of the technique. As stated earlier, attenuations in excess of 500 can be obtained quite easily but a more complex weighting function would be required.

2.9. *Application of Theory*

Weighted averaging can be obtained by several methods, analogue and digital. Analogue multipliers and integrating amplifiers could be used but there are practical difficulties associated with such analogue methods, not least of which is the difficulty of producing an analogue multiplier of sufficient accuracy and temperature stability. These difficulties can be largely overcome by employing a digital sampling technique which is in line with the general trend towards increasing use of digital techniques. Such an equipment is compatible with our analogue-to-digital converter which produces a digital output from the analogue weight signal generated by the load cell transducers.

With straight averaging the use of digital sampling techniques is quite straightforward. The digital weight signal is sampled at regular intervals during the weighing period, and the sum of all the samples is divided by the total number of samples taken.

In weighted averaging, additional complexity is introduced by the need to multiply the weight signal by the weighting function $F(t)$. One approach would be to multiply each sample prior to summation by a factor dependent upon the weighting function. This method would be rather expensive in terms of electronic components. A better method is to vary the sampling rate in accordance with the weighting function. The validity of this method can be shown by reference to Fig. 8.

We have an incoming signal $y = I(t)$ and a given weighting function $y = f(t)$. We wish to evaluate, over a time interval T, the expression:

$$E = \frac{I(t).f(t)\,dt}{f(t)\,dt} \quad \ldots\ldots(7)$$

To solve this expression, we sum samples of the incoming signal $I(t)$ at a sampling rate equal to the instantaneous value of $f(t)$. Thus if n is the number of samples,

$$(t) = \frac{dn}{dt}$$

Consider an elemental increment of time δt. The number of samples taken in this interval of time is $f(t).\delta(t)$. As each sample is a measure of the instantaneous value of $I(t)$ then the total obtained by summation of samples over time interval δt is $I(t).f(t).\delta t$.

Over time T, the total obtained is then

$$\int_0^T I(t)f(t)\,dt$$

$$\int f(t)\,dt = \int \frac{dn}{dt}.dt = \int dn$$

Over time interval T, this integral is equal to N, the total number of samples taken.

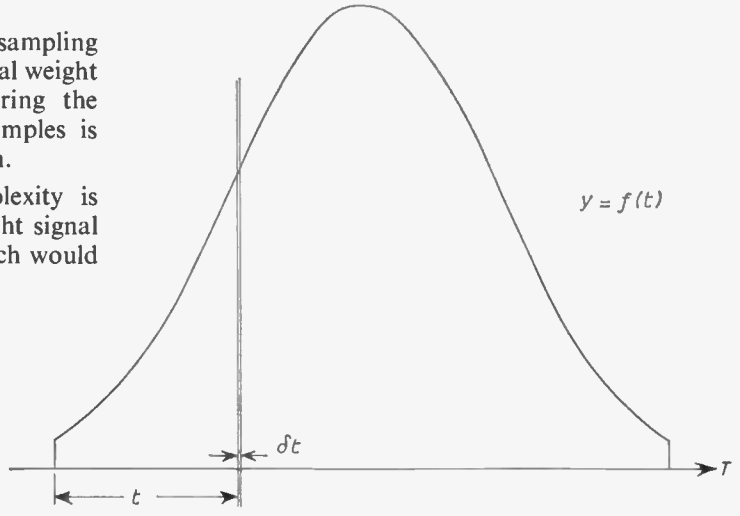

Fig. 8. Weighting function.

Thus by sampling the incoming signal at a rate equal at any instant to $f(t)$ and then dividing the total by the number of samples taken, we obtain a value for E over the time interval T. A large number of samples are taken during the weighing period whilst the sampling rate is varied according to the weighting function. Each sample is divided by the total number of samples and the quotient is stored in an accumulator. The actual weighting function as shown in Fig. 9 is a stepped approximation to the true weighting function of Fig. 8. The sampling rate is varied in equal increments of 0·5 from 1 to 14.

A practical realization of the digital filtering system applied to the weighing of rail vehicles is illustrated in Fig. 10.

Track switches located in the rails in conjunction with the track switch logic unit, recognize vehicles to be weighed and initiate the weighing sequence. On the receipt of signals from the appropriate track switches, the logic unit transmits a start signal to the control unit. Initially, the control unit resets the various counters in the system, then follows a pre-set delay or waiting period to allow the initial transient signal to reduce to an acceptable level. At the end of this period the control unit 'locks' the output of the analogue-to-digital converter or digitizer. A transfer signal is then supplied to the transfer gates which causes the digitizer output to be transferred into the buffer store. At this point, the locking signal is removed from the digitizer.

On completion of the transfer operation, a start signal is given to the 'clock pulse generator', the output of which is fed via the 'pulse rate divider' into the serializer. The function of the 'serializer' is to serialize the parallel input signal it receives from the buffer store. That is to produce a series of pulses equal in number to the minor weight increments contained in the input signal. To do this it is necessary to feed into the 'serializer' from the 'pulse rate divider' a fixed number of pulses, equal in fact, to one greater than the number of minor weight increments in the full scale capacity of the digitizer.

On completion of this serializing operation, the serializer produces a pulse which signifies the end of one sample, and this is fed to the control unit. On receipt of this pulse the control unit stops the clock pulse generator and then initiates a second transfer operation, i.e. it locks the digitizer, transfers the digitizer reading into the buffer store, and then unlocks the digitizer. Following this it again re-starts

Fig. 9. (*below*). Digital weighting function.

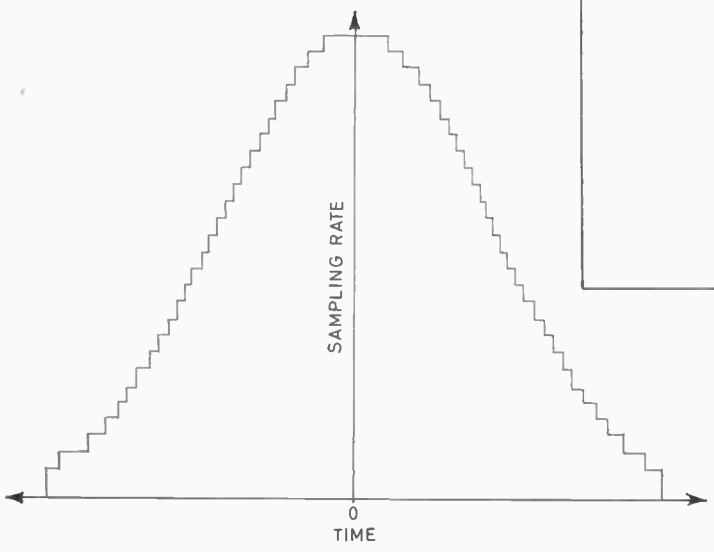

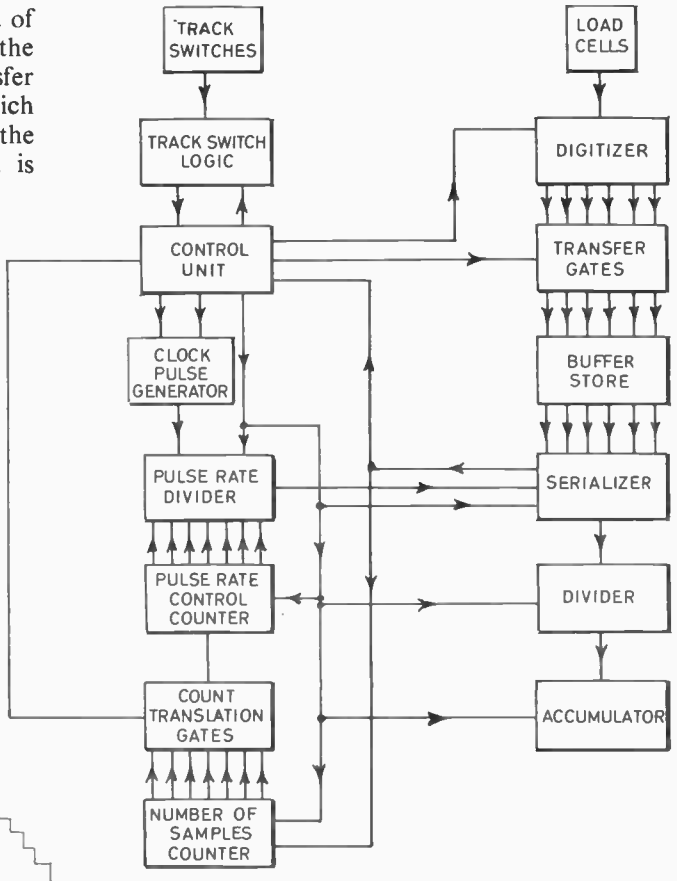

Fig. 10. Block schematic of digital filter.

the clock pulse generator thus initiating a second serializing operation. This process is repeated until the weighing cycle is completed. Each sample is fed into the accumulator via the divider which divides the sample by the total number of samples.

The time required to transfer the digitizer reading into the buffer store is small compared to the serializing time, so that the time between successive samples and hence the sampling rate, is determined by the serializing time. To perform a serializing operation, a fixed number of pulses are fed from the pulse rate divider into the serializer. Therefore the sampling rate can be varied by altering the pulse rate out of the pulse rate divider. The division ratio of the pulse rate divider is controlled by the pulse-rate-control counter. This is a straight binary counter and the pulse rate out of the pulse rate divider and hence the sampling rate, is directly proportional to the count of this counter.

The pulse rate control counter is set initially to a low count. The count is then increased progressively after predetermined numbers of samples, until the maximum sampling rate is reached at the middle of the weighing period. The sampling is then reduced in a symmetrical manner by progressively reducing the count on the counter. In order to change the count after pre-determined numbers of samples, it is first necessary to keep a progressive total of the samples. This is the function of the 'number-of-samples counter', into which are fed the 'end-of-sample' pulses from the serializer. Working in conjunction with this are the count-translation gates. These gates are required to recognize the counts on the number-of-samples counter at which the sampling is changed. Both the 'pulse-rate-control counter' and the 'number-of-samples counter' reverse automatically at the middle of the weighing period.

A system based on this design was constructed and put into operation in 1965. To date our worst results show an attenuation of greater than 600. At first sight such exceptional results seem improbable as one would not expect field results to compare with those calculated. In this case, however, the calculated results were based on worst phase conditions. The occurrence of the worst phase condition coincidentally with the minimum frequency of $2\frac{1}{2}$ Hz is extremely rare and may not have appeared in tests so far. Figure 11 shows a typical attenuation characteristic again assuming worst phase conditions. In the case of a simple sinusoid, of which $3\frac{1}{2}$ cycles are contained within the weighing period, the attenuation obtained will lie between about 50 dB and infinity, dependent upon phase conditions. Other components at different frequencies can be superimposed and the attenuations obtained. A summation of the errors contributed by each component will then yield the total weighing error. In such a system, there will always be conventional filtering in addition to variable rate integration and the effect of this filtering will be significant at the higher frequencies.

3. Conclusions

The basic problems related to dynamic weighing have been illustrated and a solution proposed. Such a solution must be found and applied in any dynamic weighing system if acceptable accuracies are to be obtained. In practice, many additional requirements arise. The object of weighing a vehicle for example is

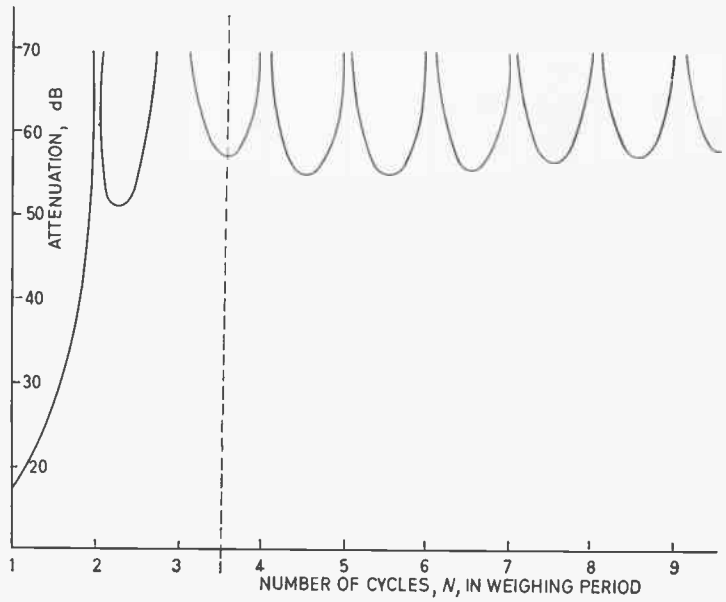

Fig. 11.
Typical attenuation characteristic.

normally to obtain the weight of its contents. The vehicle must therefore be weighed full, its gross weight stored, then weighed empty to obtain its tare weight. The tare weight must then be subtracted from the gross weight to obtain the weight of the contents. Many such functions are normally required in conjunction with dynamic weighing and they are extremely important. Nevertheless they are merely auxiliary functions which require only the exercise of elementary logic and additional fairly straightforward electronic equipment. The heart of a dynamic weighing system, the part that really matters, is that in which the effects of vibration are nullified. Without effective low frequency vibration attenuation, no amount of attractive sidelines will produce a good dynamic weighing system.

4. Acknowledgments

Acknowledgment is made to the directors of W. & T. Avery Ltd., for permission to publish the paper. The author also wishes to acknowledge the assistance of the other members of the development team whose efforts have made this paper possible.

5. References

1. 'Condition Responsive Device', U.S. Patent No. 3,108,648, October 1963 (Toledo).
2. 'Method and Apparatus for Dynamically Weighing Objects in Motion', British Patent No. 1,077,508 October 1964. French Patent No. 1,423,144 December 1964 (C.N.R.).
3. 'System for Measuring the Weight of Dynamic Loads', U.S. Patent No. 3,063,635 November 1962 (EPCCO).
4. Rogers, E. L., 'Integrated system streamlines railroad freight handling', *Control Engineering*, **15**, pp. 56–9, January 1968.
5. 'Arrangement for Weighing Oscillatory Load', U.S. Patent No. 3,173,503. March 1965.
6. 'Electronic Wagon Weigher', French Patent No. 1,295,598. April 1961.
7. 'High Speed Weighing System', Canadian Patent No. 718.547. September 1965.
8. 'Weighing on the move', *Process Engineering*, pp. 66–7, October 1966.
9. 'The Santa-Fe installs two-draft uncoupled-in-motion track scales', *Scale Journal*, **51**, No. 9, pp. 4–5, 9, June 1965.

Manuscript received by the Institution on 18th July 1968 (Paper No. 1275/IC 10).

STANDARD FREQUENCY TRANSMISSIONS—July 1969

(Communication from the National Physical Laboratory)

July 1969	Deviation from nominal frequency in parts in 10^{10} (24-hour mean centred on 0300 UT)			Relative phase readings in microseconds N.P.L.—Station (Readings at 1500 UT)		July 1969	Deviation from nominal frequency in parts in 10^{10} (24-hour mean centred on 0300 UT)			Relative phase readings in microseconds N.P.L.—Station (Readings at 1500 UT)	
	GBR 16 kHz	MSF 60 kHz	Droitwich 200 kHz	*GBR 16 kHz	†MSF 60 kHz		GBR 16 kHz	MSF 60 kHz	Droitwich 200 kHz	*GBR 16 kHz	†MSF 60 kHz
1	− 299·9	+ 0·1	0	548	468·2	17	− 299·9	+ 0·2	+ 0·1	529	458·5
2	− 299·9	+ 0·1	0	547	467·5	18	− 300·0	+ 0·1	+ 0·1	533	457·8
3	− 299·9	+ 0·1	0	546	466·3	19	− 300·1	+ 0·1	+ 0·1	534	456·9
4	− 299·8	0	0	544	466·1	20	− 299·9	+ 0·1	+ 0·1	533	455·9
5	− 299·9	+ 0·1	0	543	465·4	21	− 299·9	0	+ 0·1	532	456·0
6	− 300·0	+ 0·1	0	544	464·5	22	− 300·0	0	+ 0·1	533	456·1
7	− 299·9	0	0	543	464·4	23	− 300·1	0	+ 0·1	534	456·0
8	− 299·8	+ 0·1	0	541	463·8	24	− 300·1	0	+ 0·1	535	456·0
9	− 300·0	+ 0·1	0	541	462·8	25	− 300·0	0	+ 0·1	535	456·0
10	− 299·9	+ 0·1	0	540	461·8	26	− 300·0	0	+ 0·1	535	456·1
11	− 299·7	+ 0·1	+ 0·1	537	461·0	27	− 299·9	0	+ 0·1	534	456·0
12	− 299·7	+ 0·1	0	534	460·6	28	− 300·1	0	0	535	456·1
13	− 299·8	+ 0·1	+ 0·1	536	459·4	29	− 300·1	0	0	536	456·2
14	− 299·8	+ 0·1	+ 0·1	534	464·4	30	− 299·9	0	+ 0·1	535	456·1
15	− 299·9	+ 0·2	+ 0·1	533	462·8	31	− 300·0	0	+ 0·1	535	455·9
16	− 299·7	+ 0·1	+ 0·1	530	461·7						

All measurements in terms of H.P. Caesium Standard No. 334, which agrees with the N.P.L. Caesium Standard to 1 part in 10^{11}.

* Relative to UTC Scale; $(UTC_{NPL} - Station) = + 500$ at 1500 UT 31st December 1968.

†Relative to AT Scale; $(AT_{NPL} - Station) = + 468{\cdot}6$ at 1500 UT 31st December 1968.

Radio Engineering Overseas . . .

The following abstracts are taken from Commonwealth, European and Asian journals received by the Institution's Library. Abstracts of papers published in American journals are not included because they are available in many other publications. Members who wish to consult any of the papers quoted should apply to the Librarian giving full bibliographical details, i.e. title, author, journal and date, of the paper required. All papers are in the language of the country of origin of the journal unless otherwise stated. Translations cannot be supplied.

MICROWAVE HOLOGRAMS

Holography, which has made great progress in the light-wave region by the use of laser light, utilizes wave interference and its principle can be applied to the microwave region where a wave source of good coherence is available. However, in this region, the lack of suitable recording and indicating elements, makes it difficult for holography to develop as rapidly as in the light-wave region, where photographic dry plates and film are available as recording elements.

Experiments of hologram construction by microwaves and optical image reconstruction of the object by illuminating the microwave hologram have been carried out at Hokkaido University. The published paper describes the experimental and theoretical examinations involving the effect of scanning lines on the reconstructed image when a probe scans in the hologram construction. The relation between object magnitude, wavelength and resolution, storage of three-dimensional information in microwave hologram are also considered. In the theoretical analysis, the hologram optical system is expressed in matrix form from the standpoint of light ray optics and the experimental results are explained by using a matrix technique.

'Microwave holograms and their optical reconstruction', Yosinao Aoki, *Electronics and Communications in Japan*, (English language edition of *Denshi Tsushin Gakkai Ronbunshi*), **51**, No. 7, pp. 107–14, July 1968.

GLIDE PATH MODEL

The null reference 'glide path system' is that part of the international instrument landing system (i.l.s.) used to guide an aircraft down an appropriate slope preparatory to landing. The glide path system is operative over a distance of at least 10 miles and uses a frequency of about 330 MHz. The system relies on reflections from the ground to obtain an appropriate antenna radiation pattern and it is found that objectionable irregularities are associated with non-flat ground.

When the system was first introduced in about 1941, the highest practical frequency (330 MHz) was used to obtain a finely resolved pattern in space with a transmitting antenna of moderate size. Although a system could be produced today without ground surface effects by the use of a considerably higher frequency, the investment in equipment for the existing system makes such a change very undesirable. However, an improved system performance has become increasingly necessary to offset the reduced manoeuvrability of modern aircraft and to permit, eventually, blind or automatic landings.

As a result of a research project at the University of Queensland an Australian paper describes the development of a geometrical model system which can be used to evaluate the effects of specified ground surfaces. Initial development of this model depended on the selection of a suitable wavelength scaling factor and a convenient measuring principle. Wavelength scaling by approximately 30 : 1 (which corresponds to an operating frequency near 10 GHz) and a c.w. microwave system enabling detailed glide path characterization from single frequency measurements, were adopted.

The paper also outlines the essential details of the existing model together with experimental results which have established its accuracy, for an 'ideal' system, to be about 0·01°. It is intended to investigate terrain modifications of non-flat glide path sites using the model facility, which offers advantages in convenience, accuracy and ability to include fine detail.

Successful modelling of practical sites will enable convenient measurement of glide path performance and could reduce the full-scale flight testing which is currently the only evaluation method.

'Microwave model of the glide path system', R. E. Bogner, G. R. Haack and W. R. Belcher, *Proceedings of the Institution of Radio and Electronics Engineers Australia*, **30**, No. 4, pp. 111–20, April 1969.

RECEPTION OF SINGLE-SIDEBAND AND DOUBLE-SIDEBAND A.M. SOUND BROADCASTING

In amplitude modulated sound broadcasting use has so far been made exclusively of double-sideband modulation and the radio frequency carrier is fully transmitted. In this method the r.f. envelope of oscillations is an exact representation of the information to be transmitted and by simple detection the information may be reconstituted in the receiver. The single-sideband method of transmission has some advantages particularly in respect of reception from distant transmitters (sky-wave reception).

A paper by a German engineer at the Institut für Rundfunktechnik at Hamburg outlines some of the technical difficulties encountered in single-sideband reception and describes an arrangement which makes possible the reception of single-sideband transmissions, for example, in the m.f. and l.f. bands.

With this arrangement if the channel spacing is regular and the transmitter frequencies, as well as the intermediate frequency of the receiver, are derived from the channel frequency spacing, almost no disturbing problems of interference in the receiver due to harmonic interaction and unwanted radiation of oscillators are experienced, because the interference always produces a beat-frequency of zero.

'A novel arrangement for the reception of single-sideband and double-sideband transmissions in a.m. sound broadcasting', R. Netzband, *E.B.U. Review*, **114–A**, Technical, pp. 60–3, April 1969. (In English.)